

R82-36

TC171
.M41
.H99
no. 280



A SECOND-ORDER BUDYKO-TYPE PARAMETERIZATION OF LANDSURFACE HYDROLOGY

BY
STEFANOS A. ANDREOU
and
PETER S. EAGLESON

RALPH M. PARSONS LABORATORY
HYDROLOGY AND WATER RESOURCE SYSTEMS

Report No. 280

Prepared under the Support of
The National Aeronautics and Space Administration
Grant NAG 5-134

June 1982

MIT

Sarker Engineering Library



DEPARTMENT
OF
CIVIL
ENGINEERING

SCHOOL OF ENGINEERING
MASSACHUSETTS INSTITUTE OF TECHNOLOGY
Cambridge, Massachusetts 02139

A SECOND-ORDER BUDYKO-TYPE PARAMETERIZATION
OF LANDSURFACE HYDROLOGY

by

Stefanos A. Andreou

and

Peter S. Eagleson

RALPH M. PARSONS LABORATORY

HYDROLOGY AND WATER RESOURCE SYSTEMS

Report Number 280

Prepared under the Support of
The National Aeronautics and Space Administration
Grant NAG 5-134

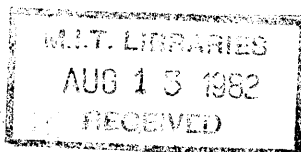
June 1982

ACKNOWLEDGEMENTS

This work was completed with the support of the National Aeronautics and Space Administration (NASA) under Grant NAG 5-134.

The work was performed by Stefanos A. Andreou, research assistant in Civil Engineering at MIT, and constitutes his thesis presented in partial fulfillment of the requirements for the degree of Master of Science in Civil Engineering. This study was supervised by Peter S. Eagleson, Professor of Civil Engineering, who also provided the theoretical background material on which it is based.

Thanks also are due to Dr. Chris P. Milly, who provided many helpful suggestions and comments, and to Antoinette DiRenzo, who performed all the necessary typing.



ABSTRACT

This work develops a simple, second-order parameterization of the water fluxes at a landsurface for use as the appropriate boundary condition in general circulation models of the global atmosphere. The derived parameterization incorporates the high non-linearities in the relationship between the near-surface soil moisture and the evaporation, runoff and percolation fluxes.

Based on the one-dimensional statistical-dynamic derivation of the annual water balance developed by Eagleson (1978), it makes the transition to short-term prediction of the moisture fluxes, through a Taylor expansion around the average annual soil moisture.

A comparison of the suggested parameterization is made with other existing techniques and available measurements.

A thermodynamic coupling is applied in order to obtain estimations of the surface ground temperature.

TABLE OF CONTENTS

	<u>PAGE NO.</u>
Title Page	1
Abstract	2
Acknowledgements	3
Table of Contents	4
List of Figures	6
List of Tables	9
Notation	10
Chapter 1 Introduction	15
1.1 Background	15
1.2 Objectives	15
Chapter 2 Literature Review	17
2.1 Landsurface Parameterization	17
2.2 Water Balance Models.	28
Chapter 3 Review of the Water Balance	31
3.1 Introduction	31
3.2 The Separate Elements of the Water Balance	33
Chapter 4 The Short-term Water Balance Model.	38
Chapter 5 Selection of the Appropriate Model Parameters	46
5.1 Introduction	46
5.2 Ecological Optimality Hypotheses	48
Chapter 6 Simulation of the Rainfall Process.	54
Chapter 7 Presentation of Results	57
7.1 The Evapotranspiration, Surface Runoff, and Percolation Functions.	57
7.2 Simulation of Soil-Moisture Concentration During the Rainy Season Using a Constant Value of $e_p = \bar{e}_p$	64
7.3 Comparison with a Numerical Model.	70
7.4 Comparison with Manabe's (1969) Parameteri- zation	78
7.5 Soil-Moisture Simulation with Changing Value of e_p	83
7.6 The Thermodynamic Coupling	88

TABLE OF CONTENTS

	<u>PAGE NO.</u>
Chapter 8	Summary, Conclusions, and Recommendations for
	Further Research. 106
	8.1 Summary. 106
	8.2 Conclusions. 108
	8.3 Suggestions for Further Research 109
REFERENCES	111
APPENDIX 1	Fortran Programs for Simulating Soil-Moisture
	at the Surface Layer 116
	1. Program Taylor.Fortran 117
	2. Program Ariz.Fortran 131
APPENDIX 2	Documentation of the Computer Program SPLASH . . . 138

LIST OF FIGURES

<u>Figure No.</u>	Title	<u>Page No.</u>
1	Surface Runoff Function	42
2	Climatic Climax Soil-Vegetation Systems: Clinton, Massachusetts	50
3	Climatic Climax Soil-Vegetation system: Santa Paula, California	51
4	Evapotranspiration Efficiency Function ($M = 0$)	58
5	Evapotranspiration Efficiency Function ($M = M_0$)	59
6	Surface Runoff Function y_s (s)	62
7	Groundwater Runoff Function y_g (s)	63
8	Simulation of Soil Moisture During the Rainy Season (Clinton, Massachusetts)	65
9	Simulation of Soil Moisture During the Rainy Season (Santa Paula, California)	67
10	Sensitivity of Fluxes to Surface Layer Thickness	68
11	Comparison of Storage Change Produced by the Analytical and Numerical Model (Santa Paula, California)	72
12	Comparison of Total Yield Produced by the Analytical and Numerical Model (Santa Paula, California)	73
13	Comparison of Evaporation Produced by the Analytical and Numerical Model (Santa Paula, California)	74
14	Comparison of Storage Change Produced by the Analytical and Numerical Model (Clinton, Massachusetts)	75
15	Comparison of Total Yield Produced by the Analytical and Numerical Model (Clinton, Massachusetts)	76

LIST OF FIGURES

<u>Figure No.</u>	Title	<u>Page No.</u>
16	Comparison of Evaporation Produced by the Analytical and Numerical Model (Clinton, Massachusetts)	77
17	Comparison of Storage Change Produced by Manabe's Model and the Analytical Model (Santa Paula, California)	80
18	Comparison of Storage Change Produced by Manabe's Model and the Analytical Model (Clinton, Massachusetts)	81
19	Comparison of Total Yield Produced by the Analytical and Manabe's Model (Clinton, Massachusetts)	82
20	Soil Moisture Concentration by the Analytical Model (Annual \bar{e}_p)	86
21	Soil Moisture Concentration by the Analytical Model (Seasonal \bar{e}_p)	87
22	Surface Temperature by Force-Restore Method ($Z_o = 0.05\text{cm}$, $T_{2_i} = 11^\circ\text{C}$, e_p calculated from the aerodynamic equation).	93
23	Soil Moisture Concentration by the Analytical Model ($Z_o = 0.05\text{cm}$, $T_{2_i} = 11^\circ\text{C}$)	94
24	Surface Temperature by Force-Restore Method ($Z_o = 0.05\text{cm}$, $T_{2_i} = 14^\circ\text{C}$, e_p calculated from the aerodynamic equation).	96
25	Soil Moisture Concentration by the Analytical Model ($Z_o = 0.05\text{cm}$, $T_{2_i} = 14^\circ\text{C}$)	97
26	Average Daily Evaporation Rate	98

LIST OF FIGURES

<u>Figure No.</u>	<u>Title</u>	<u>Page No.</u>
27	Surface Temperature by the Force-Restore Method ($Z_o = 0.5\text{cm}$, $T_{2_i} = 14^\circ\text{C}$, e_p calculated from the aerodynamic equation)	99
28	Soil Moisture Concentration by the Analytical Model ($Z_o = 0.5\text{cm}$, $T_{2_i} = 14^\circ\text{C}$)	100
29	Surface Temperature by the Thermodynamic Equili- brium Equation ($Z_o = 0.05\text{cm}$, $T_{2_i} = 14^\circ\text{C}$)	104
30	Soil Moisture Concentration (Temperature Calcu- lated by the Thermodynamic Equilibrium Equation)	105
31	Convergence Experiments (Clinton, Massachusetts)	140
32	Convergence Experiments (Santa Paula, California)	141

LIST OF TABLES

	<u>PAGE NO.</u>
TABLE 5.1	53
TABLE 6.1	56
TABLE 7.1	84
TABLE 7.2	102

NOTATION

<u>Symbols</u>	<u>Definition and Dimensions</u>	
A	albedo	[-]
A_o	gravitational infiltration rate as modified by capillary rise from water table.	$[LT^{-1}]$
B_p	biomass production	$[ML^{-2}T^{-1}]$
C_H	coefficient for the sensible heat transfer.	[-]
C_w	coefficient for the water vapor transfer	[-]
c_p	specific heat of water vapor at constant pressure	$[L^2T^{-2}deg^{-1}]$
c	pore disconnectedness index	[-]
c_s	specific heat of soil-water system	$[L^2T^{-2}deg^{-1}]$
D_{ij}	moisture transfer coefficient between layers i and j	$[LT^{-1}]$
d_1'	depth to which the diurnal moisture cycle extends	[L]
d_1	a soil depth influenced by the diurnal soil-moisture cycle	[L]
d	diffusivity index of soil	[-]
d_2	a soil depth influenced by the annual temperature cycle	[L]
E_a	drying power of the air	$[FL^{-1}T^{-1}]$
E_{PA}	annual potential evapotranspiration	[L]
E_{TA}	annual actual evapotranspiration	[L]
E_r	annual storm surface retention	[L]
E	exfiltration parameter	[-]
\bar{e}_T	average annual actual evapotranspiration rate	$[LT^{-1}]$
\bar{e}_p	average annual potential evapotranspiration rate	$[LT^{-1}]$
e_T	actual evapotranspiration rate	$[LT^{-1}]$
e_p	potential evapotranspiration rate	$[LT^{-1}]$
e_{TV}	transpiration rate from vegetation	$[LT^{-1}]$

e_s	soil evaporation rate	$[LT^{-1}]$
e_s	saturation vapor pressure at surface temperature	$[FL^{-2}]$
e_a	vapor pressure of the air at screen height	$[FL^{-2}]$
f_e	exfiltration capacity of soil	$[LT^{-1}]$
f_i	infiltration capacity of soil	$[LT^{-1}]$
G	heat flux into the soil	$[FL^{-1}]$
G	gravitational infiltration parameter	$[-]$
H	sensible heat	$[FL^{-1}]$
H_s	sensible heat	$[FL^{-1}]$
I_c	infiltration on soil surface	$[LT^{-1}]$
I_s	infiltration under vegetated surfaces	$[LT^{-1}]$
i	rainfall rate	$[LT^{-1}]$
J	evapotranspiration efficiency	$[-]$
$K(1)$	saturated hydraulic conductivity	$[LT^{-1}]$
K_{ij}	hydraulic conductivity between layers i and j	$[LT^{-1}]$
K_a	atmospheric heat conductance	$[FT^{-1}deg^{-1}]$
K_s	surface heat conductance	$[FT^{-1}deg^{-1}]$
$k(1)$	saturated intrinsic permeability	$[L^2]$
k_v	plant coefficient	$[-]$
k_s	soil thermal diffusivity	$[L^2T^{-1}]$
L	latent heat of vaporization	$[L^2T^{-2}]$
L	Monin-Obukhov length	$[L]$
M	vegetal canopy density	$[-]$
M_o	equilibrium vegetal canopy density	$[-]$
m_T	rainy season length	$[T]$

m_{t_b}	mean time between storms	[T]
m_{P_A}	mean annual precipitation	[L]
m_v	mean number of storms per year	[-]
m_i	mean storm intensity	[LT ⁻¹]
m_H	mean storm depth	[L]
m	pore size distribution index of soil	[-]
n_e	effective porosity of the soil	[-]
n	effective porosity of the soil	[-]
P_A	annual precipitation	[L]
$-$		
p	mean storm intensity	[LT ⁻¹]
P_a	atmospheric pressure	[FL ⁻²]
q^*	saturated atmospheric specific humidity	[-]
q_a	specific humidity of the atmosphere at screen elevation	[-]
q_{ij}	soil moisture flux between layer i and j	[LT ⁻¹]
$(R_i)_B$	bulk Richardson number	[-]
R_{g_A}	annual groundwater runoff	[L]
R_{S_A}	annual surface runoff	[L]
R_n	net radiation at the surface	[FLT ⁻¹]
R	gas constant	[L ² T ⁻² deg ⁻¹]
r_a	atmospheric diffusion resistance	[L ⁻¹ T]
r_i	surface diffusion resistance	[L ⁻¹ T]
S_e	exfiltration "desorptivity"	[LT ^{-1/2}]
S_i	infiltration "sorptivity"	[LT ^{-1/2}]
S_s	relative humidity at the evaporating surface	[-]
S_g	saturation ratio of the surface atmosphere	[-]

s	average soil moisture at the surface layer	[-]
s_o	average annual soil moisture at the surface layer	[-]
s_k	soil moisture concentration at time k	[-]
s_k	critical value of soil moisture	[-]
\bar{T}_a	average annual atmospheric temperature	[deg]
T_a	air temperature at screen height	[deg]
T	one year	[T]
T_g	ground temperature at the surface	[deg]
T_o	surface temperature	[deg]
T_i	soil temperature at the depth of the vapor source	[deg]
T_2	mean soil temperature of layer of depth d_2	[deg]
t_o	time when the surface becomes saturated after a precipitation	[T]
t_o	time when the surface becomes dry during an evaporation period	[T]
t_r	storm duration	[T]
t_b	time between storms	[T]
U	moisture uptake by plants	[LT ⁻¹]
U_a	wind speed	[LT ⁻¹]
w	upward capillary rise velocity from the water table	[LT ⁻¹]
W_g	surface soil moisture	[-]
W_{max}	maximum value of soil moisture for which surface runoff is equal to zero	[-]
Y	total yield	[L]
y_g	percolation rate	[LT ⁻¹]
\bar{y}_g	average annual percolation rate	[LT ⁻¹]
y_s	surface runoff rate	[LT ⁻¹]
\bar{y}_s	average annual surface runoff rate	[LT ⁻¹]
y	total yield rate	[LT ⁻¹]
Z_r	surface layer thickness	[L]

Z	distance above the soil surface	[L]
Z _a	screen height	[L]
Z _o	surface roughness	[L]
α	reciprocal of average storm intensity m_i	[L ⁻¹ T]
β	reciprocal of average time between storms t_b	[T ⁻¹]
γ	the psychrometric constant	[FL ⁻² deg ⁻¹]
Δ	slope of the saturation vapor pressure-temperature curve	[FL ⁻² deg ⁻¹]
δ	reciprocal of average storm duration t_r	[T ⁻¹]
η	reciprocal of mean storm depth m_H	[L ⁻¹]
θ	volumetric moisture content	[-]
θ_{f_c}	field capacity	[-]
κ	shape factor of Gamma-distributed rainstorm depths	[-]
λ	parameter of Gamma-distributed storm depth	[-]
E	potential humidity	[-]
ρ_α	mass density of air	[FL ⁻⁴ T ²]
ρ_w	mass density of water	[FL ⁻⁴ T ²]
ρ_s	density of soil-water system	[FL ⁻⁴ T ²]
σ	capillary infiltration parameter	[]
τ_1	one day	[T]
ϕ_e	dimensionless desorption diffusivity of soil	[-]
ϕ_i	dimensionless sorption diffusivity of soil	[-]
Ψ_g	soil matrix head	[L]
Ψ	soil matrix head	[L]
Ω	groundwater recharge potential	[-]

CHAPTER 1

Introduction

1.1 Background

Current global atmospheric general circulation models use very complex numerical techniques to solve the hydrodynamic and thermodynamic equations of motion in the atmosphere, but they generally treat the land surface thermal and moisture boundary conditions in a rather simplistic way. This study attempts to provide an improved land surface boundary condition that increases the physical fidelity while maintaining computational practicality.

There are many difficulties involved in such a parameterization. First, there are problems related to inhomogeneities of the system's inputs, such as precipitation and of the system parameters, such as soil properties. Because of the great difficulty in defining the interactions of the microscale and the macroscale dynamics and representing these in a computationally efficient way, the problem of spatial variability is treated by considering a lumped one-dimensional system, having effective areal parameters. A second problem is that of formulating the appropriate differential equations, which will account for the exchange of water and heat between the soil and the atmosphere. Special problems that arise here are those concerning the time scales of the physical processes, the number of parameters used and the selection of conceptual models representative of the real processes.

1.2 Objectives

The objectives of this work are:

1. To derive analytical expressions for the evaporation and yield rates which can be applied in dynamic mass balance equations for short term prediction of the soil moisture in the root zone.

2. To minimize the number of parameters necessary to implement this parameterization and to determine the inputs and observations required to operate the model.
3. To compare the results with those obtained from other models, which use either detailed numerical techniques or different types of parameterization.
4. To perform sensitivity analyses with respect to the critical soil parameters.
5. To estimate the ground surface temperature.

It must be noted, that the presence of snow is not taken into account in this research.

CHAPTER 2

Literature Review

2.1 Landsurface Parameterization

According to Eagleson [1981], there are six basic elements of the hydro-thermal system at the earth surface, which must be parameterized:

1. The rate of potential evapotranspiration e_p , which is a function of the incoming short and long wave radiation to the system, the wind speed, the surface roughness, the vapor pressure of the air, the temperature of the air and of the ground. The dependence of e_p on the ground temperature generates a feedback between the soil and the atmosphere, and becomes a major coupling factor between the heat and moisture fluxes. Because of the creation of an atmospheric boundary layer due to the air flow close to the surface, e_p becomes also a function of the extent of the upwind evaporating surface.

2. The actual evapotranspiration rate e_T , which is a function of the available soil moisture, the soil properties and the vegetation cover. The value of e_T is limited from above by the value of e_p , i.e., the capacity of the atmosphere to remove vapor from the surface. The following general expression relates e_T with e_p :

$$J = \frac{e_T}{e_p} = f(s, e_p, t; \text{soil and vegetation}), J \leq 1$$

where J is called the "evaporation efficiency".

3. The water yield rate y , which is divided into two components, the surface runoff rate y_s and the percolation to the water table y_g . The yield rate is functionally related to the following parameters:

$y = f(s, \text{precipitation input, } t; \text{soil properties and storage capacity of the surface layer}).$

4. The surface temperature T_g , which is dynamically related to the net radiation R_n , the latent and sensible heat losses from the soil, and the heat storage capacity of the surface soil layer.
5. The surface moisture retention capacity e_r , which can become important for certain types and density of vegetation cover and also under very arid conditions.
6. The soil moisture layer thickness Z_r , which consists of the portion of the soil close to the surface, where changes in moisture and heat content are concentrated. This zone is usually taken equal to one meter, but in fact it should be determined by the root-zone depth and by the soil and climatic properties of the area under investigation.

An overview of the methodologies proposed by prior investigators to model the above elements, will now be made following that of Eagleson (1981).

1. Potential Evapotranspiration rate e_p

The concept of potential evapotranspiration, first introduced by Thornthwaite [1948], refers to the capacity of the atmosphere to remove vapor, under given meteorological conditions, when there is unlimited water supply from the soil and the ground surface is wet.

The basis of the recent approaches for estimating e_p is Penman's [1948] equation in the modified form:

$$\rho_w L \cdot e_p = \frac{\Delta(R_n - G)}{\Delta + \gamma} + \gamma \frac{E_a(x)}{\Delta + \gamma} \quad (2.1)$$

where

$$E_a = \frac{\rho_a L}{r_a} [q^*(T_a) - q_a]$$

and

- R_n = net radiation near the surface.
 G = net heat flux into the ground.
 Δ = (de^*/dT) , the slope of the saturation vapor pressure-temperature curve.
 γ = the psychrometric constant.
 L = latent heat of vaporization
 E_a = the "drying power" of the air
 $q^*(T_a)$ = saturated atmospheric specific humidity at air temperature
 q_a = specific humidity of the atmosphere at screen elevation
 r_a = atmospheric diffusion resistance.

Equation (2.1) was applied in many theoretical and experimental studies by investigators such as Penman and Schofield, 1951; Penman, 1956; Tanner and Petton, 1960; Slatyer and McIlroy, 1961; Monteith, 1965, 1973; Rijtema, 1965; Van Bavel, 1966; Kohler and Parmele, 1967; Thom and Oliver, 1977.

The two-term structure of Equation (2.1) helps to point out the influence of large-scale advection. The first term corresponds to a lower limit to evaporation from a moist surface under steady-state conditions. When such conditions have been established, the value of q_a tends to reach the saturation value. This can happen in the downwind direction of a wet surface of infinite extent, where evaporated moisture will be advected. The second term of Equation (2.1) represents the drying power of the air $E_a(x)$. It takes its maximum value at the beginning of the uniform surface ($x=0$), where the air is driest. It was found by McNaughton [1976], that $E_a(x)$ decreases exponentially with distance x .

2. The Actual Evaporation Rate e_T

When the limiting factor for evaporation is not the available energy supplied to the system, but is the amount of soil moisture within the surface layer, then evaporation control passes to the soil. In this case, the evapotranspiration rate becomes dependent on the value of soil moisture, the soil properties and the vegetation cover, which together influence the capacity of the soil to deliver moisture upwards. Thus we can write:

$e_T = f(e_p, s; \text{soil, vegetation})$. The methods developed in order to determine this function can be categorized as follows:

a. Empirical parameterizations

Those involve long-term average relationships between precipitation and evaporation, which are derived from simple water balance equations applied to various catchments, by equating the total streamflow at the end of the catchment to the total yield produced in the basin. Such empirical relations are of no importance if one is interested in understanding the dynamics that govern the physical process, the interaction between the system's elements and their response to different hydrological and atmospheric conditions. As references one can mention the works by Schreiber [1904], Ol'dekop [1911], Tara [1954], Budyko [1956], Pike [1964], Budyko [1971].

b. Divergence of Atmospheric Vapor Flux

Rasmussen [1977]; derived a steady-state long-term regional atmospheric water balance over an area in space, by considering horizontal water vapor fluxes measured with probes well distributed in space. He used surface precipitation observations to close the water balance and estimate the long-term spatially-averaged actual evapotranspiration.

c. Advection-Aridity Approach

Brutsaert and Stricker [1979] assumed that the second term of Equation (2.1) represents the effect of larger-scale advection. They also used the concept of symmetry between potential and actual evapotranspiration introduced by Bouchet [1963] and the corresponding value of e_p for conditions of minimal advection suggested by Priestley and Taylor [1972], to derive:

$$\frac{e_T}{e_p} = \frac{\alpha(R_n - G)}{R_n - G + \frac{\gamma}{\Delta}E_a} - 1 \quad (2.2)$$

where $\alpha \simeq 1.26$

This methodology is called the "advection-aridity" approach. The time scale in Equation (2.2) is arbitrary, although they found it to work satisfactorily for daily values. It must be noted that difficulties are encountered in estimating the wind function which enters into the calculation of E_a and also advection effects were assumed to be generated only due to the regional shortage of moisture supply at the surface.

d. Soil Moisture Surrogate

Attempts have been made to derive equations for the actual evapotranspiration rate, by introducing a soil-moisture related surface parameter. All equations of this type are of the general form:

$$\frac{e_T}{e_p} = \frac{1}{1 + \frac{\gamma}{\Delta + \gamma}B} \quad (2.3)$$

where

i. $B = K_a/K_s$, Slatyer and McIlroy [1961]

K_a, K_s = atmospheric and surface heat conductances.

ii. $B = r_c/r_a$, Monteith [1965]

r_a = atmospheric diffusion resistance

r_c = surface diffusion resistance, which was related to the evaporation rate and to the difference between the vapor pressure at the leaf surface and its saturated value at leaf surface temperature.

iii. $B = (1-S_s)/S_s$, Barton [1979]

where S_s = relative humidity at the evaporating surface, which for non saturated surfaces can be very different from the relative humidity at the ground surface.

A special difficulty encountered in expressions such as Equation (2.3) is that they are not designed to represent effective areally averaged values for the atmospheric temperature and the value of B.

Tanner and Fuchs [1968] derived a more general equation for e_T , which does not assume any particular diffusion model for the leaf or other surface and does not include internal resistance to heat diffusion. The model they used is:

$$E = \frac{E_p - [\rho C_p \Delta / (\Delta + \gamma)] (T_o - T_i) / r_a}{1 + [\gamma / (\Delta + \gamma)] (r_i / r_a)} \quad (2.4)$$

where

r_i = internal resistance of the soil surface layer to the transport of water vapor [sec.m^{-1}]

T_o = surface temperature [$^{\circ}\text{K}$]

T_i = soil temperature at the boundary between the dry and moist layer in the soil, where the vapor source is.

There are also studies which derived expressions for the transpiration from plants. A category of these assumes knowledge of plant physiology, which can reduce their applicability for macroscale parameterizations, due to their inability to capture dynamic interrelationships among the various spatially variable system components. Studies of this type include those by Van de Honert [1948], Cowan [1965], Rijtema [1965], and Federer [1977].

Assuming the same albedos from the vegetation and the wet bare soil, Shuttleworth [1979] proposed a relationship similar to Equation (2.3), where he replaced e_T by e_{TV} , the transpiration rate from the plant.

Eagleson [1981] applied ecological optimality hypotheses to water-limited Natural Soil-Vegetation systems, to derive the following equation for the average evapotranspiration efficiency:

$$\frac{e_T}{e_p} = \begin{cases} 0.11 + 2.22M_o - 1.87M_o^2 + 0.54M_o^3 & , k_v = 1 \\ 0.11 + 1.25M_o + 0.27M_o^2 - 0.63M_o^3 & , k_v = 0.7 \end{cases} \quad (2.5)$$

where

M_o = percentage of vegetation cover

and $k_v = \frac{e_{TV}}{e_p}$ = plant coefficient.

e. Moisture Accounting Models

Most of the atmospheric general circulation models currently in use, apply a surface boundary conditions which incorporates an evaporation-soil-moisture relationship of the linear Thornthwaite-Budyko type. This relation has the form:

$$\frac{e_T}{e_p} = \begin{cases} 1 & \theta > \theta_{fc} \\ \theta/\theta_{fc} & 0 \leq \theta \leq \theta_{fc} \end{cases} \quad (2.6)$$

where Θ_{fc} is the soil field capacity, i.e., the upper limit of soil moisture for which water can be stored in the soil without drainage due to gravity.

A major difficulty encountered in formulations such as Equation (2.6) is the definition of the field capacity Θ_{fc} , since there is no rigorous justification for the correct value of this parameter.

As it is pointed out by other investigators (Philip, 1957; Hillel, 1971; Lowry, 1959), the relation between evapotranspiration and soil moisture can be highly non-linear, due to the influence of soil properties and vegetation cover, which play a dominant role during the exfiltration process. This non-linear relation was also theoretically supported and verified by Eagleson [1978], and it is the one used for the purposes of the present study.

Eagleson [1978] used the probability distributions of the independent climatic variables to obtain the derived distributions of the dependent elements of the water-balance, through a physically-based model of the natural process. With this statistical-dynamic approach he derived an expression of the long-term annual average evapotranspiration efficiency $\frac{\bar{e}_T}{\bar{e}_p}$ as a function of the long-term averages of soil moisture and climatic parameters, soil properties and vegetation cover. This relationship will be presented with more details in Chapter 3.

3. Water Yield Rate y

There are empirical equations which relate the long-term average annual yield with annual precipitation and potential evaporation (Lettau, 1969).

Another way of estimating the total long-term yield is by equating it with the long-term time integral of the streamflow in the catchment. This assumption can lead to errors especially under very arid conditions, where the groundwater flow does not appear as streamflow.

Empirical models developed by Budyko [1971], and Arakawa [1972], estimate the short-term yield as a function of soil moisture, precipitation, potential evapotranspiration, soil porosity, and surface layer thickness Z_r .

4. Surface Temperature T_g

The ground temperature T_g is an important parameter for determining sensible and latent heat fluxes from the soil to the atmosphere. Complicated numerical models exist, which solve the coupled moisture and heat transport equations in porous media. Recent studies include the work by Philip and DeVries [1957], Sasamori [1971], Rosema [1975], Benoit [1976], and Milly [1980].

For application in GCM's, more simplified methods for estimating T_g are needed. The most commonly used among those methodologies as presented by Deardorff [1978] are:

- a. Insulated surface (Gates et al. [1971]; Manabe et al. [1974]). The heat flux into the surface G is taken equal to zero and the energy balance equation at the surface i.e.,

$$R_n(T_g, t) - H(T_g, t) - \rho_w L e_T(T_g, t) = G \quad (2.7)$$

must be solved for T_g , given that the other elements of the equation are known.

- b. Dependence of G on the sensible heat H . Kasahara and Washington [1971] assumed $G = \frac{1}{3}H$ and solved Equation (2.7) for T_g .
- c. Dependence of G on the net radiation R_n . Nickerson and Smiley [1975] assumed $G = -0.19R_n$, when $R_n < 0$ (down) and $G = -0.32R_n$, when $R_n > 0$ (up) and solved Equation (2.7) for T_g .
- d. Bottom-insulated single soil layer. Arakawa [1972], Corby [1972], and Rowntree [1975] applied the following equation:

$$\frac{\partial T_g}{\partial t} = \pi^{1/2} G / (\rho_s c_s d_1) \quad (2.8)$$

where

$\rho_s = \rho_s(\theta) =$ density of soil-water system

$c_s = c_s(\theta) =$ specific heat of soil-water system

$d_1 =$ depth of the soil layer influenced by the diurnal temperature cycle

and $d_1 = (k_s \tau_1)^{1/2}$

where

$k_s =$ soil thermal diffusivity

$\tau_1 =$ one day

e. Force-restore method. Bhumralkar [1975] and Blackadar [1976] developed a formula that contains the deep soil temperature T_2 of the following form:

$$\alpha \frac{\partial T_g}{\partial t} = 2\pi^{1/2} G / (\rho_s c_s d_1) - 2\pi(T_g - T_2) / \tau_1 \quad (2.9)$$

where

$$\alpha = 1 + \frac{2\delta}{d_1 \pi^{1/2}} \quad \text{and} \quad T_g = T(\delta, t), \quad \delta = 1 \text{cm}$$

Deardorff [1978] considered the case where $\delta \rightarrow 0$ and Lin [1980] considered the δ layer thickness effect to be weaker than that of Bhumralkar [1975] by setting: $\alpha = 1 + \frac{\delta}{d_1 \pi^{1/2}}$

Tests performed by Deardorff [1978] and Lin [1980], proved that the force-restore method gives reasonably accurate results for estimating the ground surface temperature.

Sasamori [1970], developed a model by using the thermodynamic equilibrium relation:

$$S_g = \exp[g\psi_g(\theta)/RT_g] \quad (2.10)$$

where

S_g = saturation ratio of the surface atmosphere

$\psi_g(\theta)$ = soil matrix head as a function of θ

R = gas constant

That way he provided a coupling between the energy and mass conservation equations and the local thermodynamic equilibrium of temperature and humidity. Equation (2.10) could be solved for T_g in the case of soil controlled evaporation given that the other terms are known. A special difficulty could occur when the surface is saturated.

Then T_g should be approximated by the temperature above the evaporating surface.

5. Surface retention capacity

There is a volume of precipitation moisture which is retained at the surface due primarily to the surface texture. There are empirical relations for estimating that capacity and a collection of them is given by Wigham [1975], Blake [1975], and others. It should be noted that this water loss must depend also on the amount of precipitation, its intensity and the duration of interstorm periods.

6. Thickness of Soil Moisture Layer Z_p

This layer represents the depth from the surface within which big changes in soil moisture and heat content can occur due to forcing from the atmosphere. By using Philip's [1969] infiltration theory, Eagleson [1978] showed that this capillary penetration depth is of the order of one meter. Clearly, this depth would be a function of the soil-type, the timing of precipitation events and the depth of the root-zone system.

The diurnal thermal penetration depth has been found to be of the same order of magnitude.

Budyko assigned a value of $Z_r = 1\text{m}$ and Arakawa assumed $nZ_r = 10\text{cm}$. Gates et al. [1977] suggested $\Theta_{fc}Z_r = 30\text{ cm}$ and Shukla suggested $\Theta_{fc}Z_r = 10\text{cm}$.

Clearly, a rigorous justification of the appropriate value of Z_r does not exist and it's value is chosen rather arbitrarily. A sensitivity analysis is needed, in order to define the critical parameters that influence Z_r .

2.2 Water Balance Models

The existing water balance models can be divided into three categories:

- a. Empirical (Thorntwaite and Mather, [1955]; Lettau, [1969]).
- b. Phenomenological ("The Stanford Watershed Model", Crawford and Linsley [1966]; Holtan et al. [1974]; Peck [1976]).
- c. Dynamic (Eagleson [1978]).

For short-term predictions of soil moisture the Deardorff [1978] and Lin [1979] models are mentioned here, since results from their methodologies are compared with those obtained in this work.

Deardorff [1978] applied the "Force-restore" method to determine surface moisture and temperature. He used a value of the bulk soil moisture in the upper half-meter of the soil and wrote an equation of the form:

$$\frac{\partial W_g}{\partial t} = -C_1 \frac{(e_T - i)}{\rho_w d_1'} - C_2 \frac{(W_g - W_b)}{\tau} \quad , \quad 0 \leq W_b \leq W_{\max} \quad (2.11)$$

where

- i = storm intensity
 W_g = surface soil moisture
 C_1 = $f(W_g/W_{\max})$
 C_2 = constant
 τ = 1 day
 d_1' = depth to which the diurnal moisture cycle extends.
 W_{\max} = maximum value of soil moisture for which surface runoff is equal to zero.

Transpiration from vegetation was included by using a generalization of the Monteith and Szeicz [1962] function for evaporation, which incorporates parameters related to plant physiology. The complicated representation of vegetation can make this approach difficult to apply in an actual situation. Gravity is ignored and actual evaporation is derived from a Budyko type linear relation.

Lin [1979] developed a deterministic model to be dynamically coupled with a GCM and the groundwater zone. The ground is represented by a surface layer of 10cm depth, an intermediate 40cm layer and a deep layer which contains the groundwater zone.

The equations describing the system's dynamics are given by:

Surface layer d_1 :

$$d_1(d\theta_1/dt) = (I_s - e_s/\rho_w)(1-M) + (I_c - U_1)M - q_{12} \quad (2.12)$$

Intermediate layer d_2 :

$$d_2(d\theta_2/dt) = -U_2M + q_{12} - q_{23} \quad (2.13)$$

Deep layer:

$$\theta_3 = f(t), \text{ with very slow variations with time.}$$

where

- I_s, I_c = infiltration on soil and under vegetated surfaces
 e_s = soil evaporation rate
 M = percentage of vegetation cover
 U_1, U_2 = moisture uptake by plants
 q_{ij} = moisture flux from layer i to j

The potential evapotranspiration is derived from an aerodynamic equation and the actual evapotranspiration as a refinement of Budyko's parameterization, by using the value of the field capacity, wilting point and some empirical constants. The surface retention capacity of the soil and vegetation is ignored. The infiltration capacity is estimated by applying Holtan's [1974] method, where $I_i = A\theta_i^B$. The soil moisture flux q_{ij} , between adjacent layers is given by:

$$q_{ij} = D_{ij}(\theta_j - \theta_j) + K_{ij} \quad (2.14)$$

where

- D_{ij} = moisture transfer coefficients
 K_{ij} = hydraulic conductivity of the soil

From numerical experiments, he derived reasonable results of hydrologic variables such as soil moisture, evapotranspiration and surface temperature, for various regions of the earth. He distinguished between the variables that can be obtained from remote sensing and which are θ_1 , M , and T_g and those which cannot. The time and space varying parameters K_{ij} and D_{ij} create a special difficulty to implement in the model, since very often large scale measurements of those parameters do not exist.

CHAPTER 3

Review of the Water Balance

3.1 Introduction

The theoretical background of this work is drawn from Eagleson's (1978 a, b, c, d, e, f, g) water balance model. The physical model is one-dimensional and only vertical fluxes of water are considered in the soil column. The inputs to the system are of two types:

- a. Climatic variables, which are treated as independent random variables and are seven in total number.
- b. Soil properties, which are represented by three independent parameters considered to be deterministic.

The effect of vegetation is explicitly considered in the model through two parameters, the percentage of vegetation cover M_o , and the plant water use coefficient, k_v . Vegetation is modeled to act as a uniformly distributed sink throughout the entire surface layer of thickness Z_r , which continuously extracts moisture during the evapotranspiration period, at a rate regulated by the value of k_v .

The use of natural selection hypotheses and possible observations of the percentage of vegetation cover and total water yield from the basin, can significantly reduce the number of necessary input parameters to the model. Those techniques will be referenced with details in Chapter 5.

Uncertainty in the model is introduced through the probability distributions of several climatic variables. Precipitation events are simulated as independent and identically distributed rectangular intensity pulses having Poisson distributed arrivals. The corresponding storm depths h , are assumed as gamma distributed. The interstorm periods t_b and storm durations t_r , are

taken to be exponentially distributed. The rate of potential evapotranspiration e_p and the air temperature T_a , are set equal to their annual average values. The system dynamics for soil moisture movement are represented by Philip's (1969) infiltration and exfiltration equations. The averaged outputs from the system, i.e., the actual evaporation E_T , the surface runoff R_s and the groundwater runoff R_g are calculated through the use of derived distributions. More details for the model's assumptions are described by Eagleson (1978 a).

The mean annual water balance equation [Eagleson, 1978e] is given by:

$$E[P_A] \left\{ 1 - e^{-G-2\sigma\Gamma(\sigma+1)\sigma^{-\sigma}} \right\} = E[E_{P_A}^*]J(E,M,K_V) + m_T K(1) s_o^c - Tw \quad (3.1)$$

where

$E[]$ = expectation operator

P_A = annual precipitation

$E_{P_A}^*$ = annual potential evapotranspiration

E_{T_A} = annual actual evapotranspiration

J = $E_{T_A} / E_{P_A}^*$ = evapotranspiration efficiency.

E = exfiltration parameter

G = gravitational infiltration parameter

σ = capillary infiltration parameter

m_T = rainy season length

$K(1)$ = saturated hydraulic conductivity.

s_o = average annual soil moisture at the surface layer

c = pore disconnectedness index

T = 1 year

w = upward capillary rise velocity from the water table.

3.2 The Separate Elements of the Water Balance

The basic elements of the water balance, which will be of use in the current landsurface parameterization are the following:

a. Evapotranspiration

Eagleson (1978d) derived the total evapotranspiration during an interstorm period by using an exfiltration analogy of Philip's [1969] infiltration equation of the following form:

$$f_e \approx \frac{1}{2} S_e^{-1/2} - M \cdot e_v + w \quad (3.2)$$

where

M = vegetation fraction of surface

e_v = vegetation transpiration rate

w = velocity of capillary rise from the water table

S_e = the exfiltration "desorptivity" which is defined as follows for a dry surface ($s_1=0$)

$$S_e = 2s_o^{1+d/2} \left[\frac{n_e K(1) \psi(1) \phi_e(d)}{\pi m} \right]^{1/2} \quad (3.3)$$

where

n_e = effective porosity of the soil

K(1) = saturated effective hydraulic conductivity

$\psi(1)$ = saturated matrix potential of soil

$\phi_e(1)$ = dimensionless desorption diffusivity of soil

d = diffusivity index of soil

m = pore size distribution index of soil

s_o = initial soil moisture, constant throughout the surface boundary layer

The boundary conditions associated with the exfiltration equation are interpreted as follows:

In the beginning of the interstorm period, the surface soil moisture s_1 will take a value $s_1 = 1$, so that the exfiltration rate f_e will be equal to the potential evaporation rate e_p from a wet surface. We denote by t^* the time it takes for the surface retention to evaporate and by t_o the time it takes for the surface to become completely dry. When $t > t^* + t_o$, then $f_e < e_p$, and f_e will be given by Equation (4.1). Evaporation ceases at the time when $f_e = 0$, or when a new storm begins. Transpiration from the vegetated surface assuming unstressed conditions, will take place at a constant rate e_v , which will be given by: $e_v = k_v e_p$, where k_v = plant water use coefficient and e_p = bare soil potential evaporation.

The time t_o , after which control passes to the soil was found to be equal to:

$$t_o = \frac{s_e^2}{2\bar{e}_p^2(1+Mk_v-w/\bar{e}_p)} \cdot \left[1 - M + \frac{M^2k_v + 1(1-M)w/\bar{e}_p}{2(1+Mk_v-w/\bar{e}_p)} \right] \quad (3.4)$$

Assuming exponential distribution of the time between storms t_b and a constant potential evapotranspiration rate \bar{e}_p equal to it's annual average value, Eagleson [1978b] derived the following expression for the average annual evapotranspiration efficiency $J(E, M, K_v)$:

$$J = \frac{\bar{e}_T}{\bar{e}_p} = 1 - \left[\frac{1-M}{1-M+Mk_v} \right] \cdot \left\{ \left[1 + Mk_v + (2B)^{1/2} E \right] e^{-BE} - \left[Mk_v + (2C)^{1/2} E \right] e^{-CE} - (2E)^{1/2} \left[\gamma \left(\frac{3}{2}, BE \right) \right] \right\} \quad (3.5)$$

where

\bar{e}_T = actual annual average rate of evapotranspiration

$$B = \frac{1-M}{1+Mk_v - w/\bar{e}_p} + \frac{M^2 k_v + (1-M)w/\bar{e}_p}{2(1+Mk_v - w/\bar{e}_p)^2}$$

$$C = \frac{1}{2} / (Mk_v - w/\bar{e}_p)^2$$

$$\text{and } E = \frac{2\beta n K(1)\psi(1)\phi_e}{\pi m \bar{e}_p^2} s_o^{d+2}$$

where β , is the reciprocal of the average time between storms m_{t_b} .

b. Surface Runoff

Assuming uniform intensity $i(t)$ during a rainstorm Eagleson [1978e] applied Philip's [1969] infiltration equation, to represent the infiltration rate by:

$$f_i = \frac{1}{2} S_i t^{-1/2} + A_o \quad (3.5)$$

for a saturated surface,

$$A_o = \frac{1}{2} K(1)(1+s_o^c) - w$$

and

$$S_i = 2(1-s_o) \{ [5nK(1)\psi(1)\phi_i(d,s_o)] / 3m\pi \}^{1/2}$$

where

S_i = infiltration sorptivity

$\phi_i(d,s_o)$ = dimensionless sorption diffusivity of soil.

When the surface is saturated ($s_1=1$), f_1 becomes maximum and equal to the infiltration capacity f_1^* .

If the depth of surface retention is represented by h_o , then infiltration into the soil will start if $t_r > h_o/i$. The initial infiltration rate will be equal to the storm intensity i . The continuous rise in the internal soil moisture will cause an increase of the surface moisture. When the surface becomes saturated, at time $t_o + h_o/i$, the infiltration rate will be given from Equation (3.6). Thus, for $t_r > t_o + h_o/i$, $i > f_1$ and surface runoff is produced. It is found that:

$$t_o = \frac{s_i^2}{2i(i-A_o)} \left[1 + \frac{A_o}{2(i-A_o)} \right] \quad (3.7)$$

By solving the linearized diffusion equation with constant flux boundary condition, a similar expression can be obtained for t_o (Carslaw and Jaeger, 1959), where the coefficient $1/2$ is replaced by $\pi^2/16$.

By assuming the value of s_o to be constant at it's time-averaged value, Eagleson [1978e] approximated the expected annual surface runoff R_{sA} with the following function.

$$\frac{E[R_{sA}]}{E[P_A]} = e^{-G-2\sigma} \Gamma(\sigma+1)/\sigma^\sigma - E[E_r]/m_H \quad (3.8)$$

where

$$\sigma = \left[\frac{5n\eta^2 K(1)\psi(1)(1-s_o)^2 \phi_i(d, s_o)}{6\pi\delta m} \right]^{1/3}$$

$$G = [\alpha K(1)/2][1+s_o^c] - \alpha w$$

$$E_r = \text{storm surface retention}$$

$$\eta = \text{reciprocal of mean storm depth } m_H$$

$$\delta = \text{reciprocal of average storm duration } t_r$$

$$\alpha = \text{reciprocal of average storm intensity } m_i$$

c. Percolation to the Water Table

The average annual groundwater runoff is given by [Eagleson, 1978f):

$$E[R_{g_A}] = m_{\tau} K(1) s_o^c - Tw \quad (3.9)$$

where

m_{τ} = mean rainy season length

T = one year

CHAPTER 4

The Short-Term Water Balance Model

The purpose of this model is to make short-term predictions of the soil moisture level within the surface layer, by taking into account the atmospheric boundary conditions at the surface.

We assume that high moisture concentrations occur within a depth Z_r from the surface. That implies that a portion of the infiltrated water during precipitation will be stored within that layer of thickness Z_r . Below that depth Z_r , water will percolate downwards due to gravitational forces. If the surface reaches saturation during the precipitation period, then runoff will be produced at a rate depending on the value of the internal moisture within the layer Z_r . During evapotranspiration, the actual evaporation rate from the bare soil will be determined from the amount of available moisture within this layer and will be limited from above by the potential evapotranspiration rate e_p . Vegetation is assumed here to transpire at the potential rate under unstressed conditions, which will be independent of the level of soil moisture within the layer Z_r .

We consider a vertical soil column in contact with the atmosphere and define as the moisture state variable s_o , the concentration of soil moisture in the vegetation root zone Z_r . In a one-dimensional representation, where only vertical fluxes are considered, the conservation of water mass equation can be written:

$$nZ_r \frac{ds}{dt} = i - e_T - y \quad (4.1)$$

where

$$e_T = \text{evapotranspiration rate} = f_1(s; \text{climate, soil, vegetation}) \quad (4.2)$$

$$y = \text{yield rate} = f_2(s; \text{climate, soil}) \quad (4.3)$$

n = effective porosity of soil in vegetation root zone

Z_r = thickness of vegetation root zone (cm)

i = rainfall rate (cm/sec)

e_T = evapotranspiration rate (cm/sec)

y = yield rate (surface runoff plus percolation below the root zone)
(cm/sec)

Equations (4.2) and (4.3) establish a non-linear relation between e_T , y , and s . In order to make the transition from the long-term time averaged values \bar{e}_T and \bar{y} to their short-term values, e_T and y vary linearly around their long-term averages, with respect to the value of s . Thus, the non-linearities in the relations between e_T , y , and s will be incorporated into the model through a Taylor expansion of those functions, around the annual average soil moisture s_o . By performing that expansion, a transition is made from the long-term average values of those rates as they appear in the water balance derived by Eagleson [1978], to their short-term values.

The water balance can be written in the following form, which is more convenient for this purpose:

$$1 = EJ + e^{-G-2\sigma} \Gamma(\sigma+1) \sigma^{-\sigma} = \Omega s_o^c \quad (4.4)$$

where

E = potential humidity = $E[P_A]/E[E_{p_A}]$

Ω = groundwater recharge potential = $m_r K(1)/E[P_A]$

J = evapotranspiration efficiency = $\frac{\bar{e}_T}{\bar{e}_p}$

To a first-order approximation, we assume that the actual evapotranspiration rate e_T at anytime will vary linearly with changes in the soil moisture concentrations, s . Thus, we expand J around s_o and obtain:

$$\frac{e_T}{e_p} = \frac{\bar{e}_T}{e_p} + \frac{\partial J}{\partial s} (s-s_o) + \dots \quad (4.5)$$

From the definition of J (Equation 3.4) we can find:

$$C_1 = \frac{\partial J}{\partial s} = \left[\frac{1-M}{1-M+Mk_v} \right] \cdot \left[\left\{ -(1+Mk_v)B + (2B)^{1/2} - B(2B)^{1/2} E \right\} \cdot e^{-BE} E(1) (d+2) s_o^{d+1} \right. \\ \left. - \left\{ [-k_v C + (2C)^{1/2} - C(2C)^{1/2} E] \cdot e^{-CE} E(1) (d+2) s_o^{d+1} \right\} - \left\{ \sqrt{2E(1)} \left(\frac{d}{2} + 1 \right) s_o^{d/2} \left[\gamma \left(\frac{3}{2}, CE \right) - \gamma \left(\frac{3}{2}, BE \right) \right] \right. \right. \\ \left. \left. + (2E)^{1/2} s_o \left(\frac{3d}{2} + 2 \right) (d+2) E(1)^{3/2} \left[C^{3/2} e^{-CE(1) s_o^{d+2}} - B^{3/2} e^{-BE(1) s_o^{d+2}} \right] \right\} \right]$$

Then Equation (4.5) is:

$$\frac{e_T}{e_p} = J(s_o) + C_1 (s-s_o) \quad (4.7)$$

The following relation holds for the annual expected value of the surface runoff R_{s_A} :

$$e^{-G-2\sigma} \Gamma(\sigma+1) \sigma^{-\sigma} = \frac{E[R_{s_A}]}{E[P_A]} \quad (4.8)$$

At this point, we assume that the surface runoff occurs only during the storm duration. In order to obtain an expression for the average annual surface runoff rate \bar{y}_s we can write:

$$\frac{E[R_{s_A}]}{E[P_A]} = \frac{\bar{y}_s}{p} \quad (4.9)$$

where

$$\bar{p} = m_{PA} / m_{v} m_{tr} = \text{mean storm intensity} \equiv m_i$$

$$\text{and } \bar{y}_s = E[R_{sA}] / m_{v} m_{tr}$$

Here again, a first-order approximation is made and the surface runoff function is expanded in Taylor-series around the mean s_o .

In order to accomplish this, the derivative of the surface runoff function, with respect to s , should be derived. In attempting to evaluate the derivative of the runoff function, $e^{-G-2\sigma} \Gamma(\sigma+1) \sigma^{-\sigma}$, a difficulty is encountered because the derivative of the gamma function cannot be given in closed form. This difficulty was overcome by approximating the function $\xi = e^{-2\sigma} \frac{\Gamma(\sigma+1)}{\sigma^\sigma}$ by the polynomial:

$$\log \xi = -0.806 - 1.766(\log \sigma) - 0.980(\log \sigma)^2 \quad (4.10)$$

It is believed that this approximation represents satisfactorily the runoff function (Figure 1).

We can now evaluate the derivative of $\frac{y_s}{\bar{p}} = e^{-G-2\sigma} \Gamma(\sigma+1) \sigma^{-\sigma}$ with respect to s .

We find that:

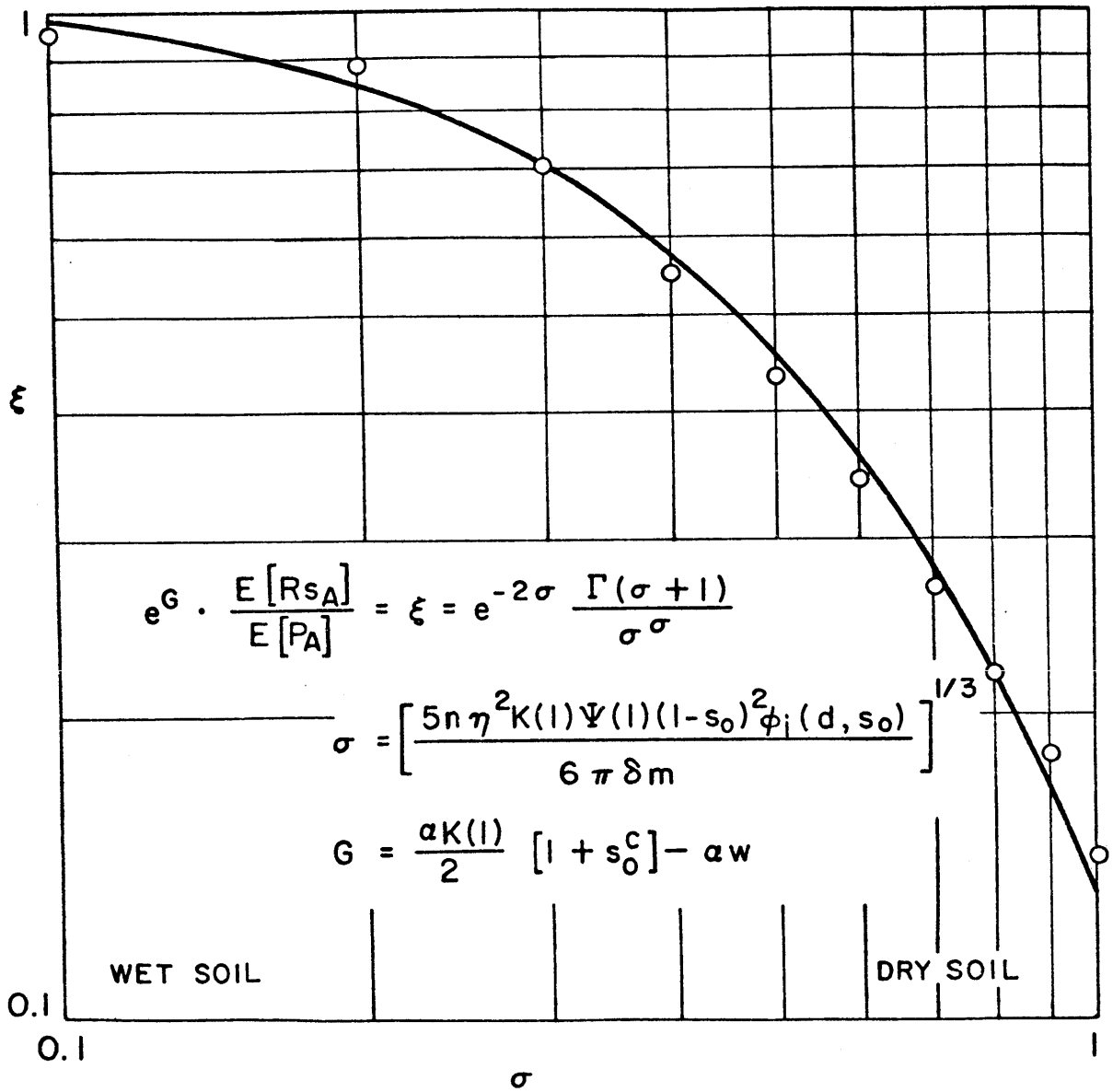
$$C_2 = \left. \frac{d(y_s/\bar{p})}{ds} \right|_{s=s_o} = e^{-G} \cdot \xi \left[\frac{-\alpha K(1) c s_o^{c-1}}{2} + U \right] \quad (4.11)$$

where

$$U = \frac{\Lambda}{\sigma} \left[-1.766 - 1.96(\log \sigma) \right]$$

$$\text{and } \Lambda = \left| \frac{5n\eta^2 K(1)\psi(1)}{6\pi\delta m} \right|^{1/3} \cdot \frac{1}{3} \cdot (1-s_o)^{-4/3}$$

$$\left[\frac{-2(1-s_o) [d(1-s_o)^{1.425-0.0375d} + 5/3] - (1-s_o)^{2.425-0.0375d} d(1.425-0.0375d)}{[d(1-s_o)^{1.425-0.375d} + 5/3]^{4/3}} \right]$$



SURFACE RUNOFF FUNCTION

FIGURE 1

Plotted points represent:

$$(\log \xi) = -0.806 - 1.766(\log \sigma) - 0.980(\log \sigma)^2$$

The following relation holds for the annual expected value of the ground-water runoff R_{gA} :

$$\Omega s_o^c = \frac{E[R_{gA}]}{E[P_A]} \quad (4.12)$$

We assume that percolation to the water table occurs during the entire rainy season of length m_τ . Thus, in order to derive a representative rate \bar{y}_g for the percolation, the following normalization is applied:

$$\Omega s_o^c = \frac{E[R_{gA}]}{E[P_A]} = \frac{\bar{y}_g}{m_{PA}/m_\tau} = \frac{\bar{y}_g}{\bar{p}} \cdot \frac{m_\tau}{m_{\sqrt{m_\tau r}}} \quad (4.13)$$

By taking the derivative of \bar{y}_g/\bar{p} with respect to s , we obtain:

$$C_3 = \left. \frac{d(\bar{y}_g/\bar{p})}{ds} \right|_{s=s_o} = \frac{m_{\sqrt{m_\tau r}} K(1) c s_o^{c-1}}{m_{PA}} \quad (4.14)$$

We also expand the groundwater runoff rate y_g around it's long-term average value. Thus, finally we can write to the the first approximation:

$$\frac{y_s}{\bar{p}} = \frac{\bar{y}_s}{\bar{p}} + C_2(s-s_o) \quad (4.15)$$

and

$$\frac{y_g}{\bar{p}} = \frac{\bar{y}_g}{\bar{p}} + C_3(s-s_o) \quad (4.16)$$

In order for the model to be applicable for both bare soil and for the presence of vegetation cover, the value of $C_1 = \frac{dJ}{ds}$ for the case of bare soil is also evaluated.

For bare soil, the value of J (Eagleson, 1978) leads to:

$$C_1 = \frac{dJ}{ds} = \left[-\sqrt{2} e^{-E} + [1 + \sqrt{2} E] e^{-E} + \Gamma\left(\frac{3}{2}, E\right) \sqrt{2} \cdot \frac{1}{2} \cdot E^{-\frac{1}{2}} \right. \\ \left. - (2E)^{\frac{1}{2}} (E^{\frac{1}{2}} e^{-E}) \right] \cdot \frac{2\beta\eta K(1)\psi(1)\Phi_e(d)(d+2)s_o^{d+1}}{\pi m e^{-\frac{2}{p}}} \quad (4.17)$$

According to the above linearizations, the conservation of water mass, Equation (4.1), can be written in the following finite difference form:

(i) Rain ($t \leq t_r$)

$$nZr \frac{\Delta s}{\Delta t} = i - y_s - y_g \quad (4.18)$$

Since surface runoff will start to be produced after time $t > t_o$ from the beginning of the storm, where t_o is the time when the surface gets saturated (Equation 3.7), we must account for y_g in Equation (4.18) only when $t_r > t > t_o$.

It also seems reasonable to assume that the percolation below the depth Z_r will not only be a function of the soil moisture s_k in the surface layer at time k but also of the soil moisture s_o below that layer. That is $y_g = f(s_k, s_o)$. In order to keep the equations simple, we will assume that y_g will vary with respect to the average value $\frac{s_k + s_o}{2}$.

Thus, finally we have:

For $t < t_o$

$$nZr \left(\frac{s_{k+1} - s_k}{\Delta t} \right) = i - \left[\bar{y}_g + C_3 \bar{p} \left(\frac{s_k + s_o}{2} - s_o \right) \right] \quad (4.19)$$

For $t > t_o$

$$nZr \left(\frac{s_{k+1} - s_k}{\Delta t} \right) = i - \left[\bar{y}_s + C_2 \bar{p} \left(s_k - s_o \right) \right] - \left[\bar{y}_g + C_3 \bar{p} \left(\frac{s_k + s_o}{2} \right) \right] \quad (4.20)$$

(ii) No rain (interstorm period) $t \leq t_b$

$$nZr \left(\frac{s_{k+1} - s_k}{\Delta t} \right) = - \left[\bar{e}_T + C_1 \bar{e}_p (s_k - s_o) \right] - \left[\bar{y}_g + C_3 \bar{p} \left(\frac{s_k + s_o}{2} - s_o \right) \right] \quad (4.21)$$

The limiting value for $e_T = \bar{e}_T + C_1 \bar{e}_p (s_k - s_o)$ will be the value of the potential rate of evapotranspiration e_p . That implies that e_T will be replaced by e_p until the time when the surface gets dry.

The above equations were solved explicitly with respect to s_{k+1} . The time step Δt was taken equal to 30 minutes, i.e., we update the soil moisture every 30 minutes. The time step was chosen to be of this order of magnitude both for reasons of numerical accuracy of the solutions and because this is the necessary time scale for conjunctive operation of the model with a GCM of the atmosphere. All other parameters appearing in Equations (4.19) through (4.21) are treated as known inputs in the model.

Two catchments were selected to test the model, Clinton, Massachusetts and Santa Paula, California. They represent two contrasting climates, the first corresponding to a humid and the second to a semi-arid region and have been well-studied elsewhere (Eagleson, 1978 a,b,c,d,e,f,g). The appropriate selection of parameters and necessary inputs in order to implement the model are presented in the next chapter.

CHAPTER 5

Selection of the Appropriate Model Parameters

5.1 Introduction

The parameters necessary to implement the model can be divided into the following categories:

a. Climatic Variables:

m_{p_A} = mean annual precipitation [cm]

m_{t_b} = mean time between storms [days]

m_{t_r} = mean storm duration [days]

m_T = average rainy season length [days]

κ = shape factor of gamma-distributed rainstorm depths

\bar{T}_a = average annual atmospheric temperature [$^{\circ}\text{C}$]

m_i = mean storm intensity [cm/day]

e_p = potential evapotranspiration rate [cm/day]

The values of m_{p_A} , m_{t_b} , m_{t_r} , m_i , m_T , and κ are derived using the statistical properties of the rainfall events (Eagleson 1978b). The value of \bar{T}_a is taken from measurements of the air temperature close to the surface during the year. The value of \bar{e}_p , as it was developed in Chapter 2, is a function of several climatic and surface characteristics. Here, it will be evaluated using a Penman-type equation. For the applications at Clinton, Massachusetts and Santa Paula, California, it will be set equal to its annual average value. In a later application, at Phoenix, Arizona this assumption will be relaxed and diurnal changes of e_p will be considered.

b. Soil parameters

Three independent soil parameters are used in the model. These are:

- n = effective porosity of the soil
k(1) = saturated intrinsic permeability [cm^2]
c = pore disconnectedness index.

By applying ecological optimality conditions (Eagleson 1982) it is possible, given the porosity, to estimate the appropriate values for k(1) and c of natural surfaces. Those conditions are described in paragraph (5.2).

c. Vegetation parameters

Vegetation is represented in the model by the percentage of vegetation cover M_o and the water use coefficient k_v . It will again be shown how the value of M_o is selected by applying ecological optimality hypotheses. Another way of obtaining M_o is through observations, sometimes by using remote sensing techniques. If this is the case, then that can help to determine more accurately the parameter k_v , as it will be shown later.

d. Surface layer thickness Z_r

The surface layer thickness Z_r is treated in the model as an independent variable, although we know that it is a function of the root zone depth, and the soil and climatic characteristics of the region. Since the exact value of this parameter is not known and the purpose of its existence is to provide us with a simple conceptual model of the physical process which accounts for some storage of water close to the surface, it will be possible to fit the value of this parameter either using available observations or solutions of more accurate numerical models. Sensitivity analysis will be performed in order to investigate the influence of Z_r on the various fluxes within the soil column, and to test the assumption of many investigators, that Z_r must be taken equal to 1m.

5.2 Ecological Optimality Hypotheses

Eagleson (1982) derived several equilibrium conditions, which he hypothesized to hold in the long-term for a natural, water-limited soil-vegetation system.

In a natural soil-vegetation system equilibrium stages can be considered to occur at different time scale.

In the short-term it is assumed that the system tends to minimize water-demand stress, so, the canopy density and the plant species will take such values that maximize the soil moisture. That implies that the following relations must hold for a given climate and soil:

$$\left(\frac{\partial s_o}{\partial M} \right)_{k_v} = 0 \quad , \quad M = M_o \quad (5.1)$$

$$\left(\frac{\partial s_o}{\partial k_v} \right)_M = 0 \quad , \quad k_v = k_{v_o} \quad (5.2)$$

where

s_o = average soil moisture concentration in the root zone

M_o = short-term equilibrium canopy density

k_{v_o} = short-term equilibrium plant coefficient

Equations (5.1) and (5.2) define the "complete vegetal equilibrium". It was shown by Eagleson [1982], that for canopy densities $M_o > 0.42$ complete equilibrium is not possible because Equation (5.2) cannot be satisfied. He further hypothesized that for a moist climate the canopy will always satisfy Equation (5.1) but that the species will only be in a quasi-equilibrium, so that the following condition is satisfied:

$$\left(\frac{\partial M_o}{\partial E} \right)_{k_v} = 0 \quad (5.3)$$

where

E = dimensionless climate-soil parameter

It was hypothesized that in long-term there is a synergistic symbiotic development of both the soil properties and the vegetation canopy which tends to maximize biomass production, B_p . For water limited systems, B_p will be proportional to the water utilization by the plants, i.e.,

$$B_p \sim M_o k_v \bar{e}_p \quad (5.4)$$

For a given climate and constant k_v , B_p is maximized, according to Equation (5.4), when M_o is maximized. The conditions for this equilibrium then, are:

$$\left(\frac{\partial M_o}{\partial c} \right)_{k(1)} = 0 \quad , \quad M_o = M_o^* \quad (5.5)$$

$$\left(\frac{\partial M_o}{\partial k(1)} \right)_c = 0 \quad , \quad M_o = M_o^* \quad (5.6)$$

The third soil property, the effective porosity n , is assumed constant during this optimization procedure.

For two contrasting climates, those of Clinton, Massachusetts and Santa Paula, California, and with the climatic and soil parameters given in Table 5.1 contours of constant M_o for different combinations of $k(1)$ and c were drawn. (Figure 2 and 3). Each contour corresponds also to a constant value of E and of the actual evapotranspiration E_{TA} . From those contours, the optimum value of the canopy density, M_o^* , can be derived. That peak value of M_o , defines a unique pair of values of $k(1)$ and c . Thus, under the previously developed hypotheses the only soil parameter that is needed to be known is the porosity n .

Eagleson and Tellers [1982] provide encouraging tests of the above hypotheses for different catchments. They also suggest algorithms for fitting

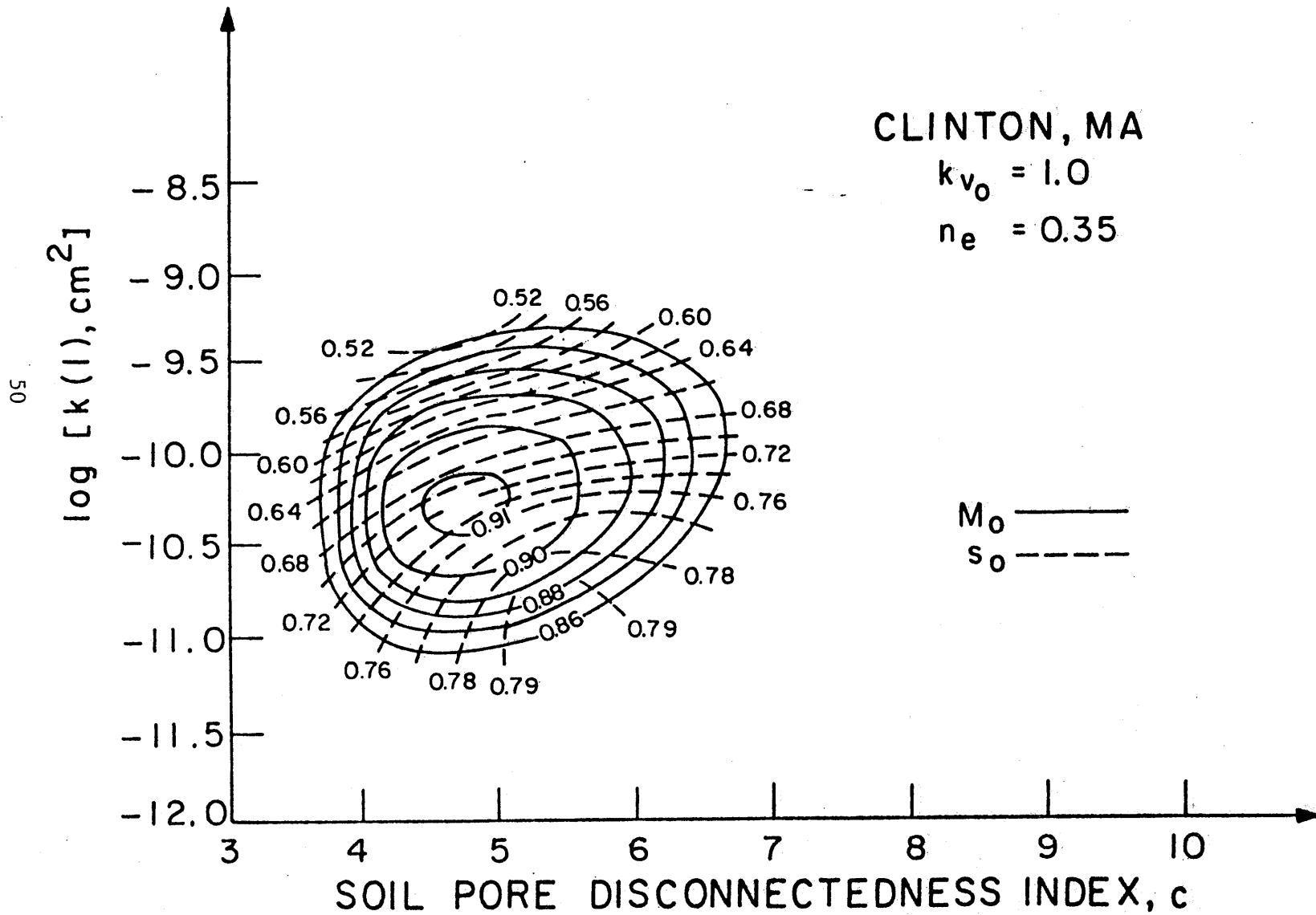


FIGURE 2 CLIMATIC CLIMAX SOIL-VEGETATION SYSTEM - CLINTON, MASSACHUSETTS
 EAGLESON, 1982

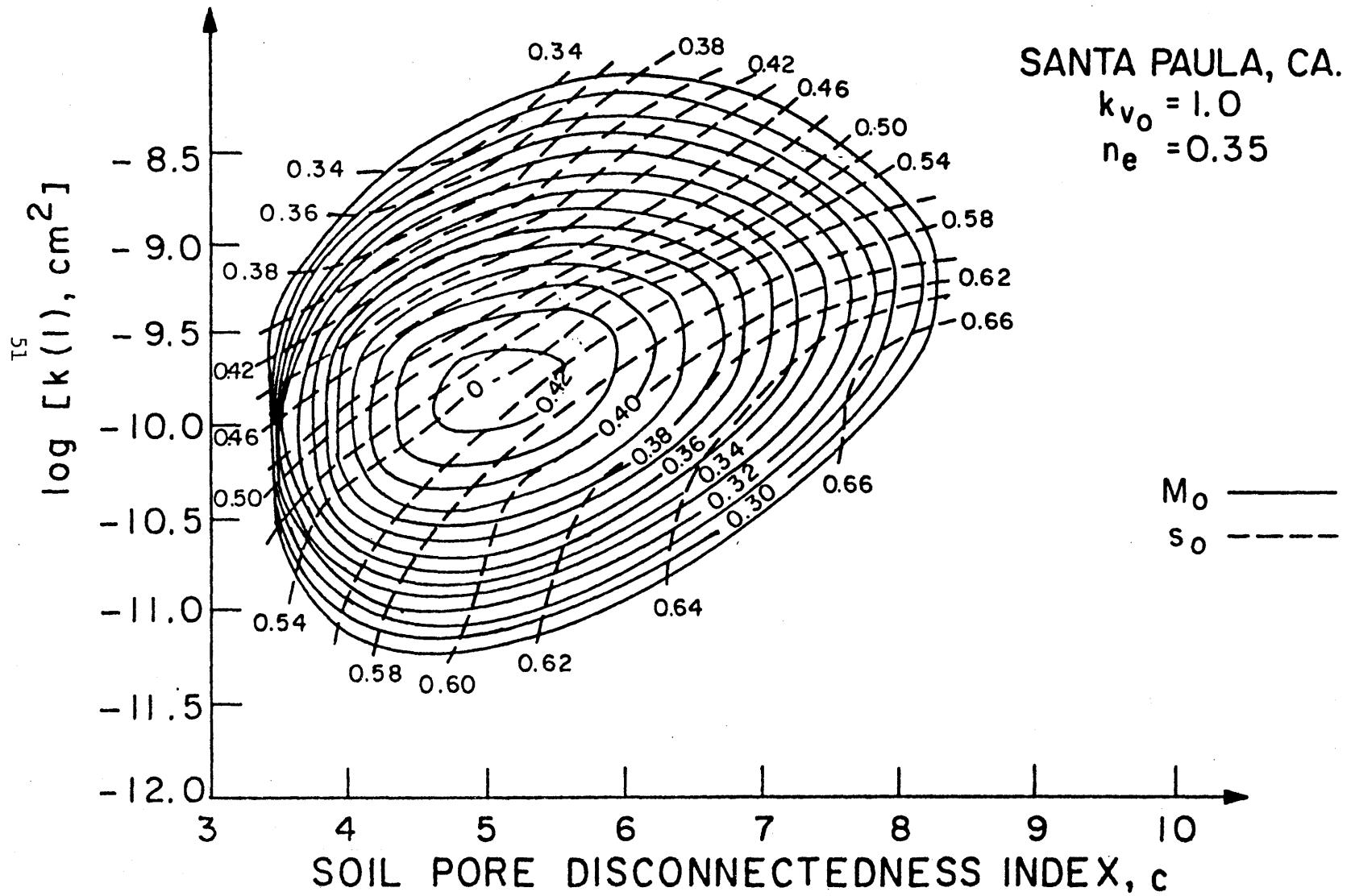


FIGURE 3 CLIMATIC CLIMAX SOIL-VEGETATION SYSTEM - SANTA PAULA, CALIFORNIA
 EAGLESON 1982

the values of k_v and n , if observations of the canopy density and the total water yield exist.

Also shown in Figure 2 and 3 are curves of constant s_o . It is noticed that the locus of optimum (maximum) s_o does not coincide with the peak value of M_o . The basic reason for that is that in the long-term evolution, the dominant factor is the maximization of the biomass production. Thus, although the system is locally optimized with respect to s_o , maximization of s_o is not the primary condition to be fulfilled. A more detailed discussion of this point is given by Eagleson [1982].

TABLE 5.1

Clinton, Massachusetts

M_o	=	0.912
\bar{e}_p	=	0.150 cm/day
m_{t_b}	=	3 days
m_{t_r}	=	0.32 days
m_τ	=	365 days
w/e_p	=	0
m_v	=	109
m_{p_A}	=	94 cm
k_v	=	1
\bar{T}_a	=	8.4°C
κ	=	0.50
λ	=	0.578
$k(1)$	=	$5.57 \times 10^{-11} \text{ cm}^2$
c	=	4.75

Santa Paula, California

M_o	=	0.424
\bar{e}_p	=	0.274 cm/day
m_{t_b}	=	10.42 days
m_{t_r}	=	1.43 days
m_τ	=	212 days
w/e_p	=	0
m_v	=	15.7
m_{p_a}	=	54 cm
k_v	=	1
\bar{T}_a	=	13.8°C
κ	=	0.25
λ	=	0.0732
$k(1)$	=	$12.27 \times 10^{-11} \text{ cm}^2$
c	=	5.25

[The values of M_o , $k(1)$, and c were set equal to those corresponding to peak climatic values, according to the vegetal equilibrium hypothesis and the ecological optimality hypothesis, as they are described by Eagleson (1982).]

CHAPTER 6

6.1 Simulation of the Rainfall Process

In order to test the model, rainfall inputs were generated, which possessed the statistical characteristics derived from historical records. Under the assumption of independently distributed rainfall depths, storm durations, and times between storms, we generated those variables with the following characteristics:

Storm depth h:

It was considered as Gamma distributed with parameters κ and λ . The corresponding pdf was

$$f_H(h) = \frac{\lambda(\lambda h)^{\kappa-1} e^{-\lambda h}}{\Gamma(\kappa)} \quad (6.1)$$

with $m_H = \kappa/\lambda$, $\sigma_H^2 = \kappa/(\lambda)^2$

Storm duration t_r :

It was taken as exponentially distributed with pdf of the form

$$f_{t_r}(t_r) = \delta e^{-\delta t_r}, \quad t_r > 0 \quad (6.2)$$

where

$$\delta = m_{t_r}^{-1}$$

Time between storms t_b :

It was also taken as exponentially distributed with pdf

$$f_{t_b}(t_b) = \beta e^{-\beta t_b}, \quad t_b > 0 \quad (6.3)$$

where

$$\beta = m_{t_b}^{-1}$$

The above distributions for h , t_r , and t_b were chosen, because it is shown by Eagleson [1978b] that they can adequately represent the rainfall process.

The generated variables, i.e., h , t_r , and t_b preserved the above-defined statistics. For their generation the IMSL library subroutine GGAMR was used. This subroutine was incorporated into the main program "Taylor. Fortran", which also calculates the statistics of the generated variables in order to check for consistency with the historical values. (Gamma and exponentially distributed variables, can both be generated with this subroutine, by making some slight modification of the parameters used.)

The storm intensity was assumed uniform during the rain and thus was derived just by dividing the value of the generated h with the corresponding value t_r . Since the storm magnitudes and storm durations were assumed independently distributed, the matching was performed arbitrarily by using the values of h and t_r in the sequence they were generated from the random number generator. Of course, such a matching could give rise to unrealistic values of i , in the extremes where independence is most invalid. However, at this stage, this fact will not be taken into account in testing the model, although its impact should be kept in mind during the interpretation of the results.

The statistics of the generated rainstorm characteristics for Clinton, Massachusetts and Santa Paula, California are presented in Table 6.1.

The observed differences are reasonable, since the generated variables which were tested, corresponded to many fewer events than the historical values derived from five years of observations. We also observe that the generated series at Clinton, Massachusetts gives an average storm depth considerably less than the average of five years, so we expect that to reflect in a smaller soil moisture on the average than the average annual soil moisture corresponding to five years of data.

TABLE 6.1

Clinton, Massachusetts		
	Historical (5 years)	Generated (1 year)
Storm depth	$E[h] = 0.86$	$E[h] = 0.73$
[cm]	$Var[h] = 1.50$	$Var[h] = 0.73$
Storm duration	$E[t_r] = 0.32$	$E[t_r] = 0.34$
[days]	$Var[t_r] = 0.10$	$Var[t_r] = 0.13$
Time between	$E[t_b] = 3$	$E[h] = 3.18$
[days]	$Var[t_r] = 9$	$Var[t_b] = 10.88$
Santa Paula, California		
	Historical (5 years)	Generated (1 year)
Storm depth	$E[h] = 3.41$	$E[h] = 3.83$
[cm]	$Var[h] = 46.65$	$Var[h] = 20.16$
Storm duration	$E[t_r] = 1.43$	$E[t_r] = 2.34$
[days]	$Var[t_r] = 2.04$	$Var[t_r] = 4.69$
Time between	$E[t_b] = 10.42$	$E[t_b] = 11.90$
[days]	$Var[t_b] = 108.57$	$Var[t_b] = 66.30$

CHAPTER 7

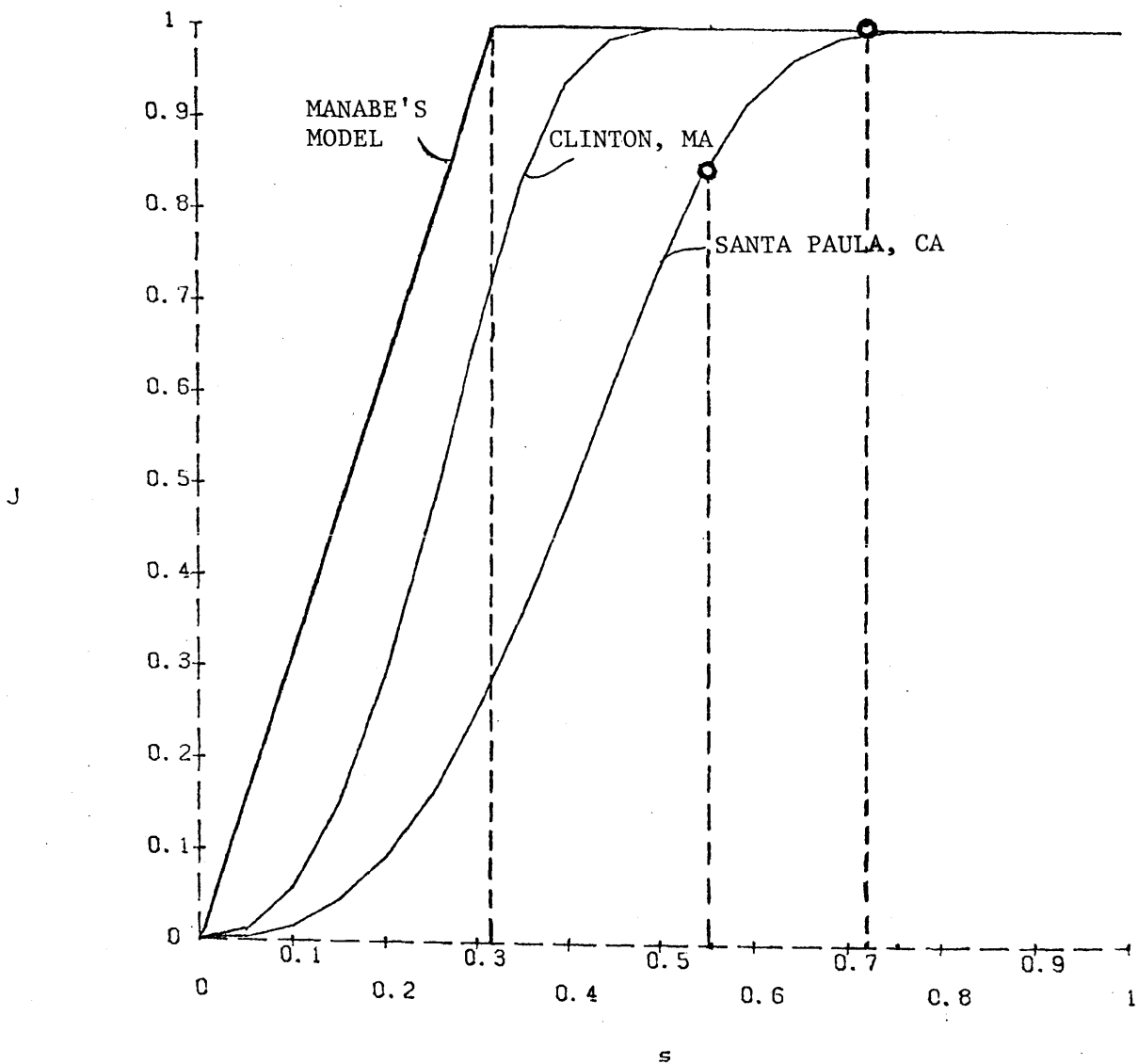
Presentation of Results

7.1 The Evapotranspiration, Surface Runoff, and Percolation Functions

Before applying the model described in Chapter 4 for simulating the soil-moisture concentration during the rainy season, it is essential to present the rate functions of evapotranspiration e_T , surface runoff y_s , and percolation y_g , which will be linearized around the average annual soil moisture, s_o .

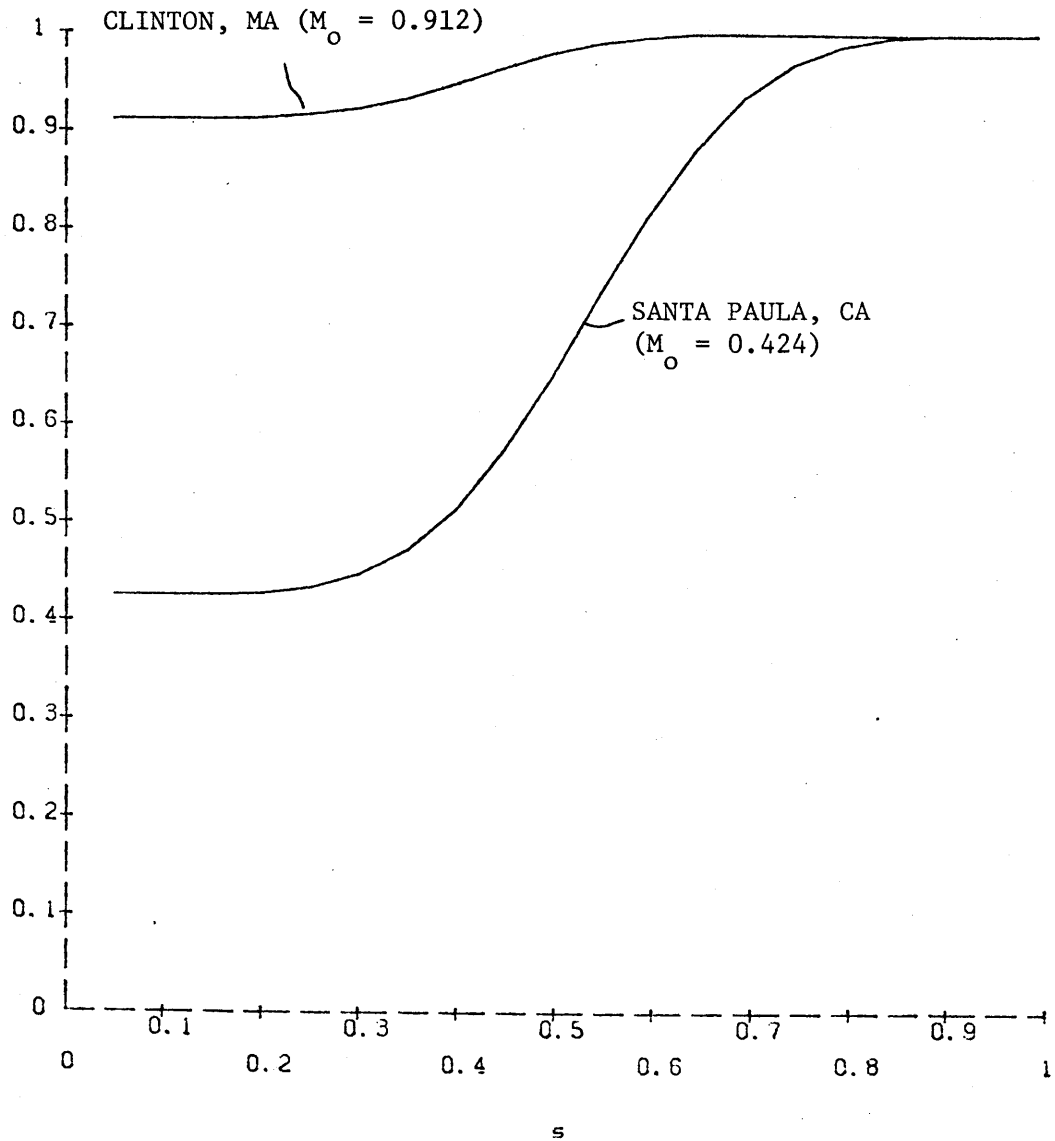
The actual evapotranspiration rate e_T is given by Equation(3.6), where it appears through the expression of evapotranspiration efficiency J , i.e., normalized with the value of the average annual (seasonal) potential evaporation rate \bar{e}_p . By using the climatic variables and the soil and vegetation parameters derived under climatic climax conditions and shown in Table 5.1, for the catchments of Clinton, Massachusetts and Santa Paula, California, the evapotranspiration efficiency J can be plotted as a function of the soil-moisture, s .

Figure 4 shows the $J(s)$ function for the bare soil case ($M_o = 0$) and Figure 5 shows $J(s)$ when the presence of vegetation is taken into account. Also, shown in Figure 4 is the evaporation efficiency function that is used by Manabe [1969] in his GCM. This follows a linear Budyko-Type parameterization for which $J = 1$ if $s > s_k$ and $J = \frac{s}{s_k}$ if $s < s_k$, where s_k is a critical value of s defined by $s_k = 0.75 \times s_{f_c}$ and s_{f_c} is the degree of soil saturation within a soil layer from the surface to 1m depth, corresponding to the field capacity θ_{f_c} . The value of the field capacity used in Manabe's General Circulation Model is held uniform over all areas of the Earth and is set equal to 15 cm.



Evapotranspiration Efficiency Function (M = 0)

FIGURE 4



Evapotranspiration Efficiency Function ($M = M_o$)

FIGURE 5

The difference in the $J(s)$ functions for Clinton and Santa Paula can be explained by the different climatic and soil properties of the two catchments. Clearly, Manabe's $J(s)$ function overestimates the evapotranspiration in both cases. In Figure 5 we observe the apparent influence of the vegetation cover M on the evaporation efficiency. In this case according to the assumptions developed in Chapter 3, the limiting value of e_T becomes $M_o k_v \bar{e}_p$. For the humid climate of Clinton, we expect that the deviations of s around the average annual value s_o , will not be very high and thus we will always operate in the region where $J = 1$. Otherwise, the linearization procedure described in Chapter 4 will not give accurate results. With a value of $s_o = 0.72$, as derived from the annual water balance, the above assumption is very reasonable for the humid climate. For the semi-arid climate of Santa Paula, we observe that the function $J(s)$ is very close to a linear form, for values of s in the neighborhood of $s_o = 0.55$. That implies, that the use of a linearized function of J around s_o , will give accurate results for this case. It must be pointed out that when a constant value of e_p is used, equal to its annual average value \bar{e}_p , then the actual evapotranspiration rate e_T will tend to \bar{e}_p as s increases above the value of s_o . Thus, this function is expected to give fairly accurate results when applied in a real case of successive rainy and dry periods, if e_p is supposed to be held constant. But if e_p is changing, as would be the case in reality, then the value of e_T obtained from this function will tend to the value of \bar{e}_p whenever the surface becomes saturated and not to the actual value of e_p . Thus, if a changing value of e_p is to be used, the time t_o from the beginning of the interstorm period until the surface gets dry must first be calculated. Before that time, evaporation will occur at the actual potential rate e_p and after that time control will pass to the soil and the value of e_T

obtained through the previously described linearization procedure will be used.

The average annual surface runoff rate \bar{y}_s is given by:

$$\bar{y}_s = e^{-G-2\sigma} \Gamma(\sigma+1) \sigma^{-\sigma} m_{PA} / m_{Vt} m_r \quad (7.1)$$

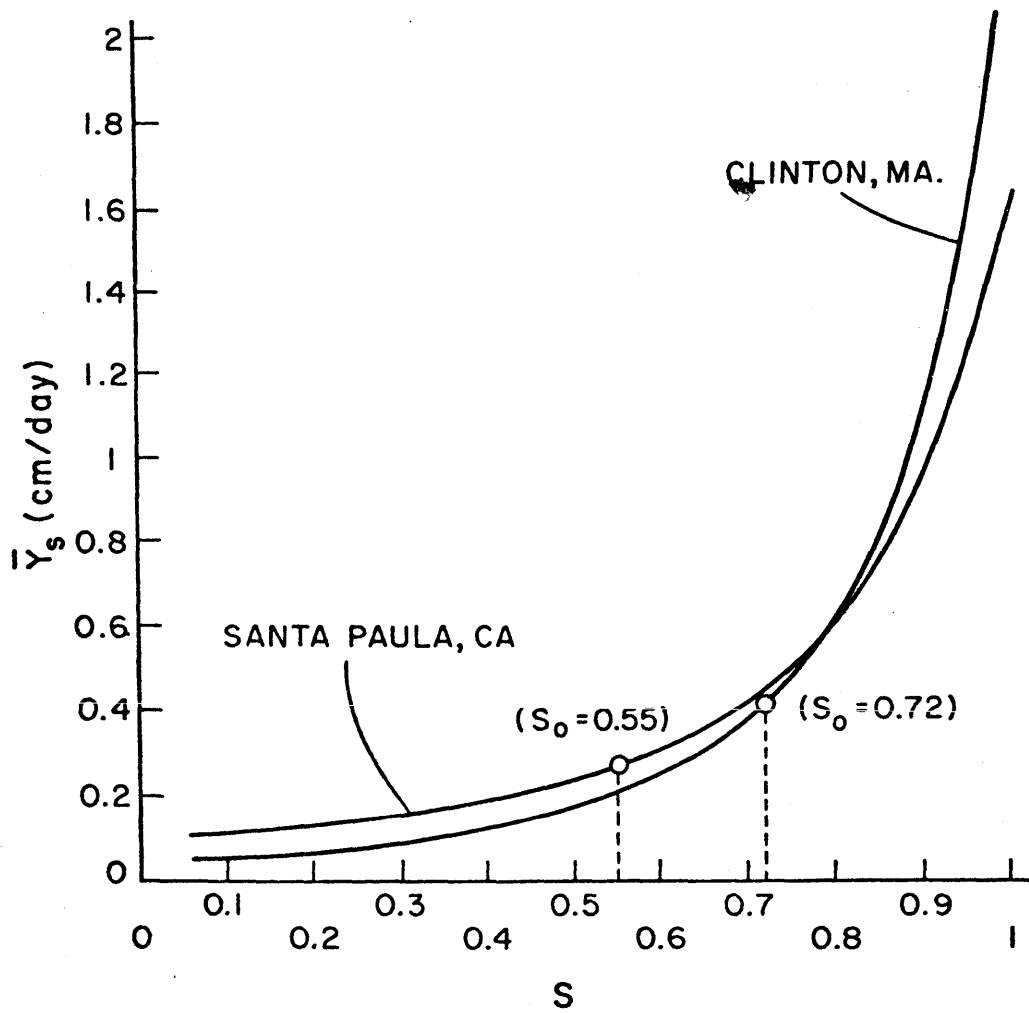
In Figure 6 \bar{y}_s is plotted versus s , for the catchments of Clinton and Santa Paula.

The average annual percolation rate \bar{y}_g to the water table is given by:

$$\bar{y}_g = K(1)s^c \quad (7.2)$$

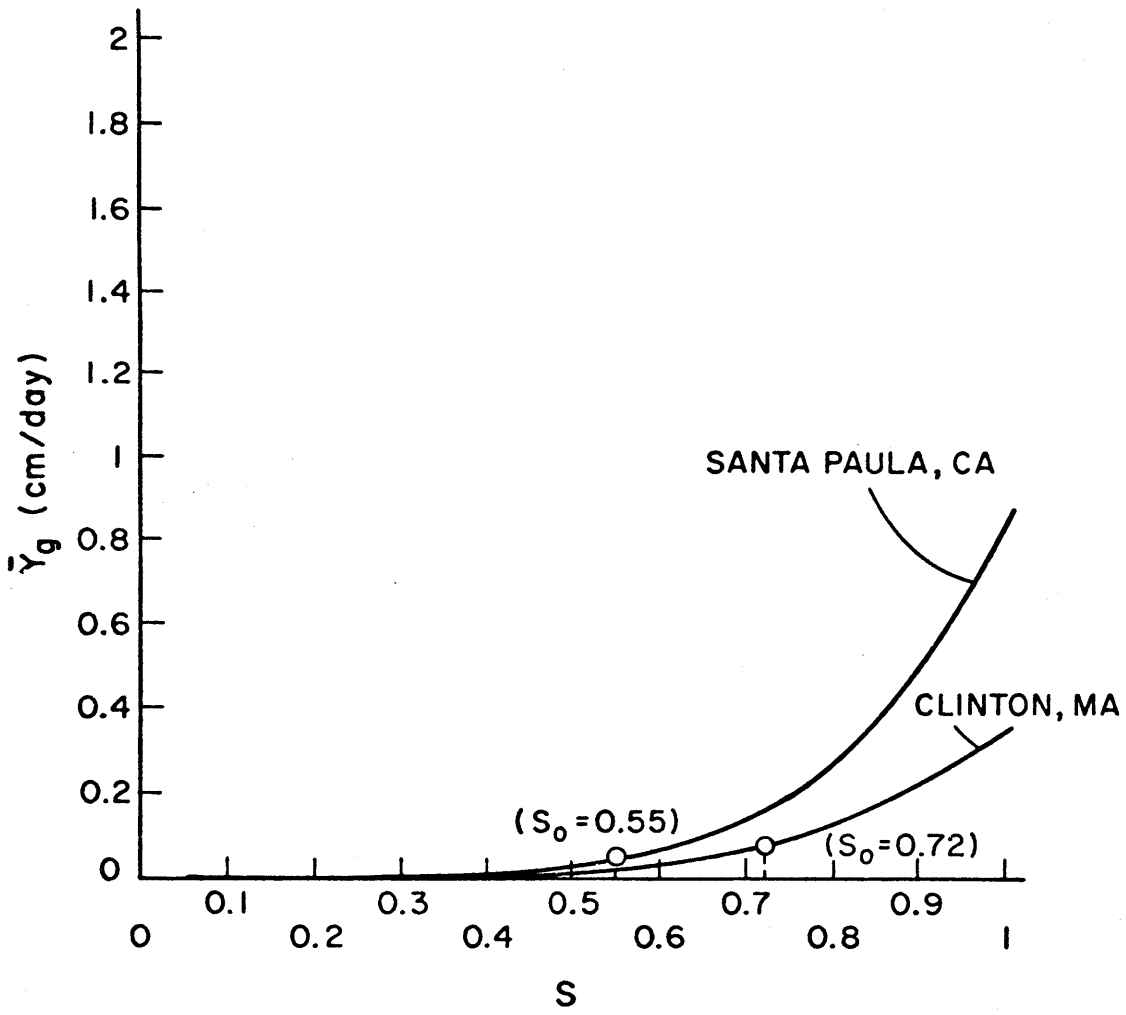
The function \bar{y}_g versus s is shown in Figure 7 for both Clinton and Santa Paula.

The functions $\bar{y}_s(s)$ and $\bar{y}_g(s)$ indicate high non-linearities between those fluxes and the soil moisture s . Thus, we must expect that a linearization around the corresponding average soil moisture s_0 , for each climate, can introduce errors in the estimation of those rates, especially when the deviations from the average value become high. This fact should be considered with attention to the interpretation of the results. That is, since those functions appear in this case to be convex, we expect to underestimate the surface runoff and percolation rates, whenever $s > s_0$ and overestimate them when $s < s_0$.



Surface Runoff Function $y_s(s)$

FIGURE 6



Groundwater Runoff Function $y_s(s)$

FIGURE 7

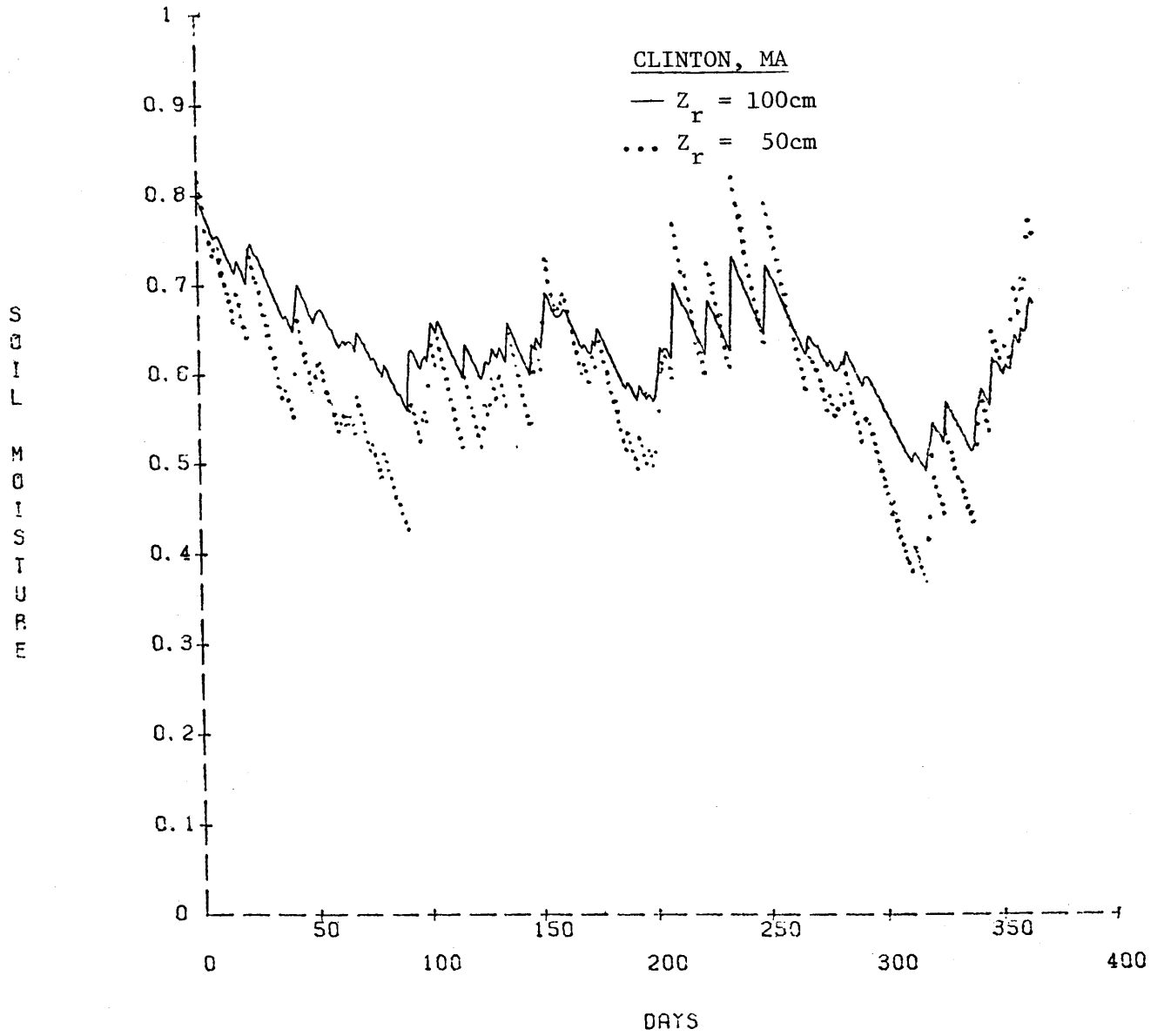
7.2 Simulation of Soil-Moisture Concentration During the Rainy Season Using

a Constant Value of $e_p = \bar{e}_p$

Equations (4.14) and (4.16) were solved for each time step ($\Delta t = 30$ minutes), with respect to s_{k+1} , using the generated rain storm events. The depth of the surface layer Z_r which accounts for storage was treated as an independent variable, i.e., many simulation runs were performed with different values of Z_r in order to observe the sensitivity of the fluxes with respect to that parameter. The capillary rise from the water table was taken equal to zero, assuming that the water table was deep enough that it did not have any impact on the fluxes occurring close to the surface. The climate and soil properties for Clinton and Santa Paula were those presented in Table 5.1 which were derived using ecological optimality hypotheses (Eagleson 1982).

The computer program named "TAYLOR.FORTRAN" was set up to perform a simulation of the soil-moisture concentration in the surface layer. A complete description of this program is given in Appendix 2.

The soil-moisture concentration, s , as a function of time, for Clinton, Massachusetts is shown in Figure 8. Two different cases are presented; one with $Z_r = 100$ cm and one with $Z_r = 50$ cm. As is expected for the case where Z_r is smaller, the soil moisture fluctuates over a larger range. The results shown in Figure 9 correspond to a vegetation cover $M_0 = 0.912$, which is the climatic climax value (Eagleson and Tellers, 1982). When bare soil was assumed ($M = 0$), there was no change in the results, because in the humid climate of Clinton, evaporation from the bare soil occurs at the potential level (climate controlled) and because we have taken $k_v = 1$, its optimum value (Eagleson and Tellers, 1982).

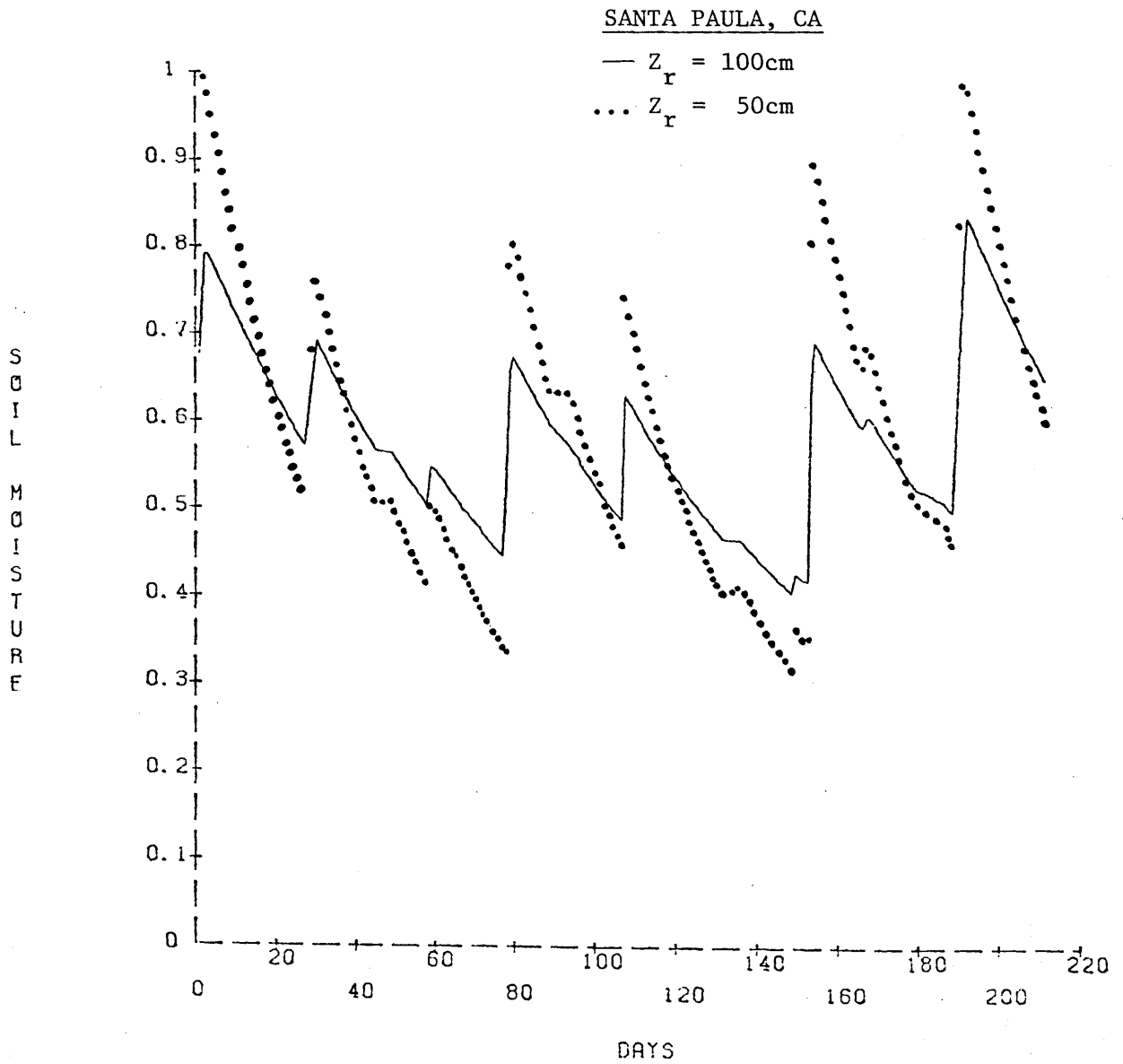


Simulation of Soil Moisture During the Rainy Season
 (Clinton, Massachusetts)

FIGURE 8

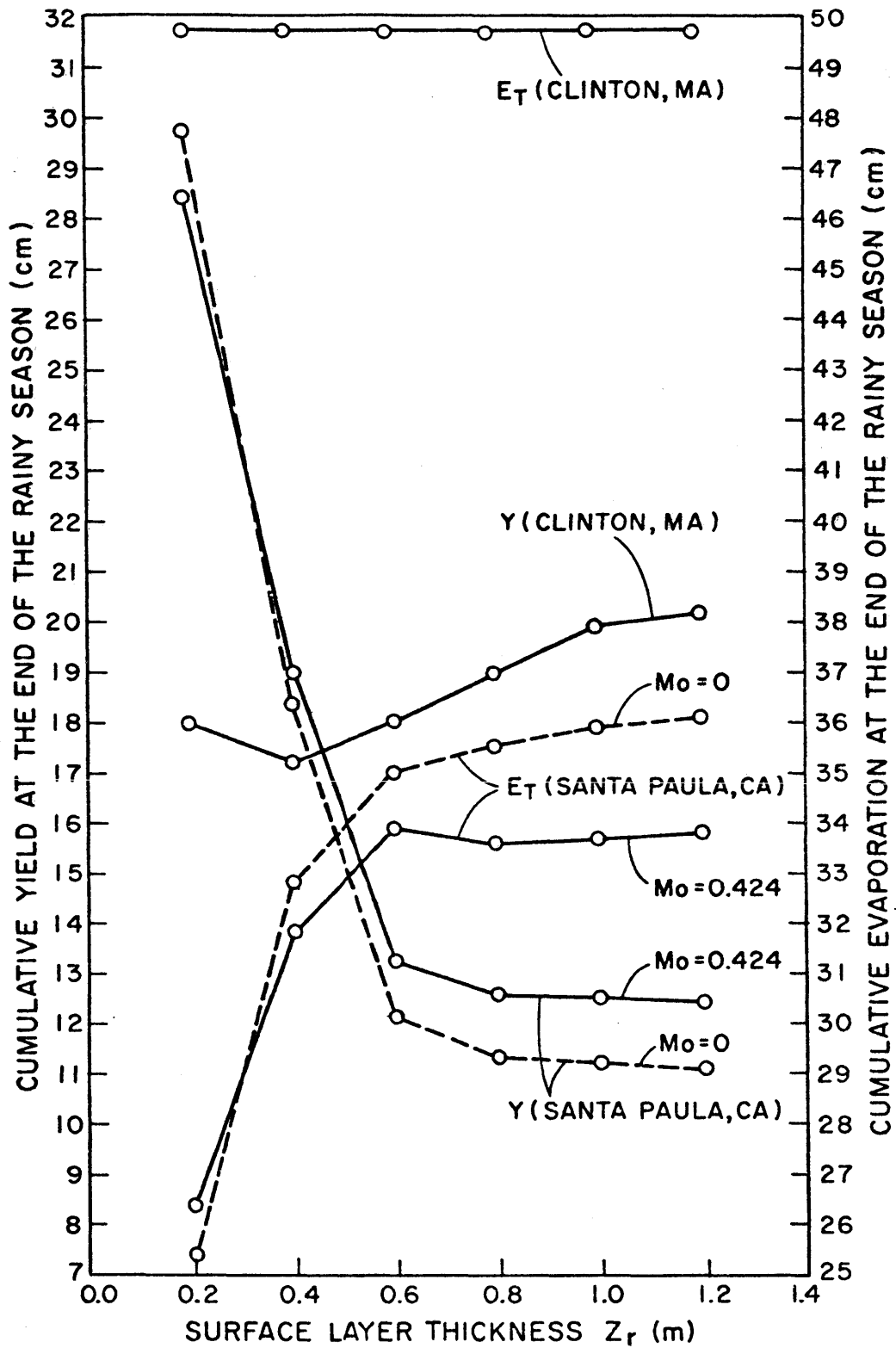
Analogous results of s versus time for Santa Paula, California and $Z_r = 100$ cm and $Z_r = 50$ cm, are shown in Figure 9. We observe that at Santa Paula we have larger deviations of s around the mean s_0 compared to those at Clinton. This is due to the much longer interstorm periods and longer storm durations of the climate of Santa Paula. The results shown in Figure 10 correspond to a vegetation cover $M_0 = 0.424$ (optimum value). When M was set equal to zero (bare soil), small differences occurred in the soil-moisture concentration. This was due to the fact that here also the evaporation from the bare soil is, on the average, rather high ($J(s_0) = 0.84$) and again $k_v = 1$.

A sensitivity analysis was performed for the humid climate of Clinton and the semi-arid climate of Santa Paula, with respect to the value of the parameter Z_r . The results are shown in Figure 10. The horizontal axis corresponds to values of Z_r ranging from 20 cm to 120 cm. On the vertical axis, the cumulative yield and cumulative evaporation at the end of the rainy season are plotted. For Santa Paula, California, it is interesting to observe that there is a range of values of Z_r from approximately 60-120 cm, where those fluxes are insensitive to the value of Z_r . When Z_r becomes small enough, evaporation is rapidly reduced. This is due to the fact that soil moisture is exhausted very fast during the interstorm period, the surface becomes dry faster and control passes to the soil earlier than before. On the contrary, yield increases rapidly with small values of Z_r , because in that case, during the rain, the soil-moisture concentration in the surface layer increases very fast and the surface becomes saturated at earlier times. Thus, surface runoff is produced more frequently and at earlier times during the rain.



Simulation of Soil Moisture During the Rainy Season
 (Santa Paula, California)

FIGURE 9



Sensitivity of Fluxes to Surface Layer Thickness

FIGURE 10

For Clinton, Massachusetts, the cumulative yield does not seem to become very sensitive to the value of Z_r , when the latter becomes small. For values of Z_r ranging from 0.4-1m, there is a maximum change of 3cm in the cumulative yield. The rate of change becomes much smaller when Z_r exceeds 1m. Cumulative evaporation was found to remain constant for all values of Z_r , indicating that the exfiltration process was always under climate control. At this point, it must be noted that, because of the model's structure, this sensitivity analysis becomes invalid for the humid climate of Clinton when Z_r is low and the value of s is such that control must pass to the soil. That is, the linearization around the value of the average annual soil moisture s_0 , is not valid in this case of $e_T \ll e_p$. However, for a humid climate, we can say apriori that Z_r should not be very low and so assume that soil control does not occur. Otherwise, it would be necessary to change the linearization procedure, and thus reduce the general applicability of the model.

It must be noted that in all cases examined for both climates, the moisture in the surface layer was never completely exhausted. It would be exhausted however, if even smaller values of Z_r are assumed. However, such Z_r are physically unrealistic because Z_r is defined to include all exchangeable moisture.

We also observe that, because of earlier passage to soil-control when $M \neq 0$, the cumulative evaporation is greater when $M = 0$, for most values of Z_r .

7.3 Comparison With A Numerical Model

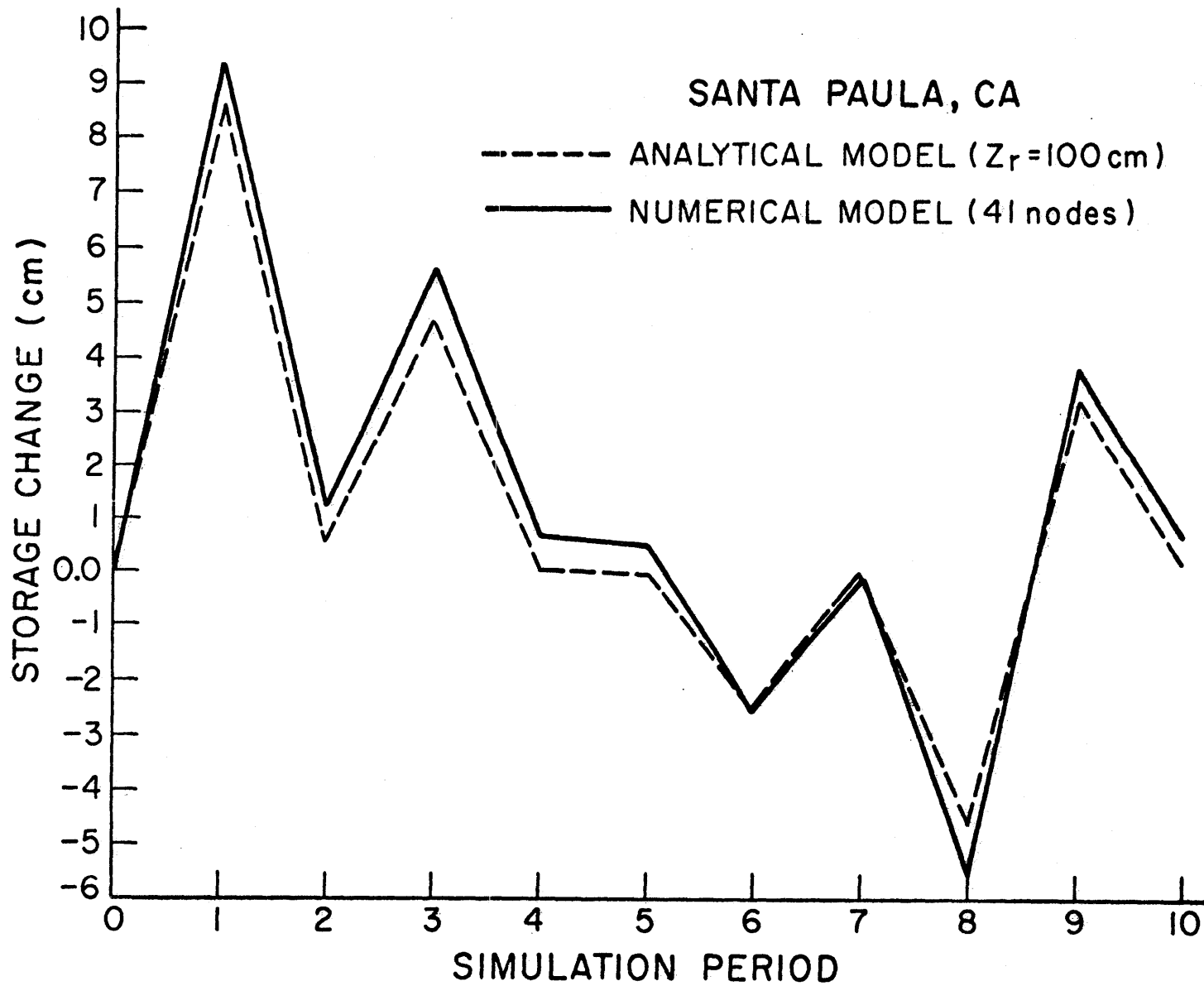
In order to test the predictive capability of the model developed in this study, the soil-moisture concentration and the water fluxes obtained from it, were compared to those obtained by an "exact" numerical model. The numerical model used was that developed by Milly and Eagleson [1980]. This model assumes a one-dimensional representation of the physical system and solves the coupled, non-linear partial differential equations governing mass and heat transport in the soil, using the Galerkin finite element method. In the present comparison, an isothermal version of the model was applied. The vertical soil column was taken equal to 5m and the influence of the water table was considered to be negligible. A constant flux ($K(\theta_0) = \text{constant}$) boundary condition was assumed at the bottom. The surface boundary condition was changed according to the surface moisture state. During precipitation, infiltration takes place at the precipitation rate, until the soil surface reaches saturation. After that happens, ponding of water on the surface occurs, thus producing surface runoff. During evaporation, the evaporation rate is equal to the potential value until the surface becomes completely dry and control passes to the soil. After this time, evaporation proceeds according to the exfiltration capacity of the soil. The values for the precipitation intensities, storm durations, and interstorm periods used were those obtained from the simulated rainstorm events, as described in Chapter 6. The value of the potential evapotranspiration was assumed constant throughout the simulation period and equal to it's annual average value, and thus, as discussed in Section 7.1 it was not necessary to calculate a time t_0 during the evaporation period.

The computer program SPLASH.FORTRAN developed by Milly [1980] was used in order to obtain the numerical solution. Many runs were performed, varying

the number of finite elements within the soil column and several other parameters, in order to achieve convergence of results. This procedure is described with more details in Appendix 2. The results from this comparison are shown in Figure 11-16, and correspond to solutions of the numerical model where convergence was achieved. Figures 11-13 show the storage change, the total yield (surface runoff and percolation) and evaporation flux respectively, for Santa Paula, California and for 10 consecutive simulation periods. Each simulation period corresponds to either a storm or an interstorm period, with intensities and durations as generated by the procedure described in Chapter 6. The storage change represents the deviation from the initial soil-moisture concentration. From the results of the numerical model, it was found that the surface became dry at the eighth simulation period which implies that control passed to the soil at that time.

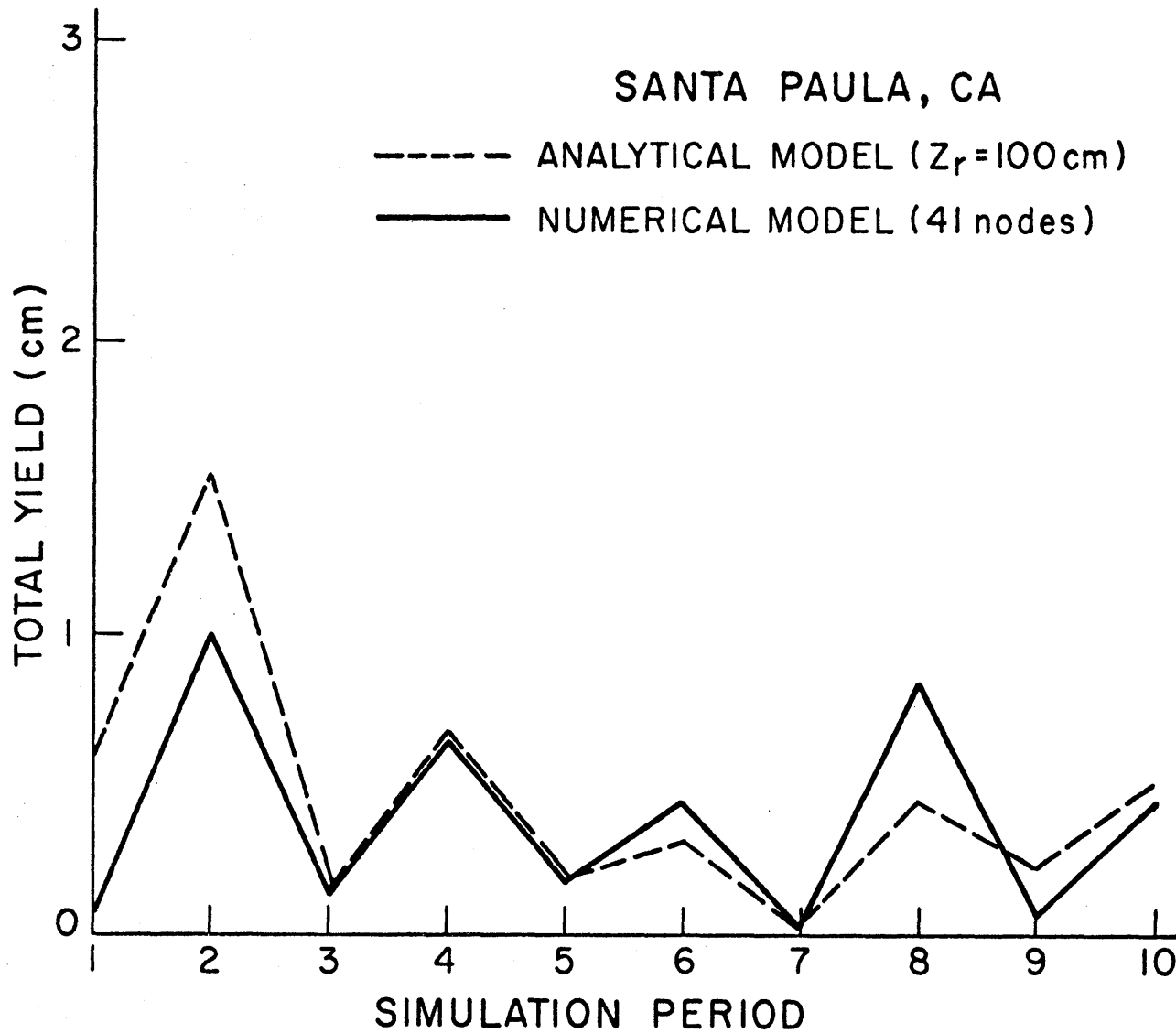
It is observed that the differences between the two models are not big and never exceed 1 cm of storage. The analytical model follows the numerical solution very faithfully. The water fluxes outside the surface layer are shown in Figure 12. Again, the differences between the two models are very small. The evaporation flux is shown in Figure 13. The differences here do not exceed 0.5 cm.

Figure 14-16 show the same comparison for Clinton, Massachusetts, and for 20 simulation periods, generated as discussed before. From Figure 14, we observe that the storage change is consistently underestimated by the analytical model, but again the differences between the two are relatively small and never exceed 0.6 cm of storage. In Figure 15, the total yield at each simulation period is plotted and the agreement between the two models is considered as very satisfactory. Evaporation fluxes are shown in Figure 16. For the humid climate



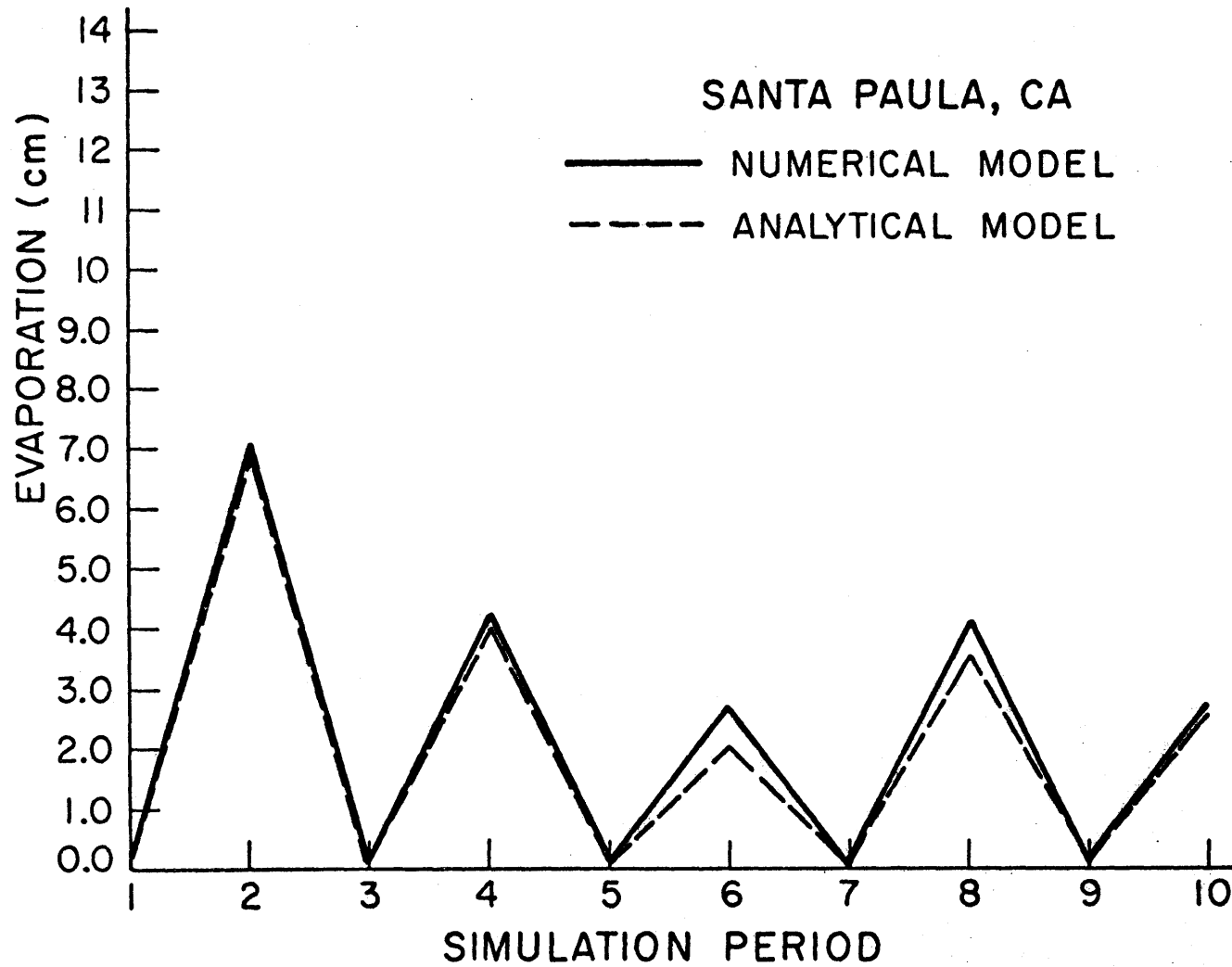
Comparison of Storage Change Produced by the Analytical and Numerical Model
(Santa Paula, California)

FIGURE 11



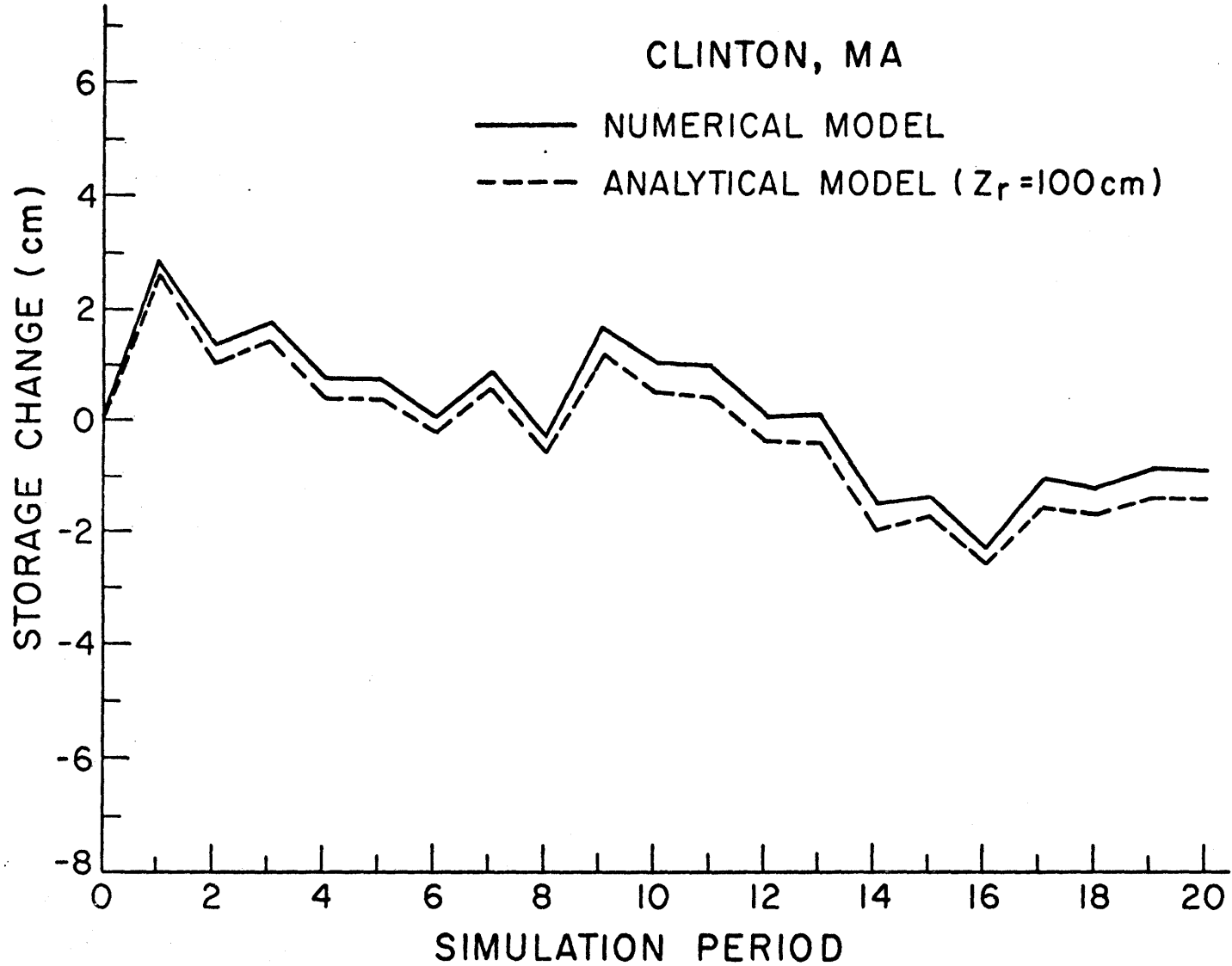
Comparison of Total Yield Produced by the Analytical and Numerical Model
(Santa Paula, California)

FIGURE 12



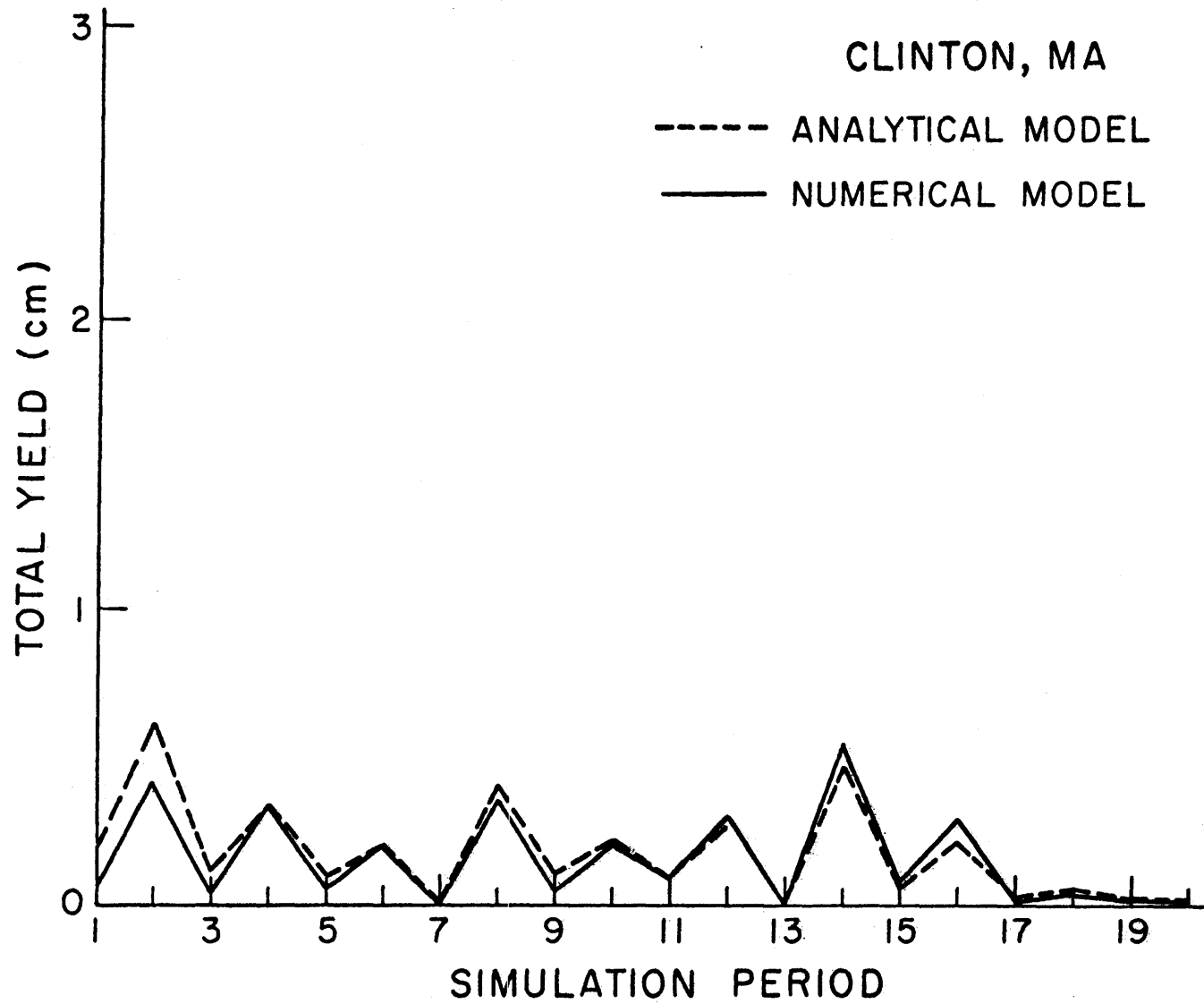
Comparison of Evaporation Produced by the Analytical and Numerical Model
(Santa Paula, California)

FIGURE 13



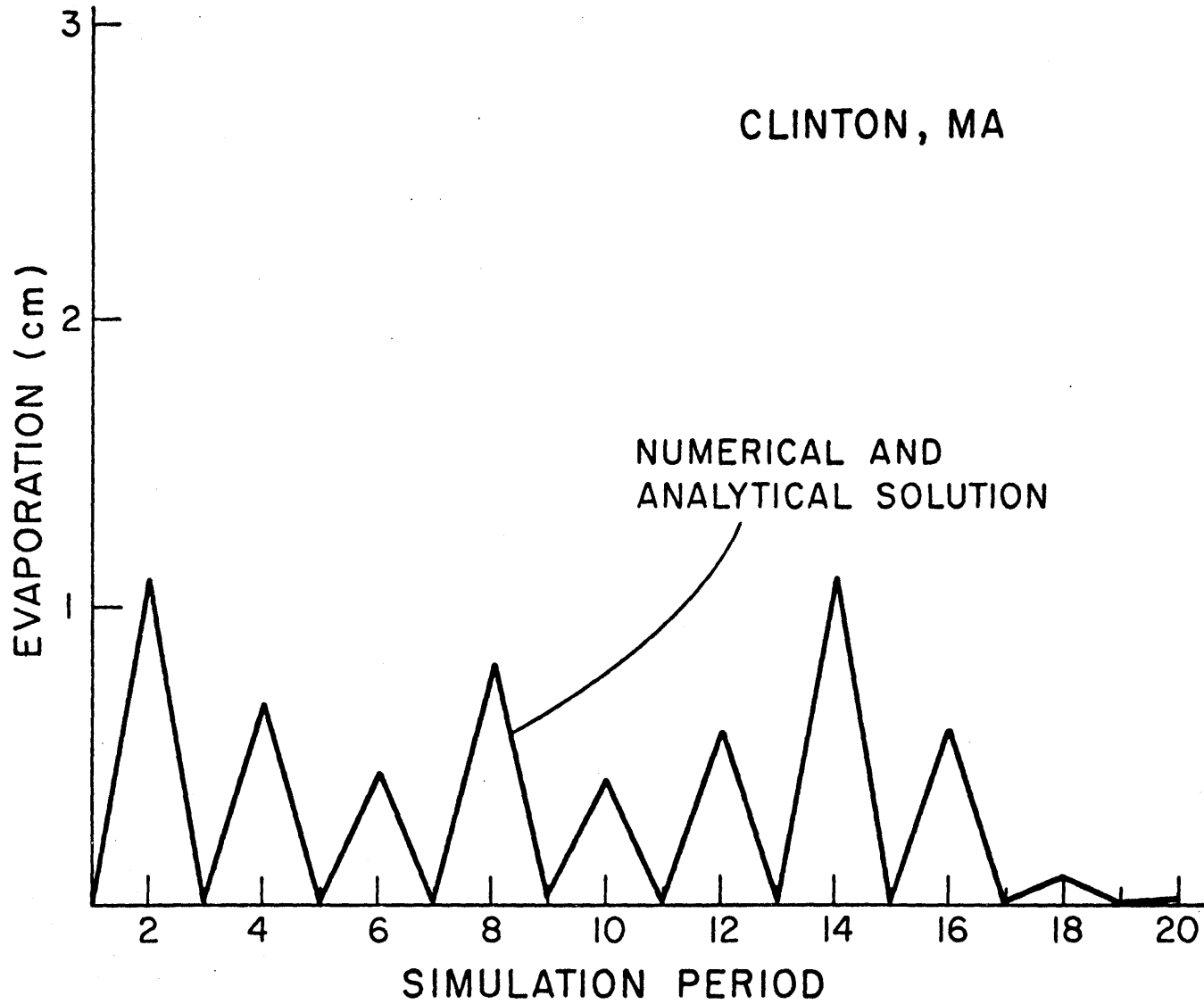
Comparison of Storage Change Produced by the Analytical and Numerical Model
(Clinton, Massachusetts)

FIGURE 14



Comparison of Total Yield Produced by the Analytical and Numerical Model
(Clinton, Massachusetts)

FIGURE 15



Comparison of Evaporation Produced by the Analytical and Numerical Model (Clinton, Massachusetts)

FIGURE 16

of Clinton, evaporation was always at the potential level and thus there is no difference between the two models. Thus, all differences in storage change can be explained by the differences occurring in the prediction of the yield.

In general, it should be noted that the solution obtained by the analytical model is in very satisfactory agreement with the numerical solution for both climates. Of course, it must be kept in mind that the tested version of the numerical model was a simplified one, since isothermal conditions were assumed.

7.4 Comparison with Manabe's [1969] Parameterization

Manabe's [1969] landsurface parameterization was also compared with the model developed in this study.

Manabe [1969] uses the concept of field capacity s_{fc} in his soil-moisture model. He assumes a surface layer of 1m and defines a critical value of soil-moisture s_k given by: $s_k = 0.75 \times s_{fc}$. Then he assumes the following equations to hold for the water and vapor fluxes at the surface:

i. Evaporation

$$\text{if } s > s_k, e_T = e_p$$

$$\text{if } s < s_k, e_T = e_p \cdot \frac{s}{s_k}$$

where

e_p is estimated from an aerodynamic type equation

ii. Soil moisture

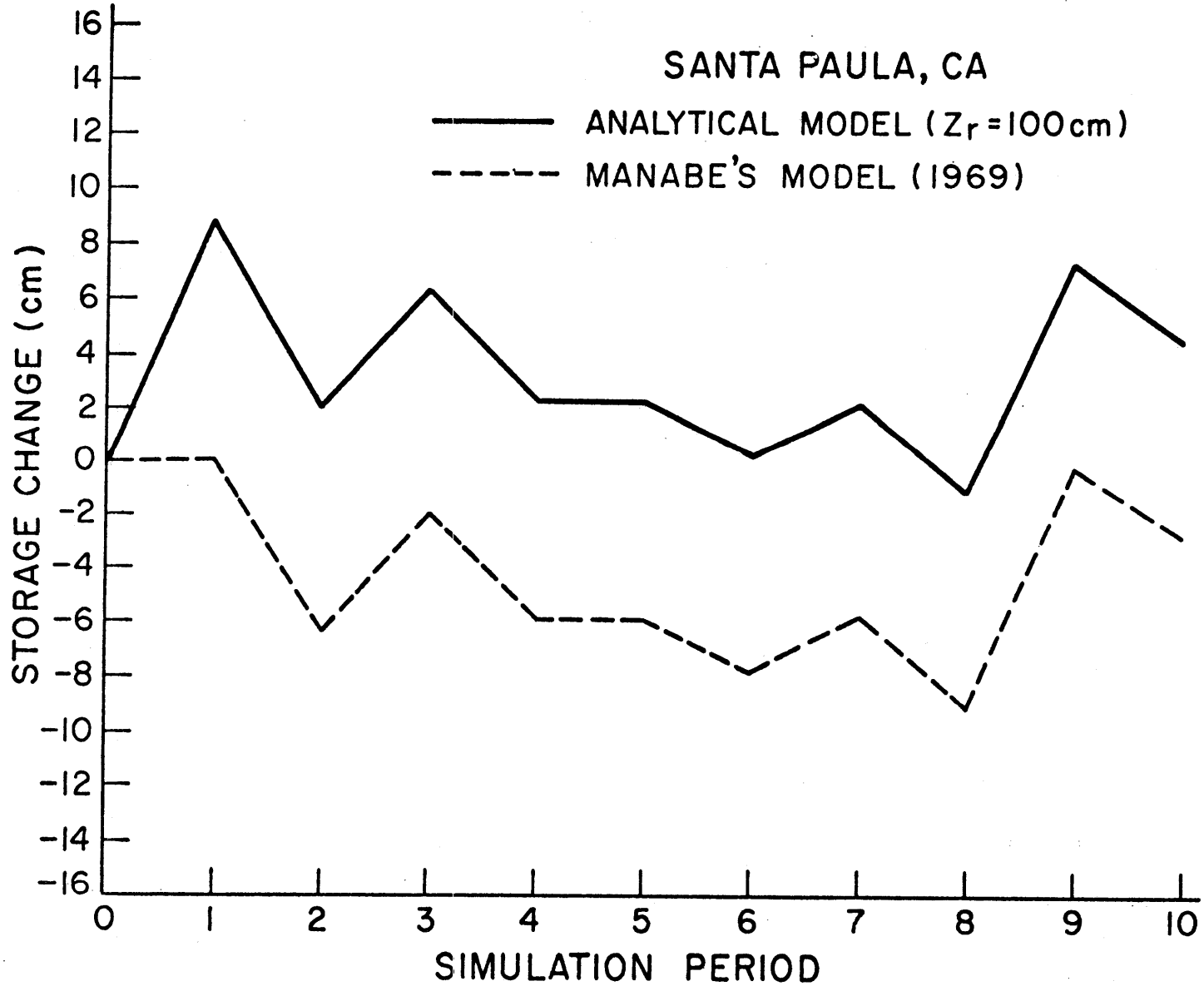
$$\text{if } s = s_{fc} \text{ and } i > e_p, \frac{\partial s}{\partial t} = 0 \text{ and } y_s = i - e_p$$

$$\text{and if } s < s_{fc}, \frac{\partial s}{\partial t} = i - e_T$$

The value of the field capacity chosen by Manabe for all applications was 15cm, which for a soil layer of 1m and a porosity of 0.35 corresponds to a soil-moisture concentration given by $s_{fc} = 0.42$.

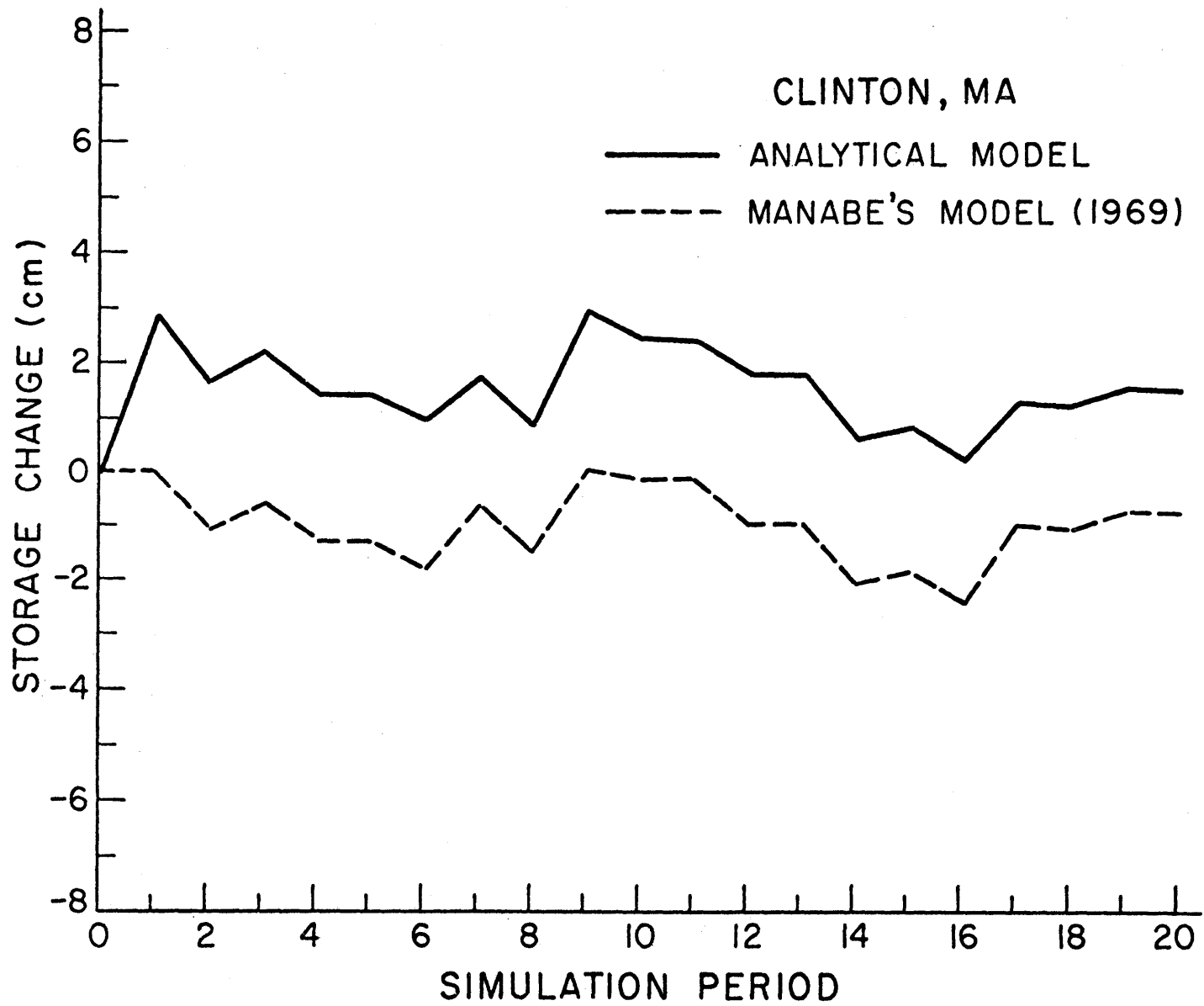
Using the same initial condition ($\theta = \theta_{fc}$) for both models, the storage change versus the simulation period, is shown in Figures 17 and 18 for Santa Paula, California and Clinton, Massachusetts. It is observed that there is a big difference between the two, which is on the order of 4cm for Santa Paula and 3cm for Clinton. Since the first simulation period corresponds to a storm and the initial condition of soil moisture is set equal to the field capacity, it is expected that Manabe's model will not produce a storage change during that period because according to his assumption, soil moisture cannot exceed the value of field capacity. If the first simulation period was an interstorm period, the storage changes produced by both models would not have so much difference. But big differences in storage will occur later on, when a precipitation event comes and soil-moisture reaches the value of the field capacity.

Since good agreement between the presently developed analytical model and the "exact" numerical model has already been established, it appears that Manabe's model does not represent the system very well. His model fails to capture the time variations of yield. This is shown for Clinton, Massachusetts in Figure 19. Values of the yield for Santa Paula obtained using Manabe's model are not shown graphically here. It was found, however, that a total yield of 8.7 cm was predicted for Santa Paula during the first simulation period by this model, while the yield was zero for all other simulation periods. As is shown in Figure 12, this is much different from the value predicted by both the numerical model and the analytical model developed here. Better results could possibly be obtained if a different value for the field capacity was chosen for Manabe's model, but what means can be used to evaluate this field capacity a priori?



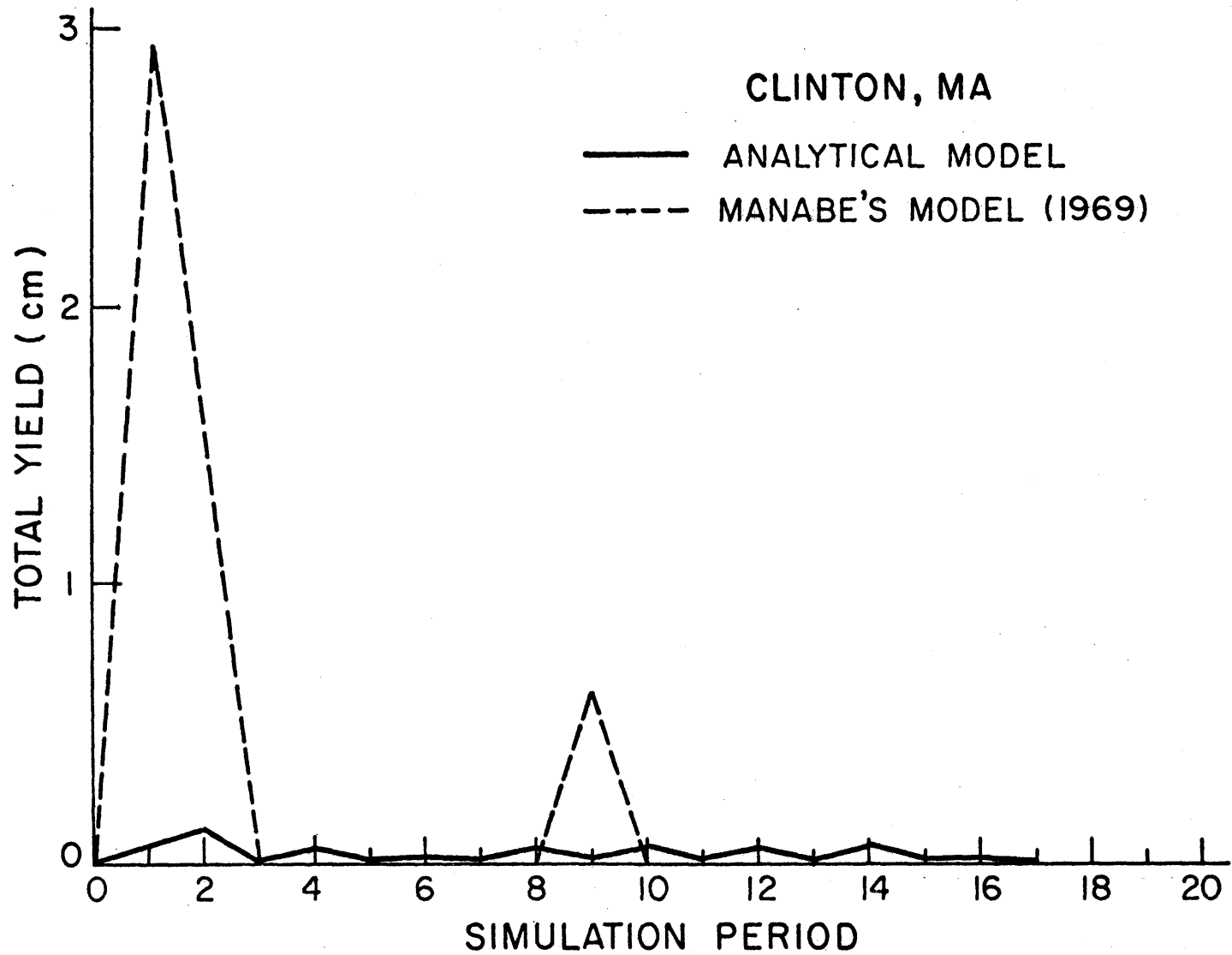
Comparison of Storage Change Produced by Manabe's Model and the Analytical Model (Santa Paula, California)

FIGURE 17



Comparison of Storage Change Produced by Manabe's Model and the Analytical Model
(Clinton, Massachusetts)

FIGURE 18



Comparison of Total Yield Produced by the Analytical and Manabe's Model
(Clinton, Massachusetts)

FIGURE 19

In general, the analytical model suggested in this study seems to be an improvement to the landsurface parameterization, mainly because it is simple, physically based and gives consistent and accurate results when compared to numerical solutions.

7.5 Soil Moisture Simulation with Changing Value of e_p

The model was also tested with real measurements of soil-moisture concentrations obtained from an experimental field at Phoenix Airport, Arizona. Values of the meteorological variables were available every half-hour, so that it was possible to estimate a changing value of e_p , using either a Penman-type equation or an aerodynamic equation. More precisely, the following measured data were available: Net radiation R_n at the surface, Air Temperature T_a , wind speed U_a , and vapor pressure e_o at screen height, surface temperature T_g at depth of 1 cm and average soil-moisture concentration in three layers below the surface (from 0 - 10cm, from 10 - 50cm, and from 50 - 100cm). The data corresponded to seven days of measurements from 5 March - 11 March, 1971. Details of the experimental field and measurement procedures are given by Jackson [1976]. Briefly, the soil consisted of Adelanto Loam, was reasonably uniform to about 100cm and had been cultivated numerous times during past years. The soil properties for the Adelanto Loam and the climatic variables at Phoenix Airport, are given on Table 7.1. A graph of hydraulic conductivity and diffusivity as a function of soil moisture θ is given by Jackson [1976]. Before the experiment took place, the field was irrigated and during the seven-day period of measurements, no precipitation was measured by rain gages at the Phoenix Airport, although some traces did occur.

In order to compare the results of the model with the measured values of soil-moisture, the latter were averaged over the 1m surface layer depth.

TABLE 7.1

Phoenix Airport - Arizona

\bar{e}_p	=	0.263 cm/day
m_{t_b}	=	7.27 days
m_{t_r}	=	0.11 days
m_t	=	365 days
κ	=	0.50
w/\bar{e}_p	\approx	0
\bar{T}_a	=	21.3 °C
m_v	=	45
m_{p_A}	=	19.05 cm
n	=	0.35 (assumed)
$k(1)$	=	$2.68 \times 10^{-9} \text{ cm}^2$
c	=	6.5

[The climatic variables shown in this table were derived by using the computer programs HODCOP and RAINSTAT developed by Restrepo and Eagleson (1978) for the interpretation and analysis of NOAA hourly precipitation data tapes. The soil properties for the Adelanto loam are given by Jackson (1965, 1979) and Mualem (1976).]

The value of the potential evaporation rate e_p was first estimated from a Penman-type equation, as described in Chapter 2, where the surface heat flux was neglected and the surface roughness was taken equal to 0.03cm.

As is also mentioned by Jackson [1976], the surface became dry after the fourth day of the experiment. This implies that after that time, flux control passed to the soil. Since the model used accounts only for soil moisture within the bulk volume and since it uses an evaporation efficiency function derived using the value of the annual (or seasonal) average evapotranspiration rate \bar{e}_p , it cannot accurately locate this change, especially when e_p is much higher than \bar{e}_p , as it was also discussed in Section 7.1. To surmount this problem, it was necessary to calculate a priori the average time t_o , until the surface becomes dry. This time is given by: (Eagleson, 1978d)

$$t_o = \frac{S_e^2}{2\bar{e}_p^2} \quad (7.3)$$

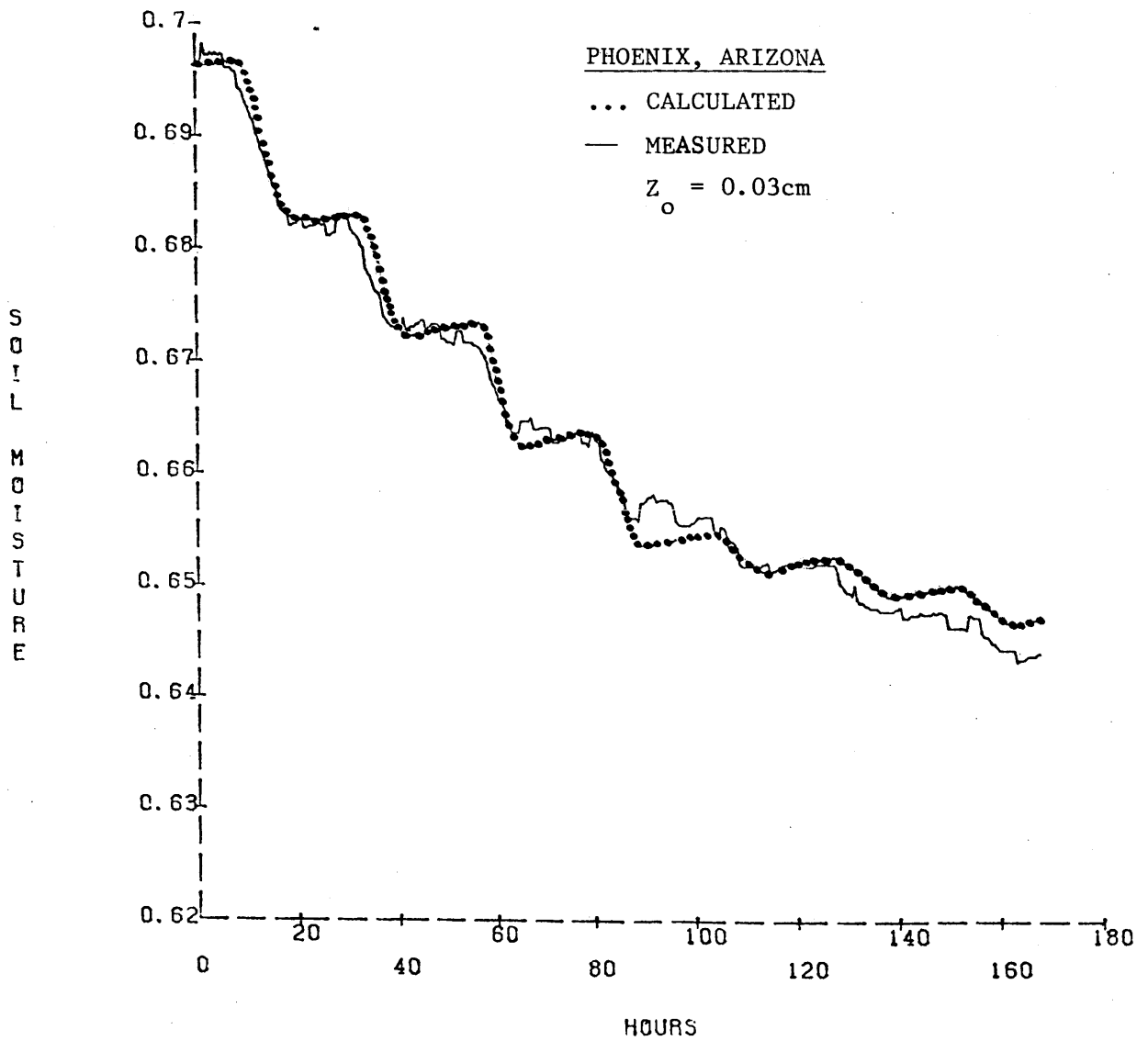
where S_e is the exfiltration "desorptivity" defined for a dry surface by:

$$S_e = 2s_o^{1+d/2} \left[\frac{nK(1)\psi(1)\phi_e(d)}{\pi m} \right]^{-1/2} \quad (7.4)$$

and M was assumed equal to zero.

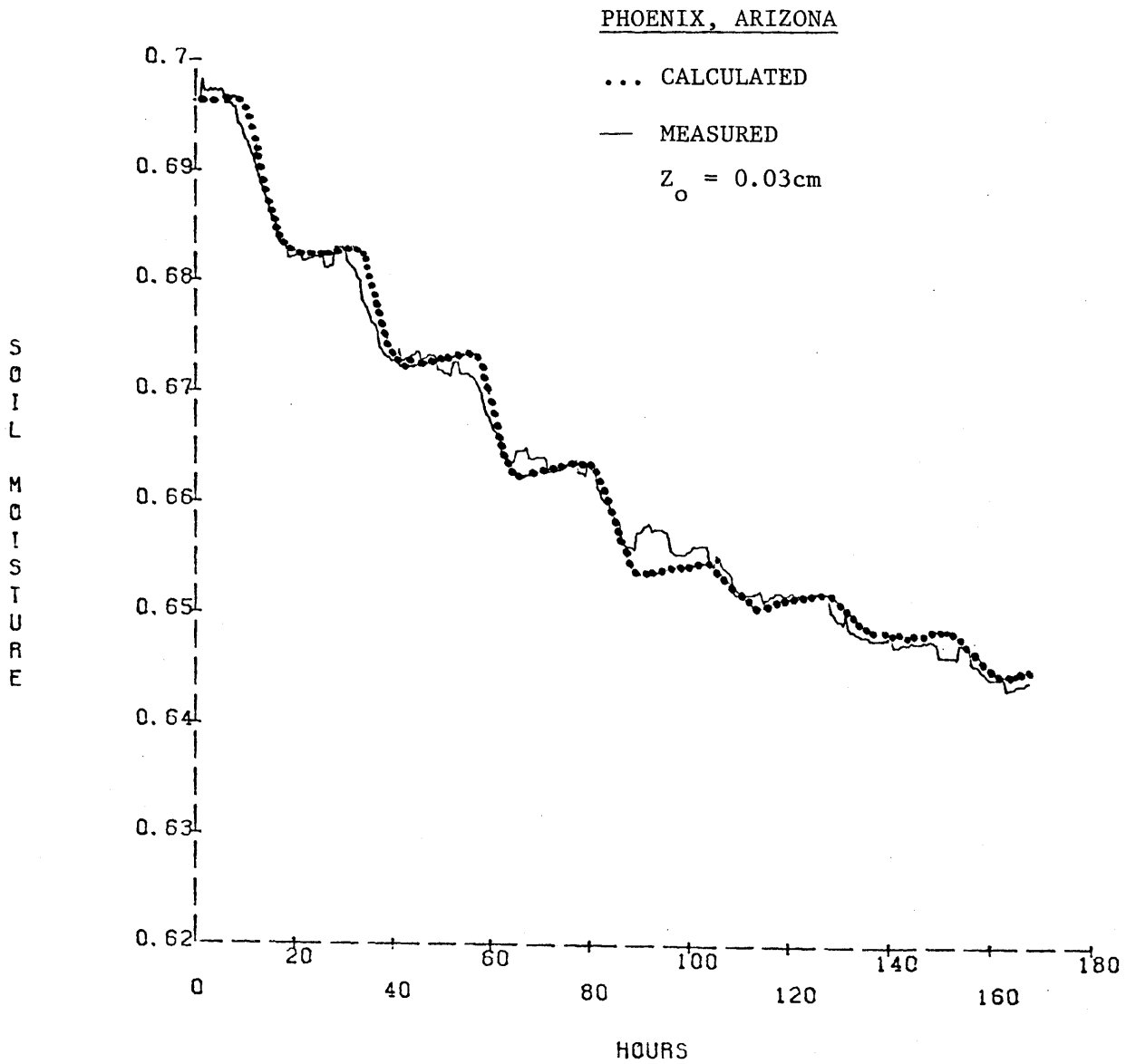
Using the values of the parameters as defined in Table 7.1, it was found that $t_o = 3.92$ days, which is very close to the value of four days mentioned by Jackson.

Equation (4.16) was now solved as before. The results for the soil-moisture concentration in the layer of 1m, are shown in Figures 20 and 21, evaluated using two different values of \bar{e}_p (the annual average value $\bar{e}_{pA} = 0.263$ cm/day, and the average value of \bar{e}_p during the seven-day period, equal to 0.323 cm/day). It is observed that the results are extremely encouraging and also,



Soil Moisture Concentration by the Analytical Model (Annual \bar{e}_p)

FIGURE 20



Soil Moisture Concentration by the Analytical Model (Seasonal \bar{e}_p)

FIGURE 21
87

as expected, the fitting is better when \bar{e}_p is the actual average for the seven-day period.

Some of the small discrepancies in these comparisons may be due to the un-gaged (trace) precipitation that occurred during this period.

In order to perform the simulation described above, the computer program ARIZ.FORTRAN was prepared. It uses as an input file the available meteorologic and soil-moisture characteristics, obtained every half-hour.

It must be noted that the ecological optimality hypotheses were not applied for soil-parameterization in the Arizona experiment for two reasons. First, because the field has been cultivated and is thus not in its natural state, and second, because soil properties were available from measurements.

Evaluation of the soil moisture concentration and the evaporation fluxes during the seven-day period will be shown in the following Section 7.6, where the thermodynamic coupling will be applied.

7.6 The Thermodynamic Coupling

The developed soil-moisture model was operated conjunctively with a thermal balance model, in order to estimate the surface temperature T_g . Two methods were tested, using the Arizona data. One used the force-restore method [Deardorff, 1978] and another used the thermodynamic equilibrium equation [Edlefsen and Anderson, 1963].

a. The force-restore method.

The force-restore method was described in Chapter 2, but the basic equations used are repeated here for convenience. Written in finite difference form, as they were solved in the present study, those equations take the form:

$$\frac{T_g^{k+1} - T_g^k}{\Delta t} = \frac{2G\pi^{1/2}}{\rho_s c_s d_1} - \frac{2\pi}{\tau_1} (T_g^k - T_2^k) \quad (7.5)$$

$$G = R_n - H_s - LE \quad (7.6)$$

and

$$\frac{T_2^{k+1} - T_2^k}{\Delta t} = G/(\rho_s c_s d_2) \quad (7.7)$$

where

- T_g^k = ground temperature at the surface ($^{\circ}\text{K}$)
- G = heat flux into the soil [$\text{cal}/\text{cm}^2 \cdot \text{sec}$]
- R_n = net radiation at the surface [ly/sec]
- H_s = sensible heat flux [$\text{cal}/\text{cm}^2 \cdot \text{sec}$]
- E = water vapor flux [$\text{g}/\text{cm}^2 \cdot \text{sec}$]
- τ_1 = 86400 sec
- T_2^k = mean soil temperature over layer of depth d_2 ($^{\circ}\text{K}$)
- L = latent heat of vaporization [cal/g]
- c_s = specific heat of soil [$\text{cal}/\text{g} \cdot ^{\circ}\text{K}$]
- ρ_s = density of soil [g/cm^3]
- d_1 = soil depth influenced by the diurnal temperature cycle [cm]
- d_2 = soil depth influenced by the annual temperature cycle [cm]

The value of d_1 is given by: $d_1 = (k_s \tau_1)^{1/2}$, where k_s is the soil thermal diffusivity. Assuming a soil porosity $n = 0.35$, the volumetric heat capacity of the soil $\rho_s c_s$ is estimated by (DeVries, "Heat Transfer in Soils").

$$\rho_s c_s = (1-n) 2 \times 10^6 + \theta (4.2) \times 10^6 + (n-\theta) c_a$$

where

- θ = volumetric water content
- c_a = heat capacity of the air

Using the Arizona data, we obtain:

$$\rho_s c_s = (1 - 0.35)2 \times 10^6 + 0.0805 \times 4.2 \times 10^6 + 0.269 \times 1.25 \times 10^3 = 1.6384369 \times 10^6 \text{ J/m}^3 \text{ } ^\circ\text{K}$$

$$\text{or } \rho_s c_s = 0.39 \text{ cal/cm}^3 \text{ } ^\circ\text{K}$$

The thermal conductivity of the soil λ is obtained using the value given by deVries for loam and for $n = 0.35$. It is found that $\lambda = 1.44 \text{ cal.cm}^{-1} \text{ sec } ^\circ\text{C}^{-1}$. Thus, the soil thermal diffusivity will be given by:

$$k_s = \frac{\lambda}{\rho_s c_s} = 0.013 \text{ cm}^2/\text{sec.}$$

and

$$d_1 = (0.013 \times 86400)^{1/2} = 33.51 \text{ cm.}$$

This value is close to the value of 31.89 applied by Lin [1980] for the same experimental field.

The value of d_2 is given by:

$$d_2 = (365 k_s \tau_1)^{1/2} = 640.21 \text{ cm}$$

The sensible heat flux H_s was evaluated from the equation suggested by Anderson [1976]:

$$H_s = \rho_a c_p \cdot C_H \cdot U_a (T_g - T_a) \left[\frac{\text{cal}}{\text{cm}^2 \text{ sec}} \right] \quad (7.8)$$

Under climate-controlled conditions where $E \equiv E_p$, the water vapor flux was evaluated by the aerodynamic relation:

$$E_p = \frac{\rho_a \times 0.622}{P_a} \cdot C_w U_a (e_s - e_a) \left[\frac{\text{g}}{\text{cm}^2 \text{ sec}} \right] \quad (7.9)$$

In these equations:

e_s = saturation vapor pressure at surface temperature

e_a = vapor pressure of the air at screen height

U_a = wind speed at screen height

T_a = air temperature ($^{\circ}$ K) at screen height

ρ_a = density of air

c_p = specific heat of dry air

P_a = atmospheric pressure

C_H and C_w are coefficients equivalent to the drag coefficient for sensible heat and water vapor flux respectively. Under neutral conditions those are given by (Anderson 1976):

$$(C_H)_N = (C_w)_N = \frac{k^2}{[\ln \frac{z_a}{z_o}]^2} \quad (7.10)$$

where

k = Von Karman's constant (0.4)

z_a = screen height

z_o = surface roughness

Deardorff [1968] computed the ratio of each of those coefficients to its value under neutral conditions, and his results are described by:

$$\frac{C_H}{(C_H)_N} = \frac{C_w}{(C_w)_N} = \left[1.0 - \left(\ln \frac{z_a}{z_o} \right)^{-1} \cdot \left[\ln \left(\frac{1+x}{2} \right) + 2 \ln \left(\frac{1+x}{2} \right) - 2 \tan^{-1} (x) + \frac{\pi}{2} \right] \right]^{-1} \cdot \left[1 - 2 \ln \left(\frac{z_a}{z_o} \right)^{-1} - \ln \left(\frac{1+x}{2} \right) \right]^{-1} \quad (7.11)$$

where

$$x = \left(1 - 16 \frac{z_a}{L} \right)^{1/4}$$

and L is the Monin-Obukhov length which can be related to the bulk Richardson number $(R_i)_B$ through the relation:

$$\frac{Z_a}{L} = \frac{k \cdot C_H / (C_H)_N \cdot (R_i)_B}{(C_H)_N^{1/2} \cdot [1 - (\ln \frac{Z_a}{Z_0})^{-1} [\ln(\frac{1+x}{2}) + 2 \ln(\frac{1+x}{2}) - 2 \tan^{-1}(x) + \frac{\pi}{2}]^{-3}} \quad (7.12)$$

where

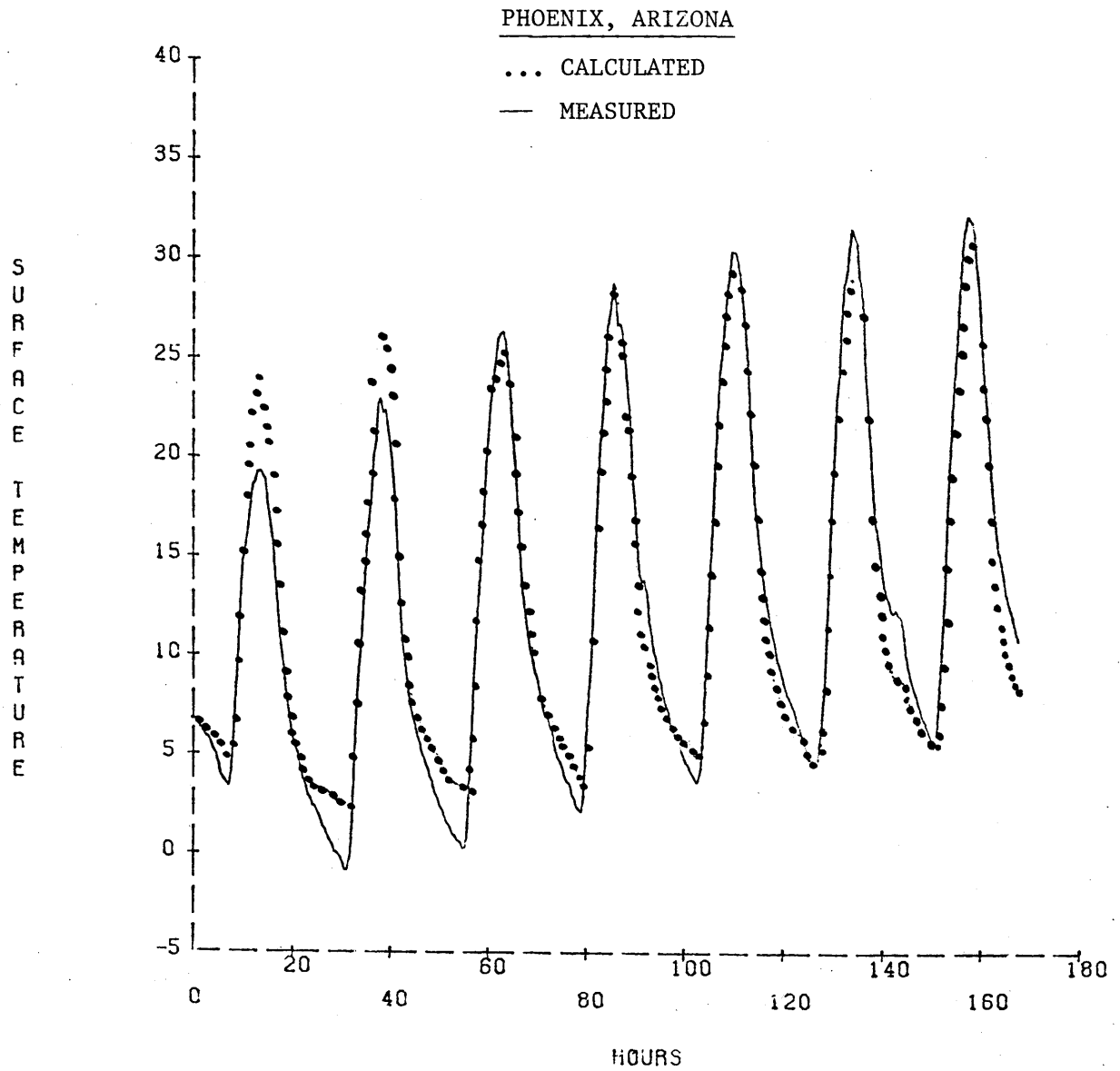
$$(R_i)_B = \frac{2g \cdot Z_a (T_a - T_g)}{(T_g + T_a) \cdot U_a^2} \quad (7.13)$$

Using equations (7.10), (7.11), and (7.12), a table of corresponding values of the ratio of bulk transfer coefficients C_H and C_w to their neutral value for different Richardson numbers $(R_i)_B$ and for different values of surface roughness Z_0 , can be constructed. Such a table is shown by Anderson [1976, page 19]. That kind of table was used in the analysis performed here in order to determine the transfer coefficients to be used.

Equations (7.5), (7.6), and (7.7) were solved simultaneously with the soil-moisture Equation (4.16). At each time-step, which was equal to 30 minutes, new values of T_g^{k+1} for the surface temperature and of s_{k+1} for the soil-moisture, were estimated. The parameters of the surface roughness Z_0 and of the initial deep soil temperature T_2 were varied in order to obtain the best fit with the measurements of surface temperature and soil moisture.

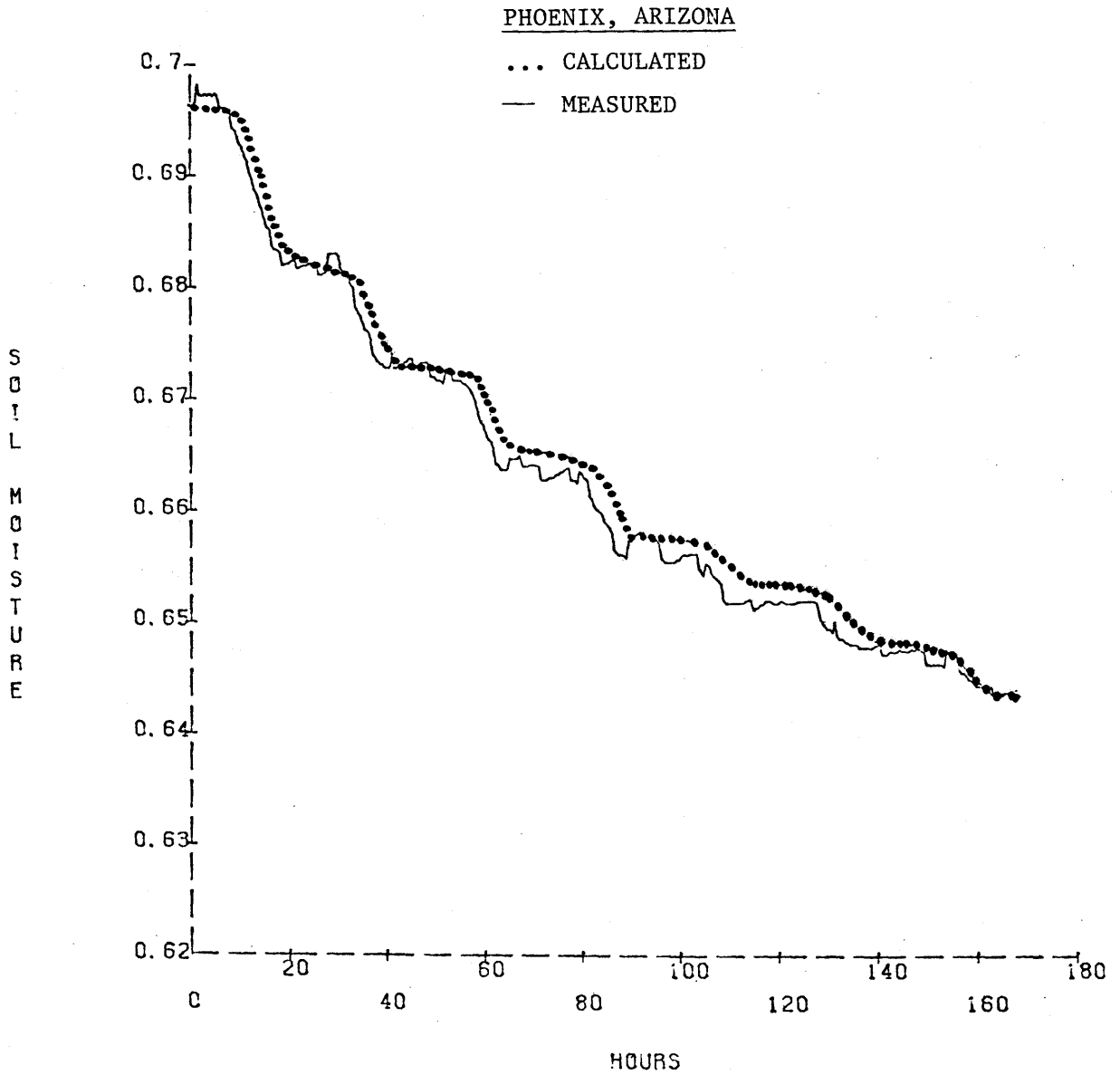
The changing value of e_p was evaluated through the use of the aerodynamic Equation (7.9). This value is used until control passes to soil.

The results are shown in Figures 22 through 29. In Figure 22 the surface temperature is plotted and compared with the solid line which represents the measured values. The transfer coefficient was set equal to $(C_H)_N = 0.00277$ and the initial deep soil temperature was set equal to $T_2 = 11^\circ\text{C}$. The fitting can be considered as satisfactory, although we observe that for the first 60 hours the surface temperature is overestimated by the model at the peaks and after that point it is underestimated at the peaks.



Surface Temperature by Force-Restore Method
 ($Z_o = 0.05\text{cm}$, $T_2 = 11^\circ\text{C}$, e_p calculated from
 the aerodynamic equation).

FIGURE 22



Soil Moisture Concentration by the Analytical Model
 $(Z_o = 0.05\text{cm}, T_{2_i} = 11^\circ\text{C})$

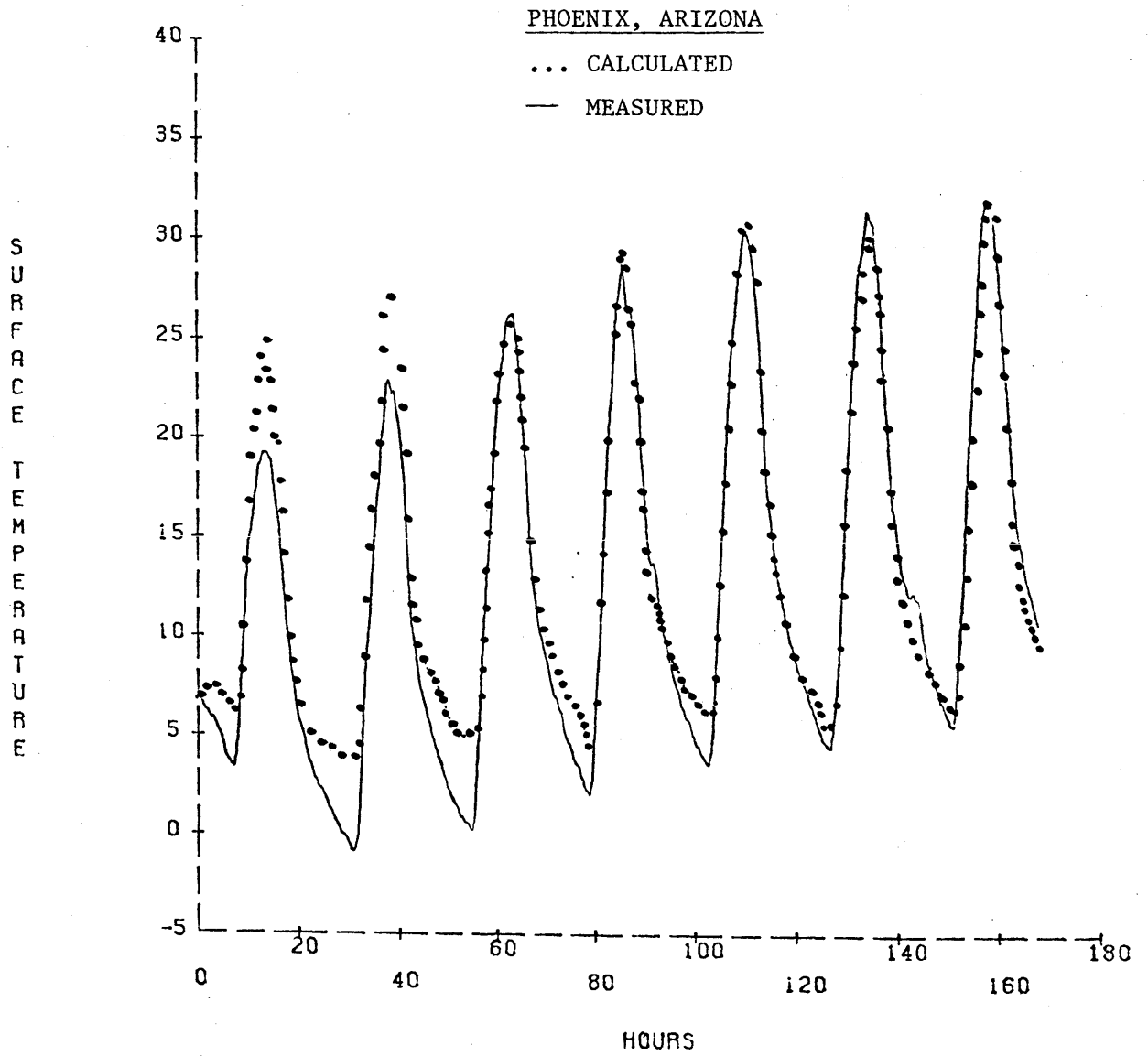
In Figure 26, the daily evaporation rate obtained from the model is compared with that measured by lysimeter (Jackson, 1976). It is seen that the calculated evaporation from the first day is less than the measured one. That could explain the overprediction of surface temperature observed in Figure 22, at the first day. That is, the higher actual evaporation makes the surface cooler than that predicted from the model.

Another fact that must be mentioned is that the measurements of surface temperature are at a depth of 1cm below the surface. Since the model assumed evaluates the temperature exactly at the surface, a discrepancy between the two could be justified. J. D. Lin (1980) mentions that high temperature gradients, as high as a difference of 20°C in 2cm, can occur near the ground surface during most of the daytime, which supports what was said before.

Figures 24 and 25 show the results obtained using the same value for the transfer coefficient $(C_H)_N = 0.00277$ as before, but with a different initial value for the deep temperature $T_{2_i} = 14^\circ\text{C}$. We observe that soil-moisture concentration is not predicted as well as before.

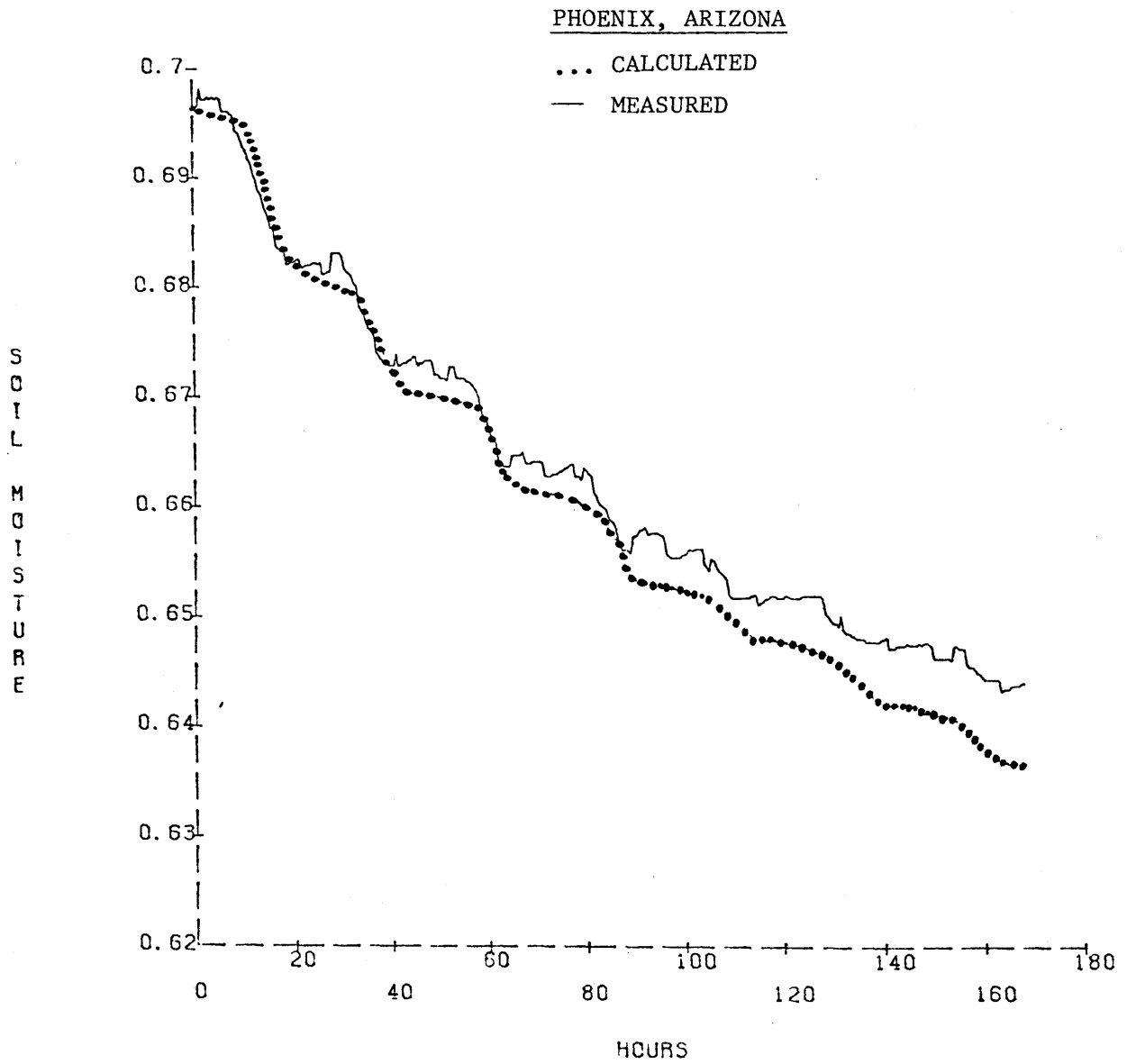
It has been argued by Bhumralkar (Deardorff, 1978) that T_2 can be estimated as the average air temperature during the previous 24 hours. If this argument is correct, it is possible that an initial value of $T_2 = 11^\circ\text{C}$, although it seems low for the Phoenix climate (where the annual average air temperature is about 21°C) could indeed have occurred.

Figures 27 and 28 show the results of the comparison, when a larger transfer coefficient $(C_H)_N = 0.0057$ is assumed. Clearly, for this high value of $(C_H)_N$ the soil-moisture concentration (Figure 28) is very much underpredicted by the model.



Surface Temperature by Force-Restore Method
 ($Z = 0.05\text{cm}$, $T_{2_1} = 14^\circ\text{C}$, e_p calculated from the
 aerodynamic equation).

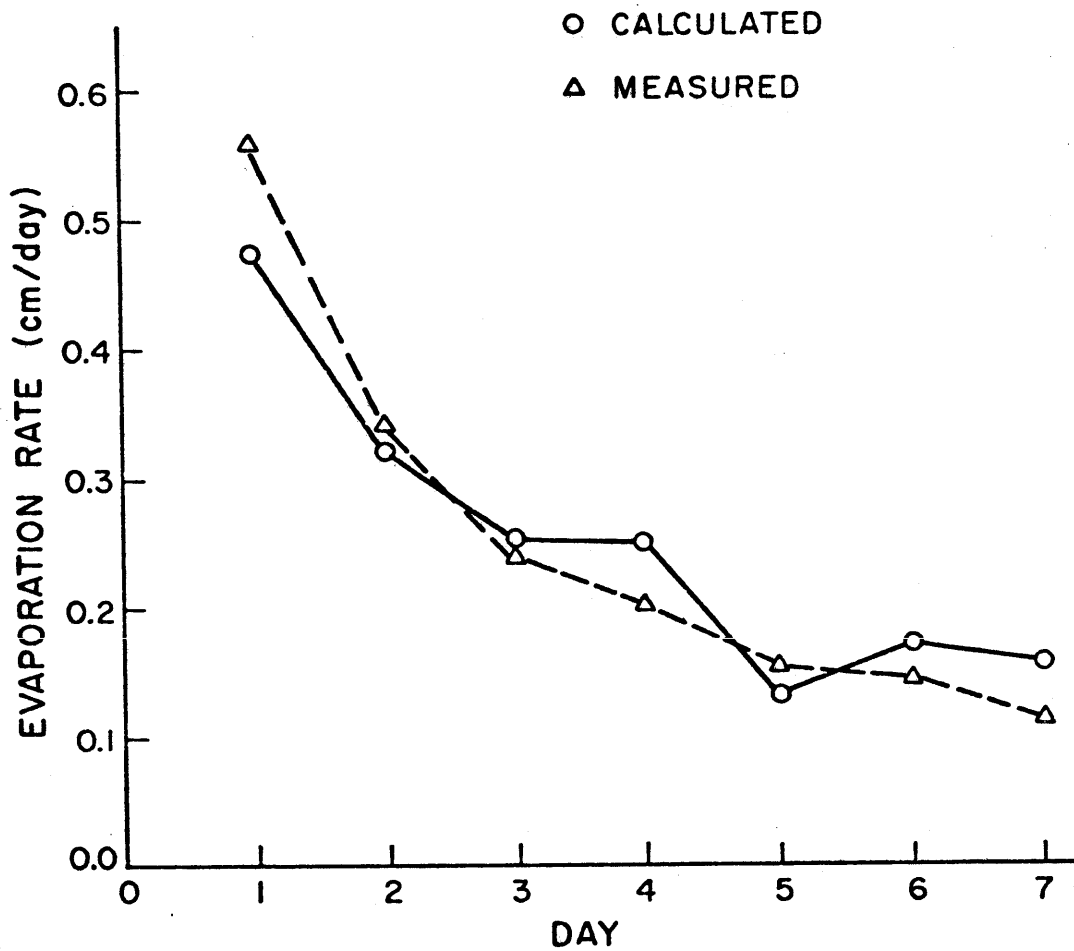
FIGURE 24
 96



Soil Moisture Concentration by the Analytical Model
 $(Z_o = 0.05\text{cm}, T_{2_i} = 14^\circ\text{C})$

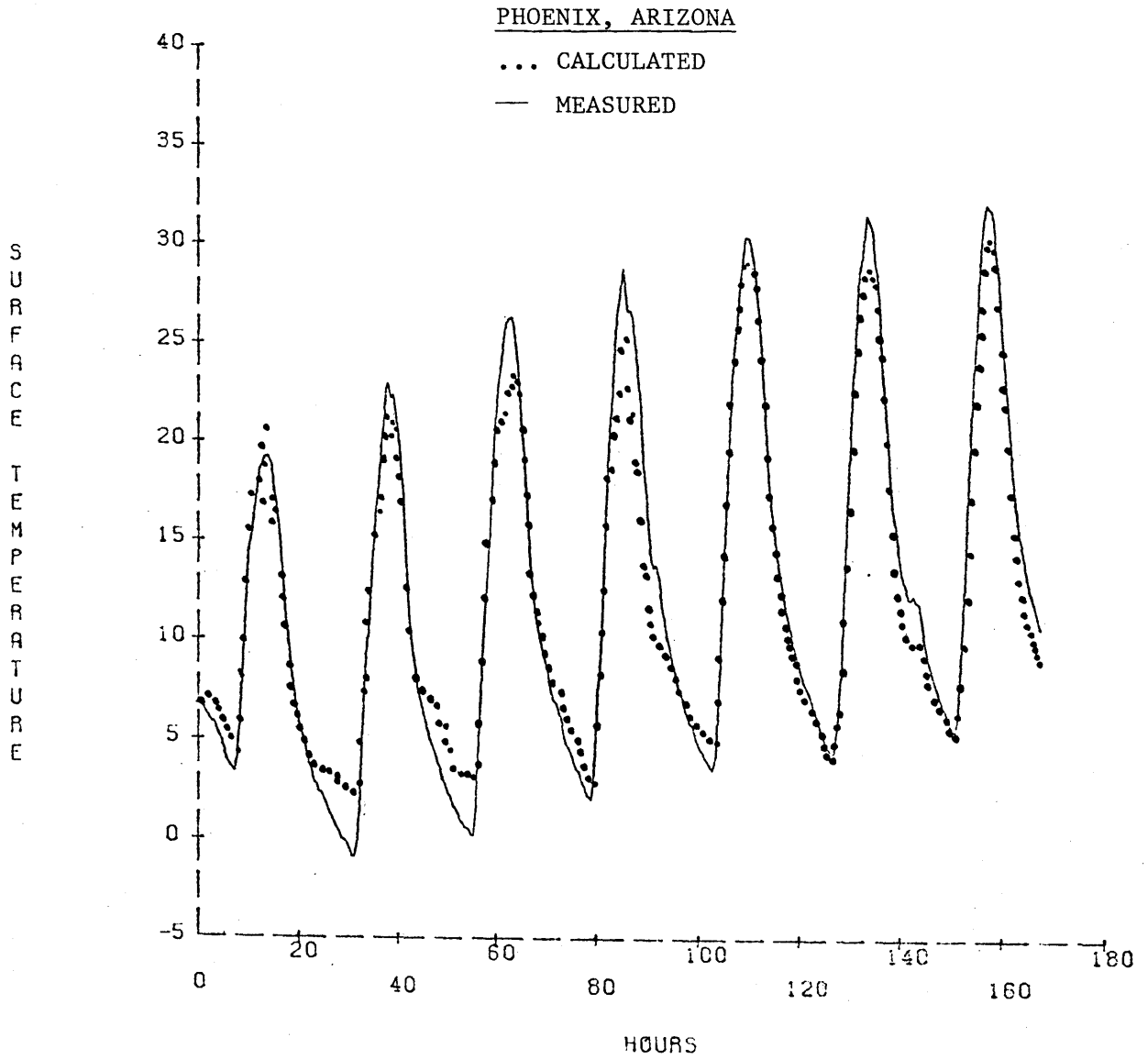
FIGURE 25

PHOENIX - ARIZONA



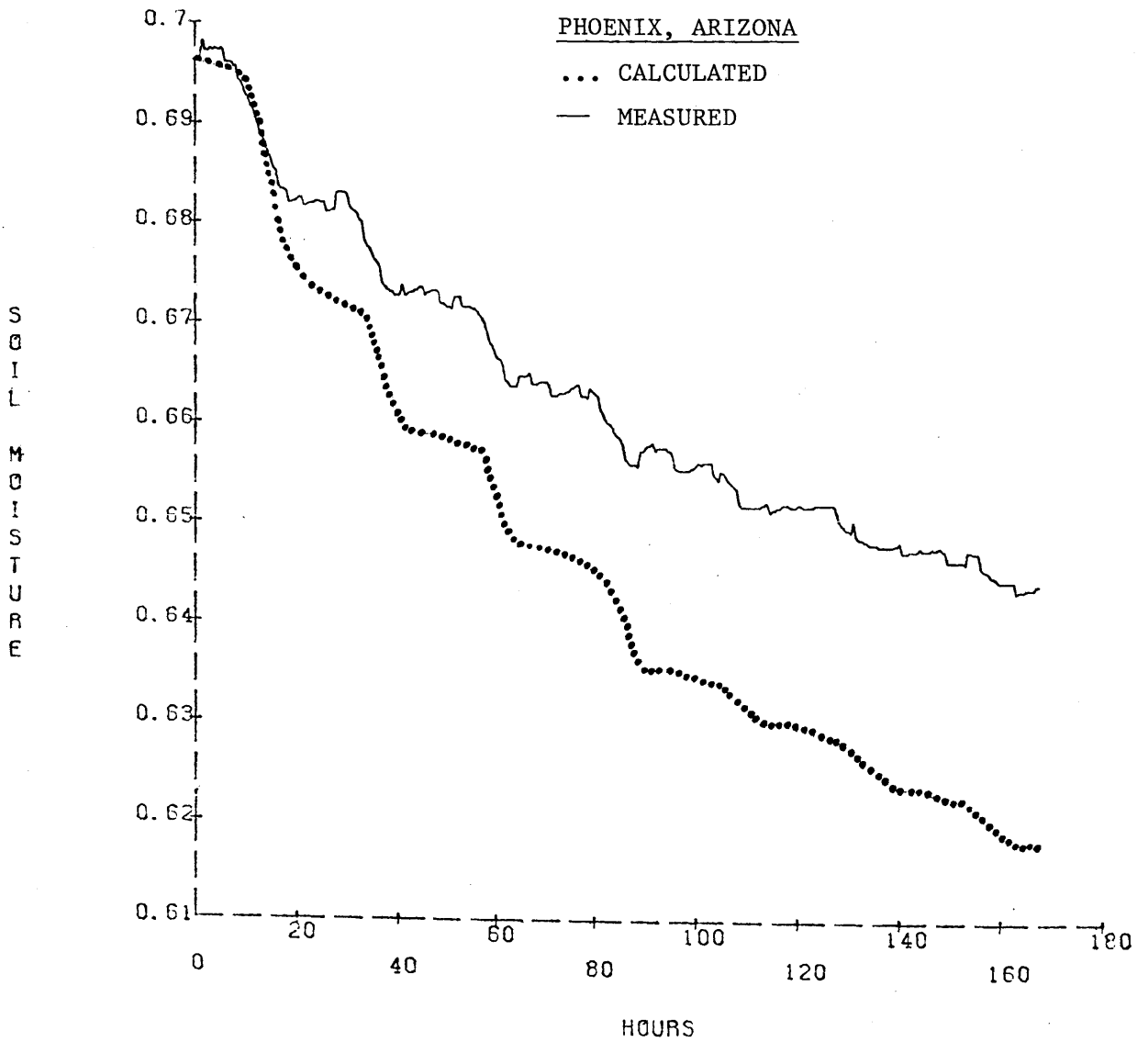
Average Daily Evaporation Rate

FIGURE 26



Surface Temperature by the Force-Restore Method
 ($Z_o = 0.5\text{cm}$, $T_2 = 14^\circ\text{C}$, e_p calculated from the
 aerodynamic equation).

FIGURE 27



Soil Moisture Concentration by the Analytical Model
 $(Z_o = 0.5\text{cm}, T_{2_i} = 14^\circ\text{C})$

A complete sensitivity analysis of the errors in the predictions of soil moisture and surface temperature with the values of surface roughness and initial deep soil temperature is shown in Table 7.2. It seems that a value of $Z_o = 0.05\text{cm}$ and of $T_{2_i} = 11^\circ\text{C}$ gives us results which predict fairly accurately both surface temperature and soil moisture. This can be confirmed both from Table 7.2 and from Figures 22 and 23. From Table 7.2, it is observed that combinations of Z_o and T_{2_i} with even smaller errors do exist, but the differences are very small compared with the errors obtained when $Z_o = 0.05\text{cm}$ and $T_{2_i} = 11^\circ\text{C}$ are selected. The problem of a priori selection of Z_o and T_{2_i} remains however.

It should be specially noted that when control passes to the soil (after the fourth day), the prediction of surface temperature is very accurate, which implies that the analytical model developed here for soil moisture fluxes, gives reasonable estimates of the actual rate of evaporation.

Manabe's model cannot be compared to the analytical model developed here for the Phoenix, Arizona experiment because the value of the soil field capacity, s_{f_c} , is not known.

b. The thermodynamic equilibrium equation.

The thermodynamic equilibrium equation is given by:

$$\frac{e}{e_s(T_g)} = \exp \left[\frac{g(s, T_g)}{R T_g} \right]$$

where e is the vapor pressure at the soil surface.

Equation (7.14) was developed by Edlefsen and Anderson (1943) and implies that the water and vapor are in thermodynamic equilibrium. It has the attraction of involving only known variables and thus does not require esti-

TABLE 7.2

Phoenix, Arizona

Surface roughness Z_o (cm)	Initial deep soil temperature T_{2i} ($^{\circ}$ C)	Cumulative Error of Soil moisture predictions $\sum_{i=0}^{337} s_i^{MES} - s_i^{CAL} $	Cumulative Error of surface Temperature predictions $\sum_{i=0}^{337} T_{g_i}^{MES} - T_{g_i}^{CAL} $
0.5	13	4.898	563.78
	11	3.815	629.19
	9	2.738	683.88
	7	1.935	1008.22
	5	1.063	1327.97
	3	0.457	1696.69
0.05	15	1.300	724.60
	13	0.541	610.21
	11	0.582	571.49
	9	1.373	628.97
	7	2.155	824.57
	5	2.790	1135.92
0.1	15	2.339	639.97
	13	1.422	561.12
	11	0.535	550.40
	9	0.547	627.94
	7	1.381	842.12
	5	2.016	1162.72
0.25	15	4.310	539.42
	13	3.250	519.76
	11	2.253	565.17
	9	1.278	685.42
	7	0.474	920.04
	5	0.550	1254.45

mates such as T_2 and C_H of the force-restore method. In order to apply it during the exfiltration process, it must be assumed that a quasi-steady state thermodynamic condition is reached at each time-step, when e_T is calculated. It must also be noted that Equation (7.14) ignores the influence of the adsorptive force-field, which can become important for a dry soil. In order to apply Equation (7.14), the dependence of ψ on T_g was ignored, assuming that the influence of T_g on ψ is not important and that the primal variability of ψ comes from variations in soil moisture.

Also (7.14) was applied only for the case where the surface is dry. When the surface is wet, the surface temperature was estimated by using again the force-restore method. If instead of doing so, it was set equal to the air temperature, a big discrepancy between the measurements and predictions would have been observed.

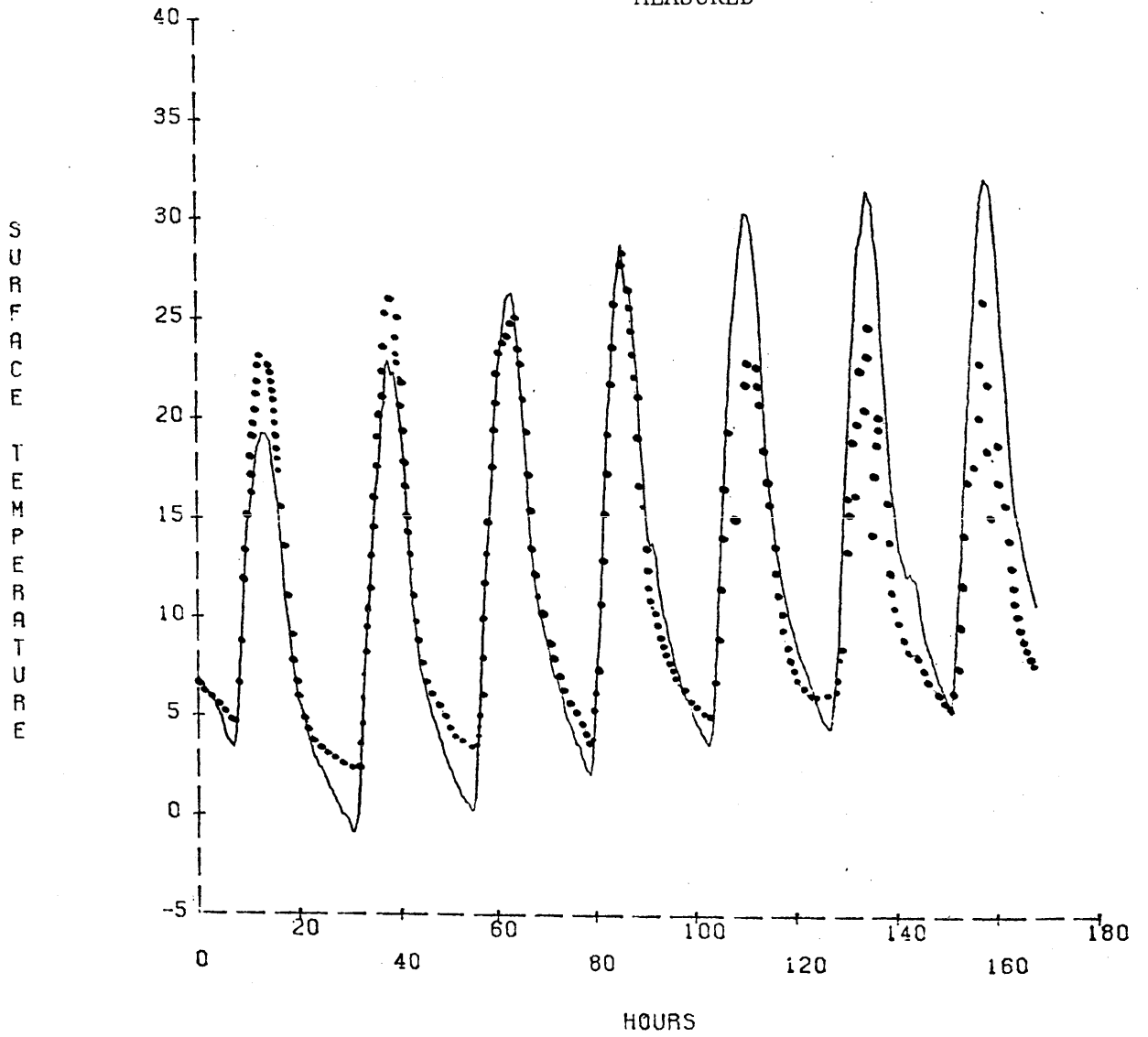
At each time step a value of the actual evaporation was determined by the model. By using the aerodynamic equation, a value for the vapor pressure e at the surface was calculated. From the soil-moisture model, the value of ψ was estimated by using the current value of s . The value of the surface temperature T_g^k of the previous time step k was used to evaluate (RT_g^k) since this factor is not very sensitive to changes at T_g . Then, Equation (7.14) was solved for T_g^{k+1} , since the only unknown now was $e_s(T_g^{k+1})$, which is a function of T_g^{k+1} .

The results are shown in Figures 29 and 30. It does not seem that the surface temperature is well estimated compared to the results of the force-restore method. After the fourth day when the surface dries and the thermodynamic equation starts to apply, the surface temperature is systematically underpredicted.

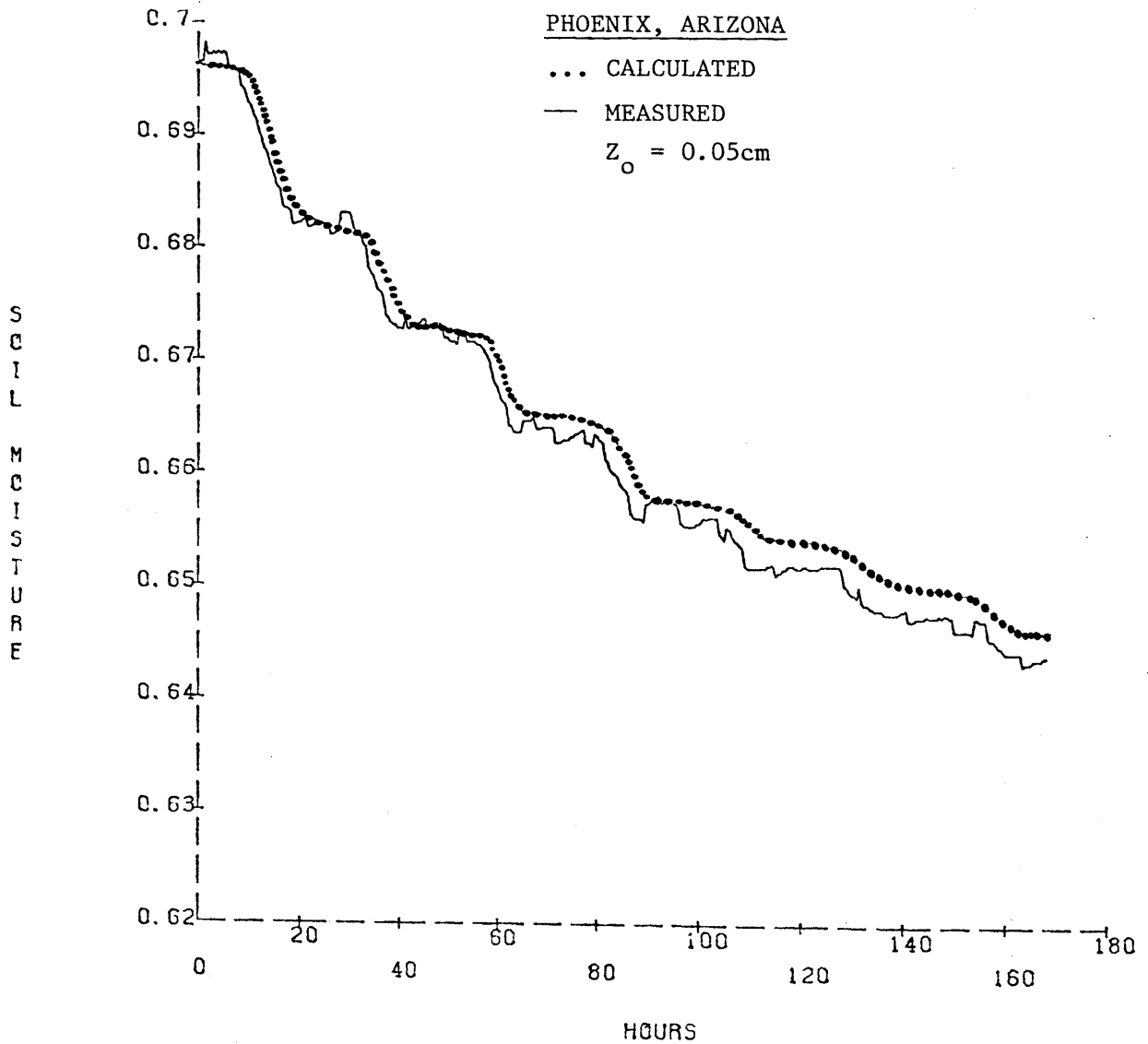
PHOENIX, ARIZONA

... CALCULATED

— MEASURED



Surface Temperature by the Thermodynamic Equilibrium Equation



Soil Moisture Concentration
(Temperature Calculated by the Thermodynamic equilibrium Equation)

FIGURE 30
105

CHAPTER 8

Summary, Conclusions, and Recommendations for Further Research

8.1 Summary

In this study, a simple analytical model was formulated to parameterize the water fluxes at the landsurface. A short-term water balance equation was solved during precipitation and interstorm periods, assuming all exchange of moisture to take place within a single surface layer. The evaporation and yield fluxes were assumed to vary linearly around their annual average values, as given by Eagleson (1978).

Successive rainstorm events and interstorm periods were generated in order to test the model. Soil-moisture concentration, within the surface layer was predicted every half-hour. The storage change and the evaporation and yield fluxes obtained from the analytical model during long simulation periods, were compared with those obtained from a numerical model (Milly 1980) and with a simple parameterization model (Manabe 1969) currently used in GCM's. This was done for two contrasting climates, those of Clinton, Massachusetts and Santa Paula, California.

Finally, the analytical model developed here for soil-moisture fluxes was operated conjunctively with thermal balance models, in order to predict the surface temperature. Results of the obtained soil-moisture concentration and surface temperature for this latter case, were compared with available measurements.

Two cases, one in which the potential evapotranspiration rate e_p was held constant at its annual average value and one in which e_p was allowed to change with time, were considered and the necessary modifications of the model for each case were discussed.

Sensitivity analysis was performed with respect to the depth of exchangeable moisture within the soil and also with respect to the surface roughness and deep soil temperature, when the thermodynamic coupling was considered.

For the catchments of Clinton, Massachusetts and Santa Paula, California, the soil and vegetation properties used were those obtained from the application of ecological optimality hypotheses (Eagleson 1982). According to these hypotheses only effective soil porosity n and the climate are necessary in order to determine $k(1)$, c and the optimum vegetation properties M_o and k_{v_o} .

In order to apply the analytical model developed here to determine the landsurface boundary condition for use in GCM's of the atmosphere, the following steps should be followed:

1. Obtain at each grid point on the landsurface the representative climatic and soil parameters necessary to implement the model. Those parameters are described in Chapter 4 and the use of ecological optimality hypotheses, in order to reduce their number is also discussed.
2. Make an estimate of the surface layer thickness.
3. Estimate the average storm intensity and average potential evaporation rate every half-hour (or appropriate Δt) according to whether it is a precipitation or an interstorm period, respectively. If there is a precipitation period, calculate the time t_o until the surface becomes saturated and let surface runoff be produced after that time if rain continues. If there is an interstorm period, calculate the time t_o until the surface becomes dry and calculate evaporation before that time by setting it equal to the value of the (changing) potential evaporation rate.

4. Solve the linearized Equations (4.14) and (4.15) if a storm has occurred, or Equation (4.16) if it is an interstorm period, every time period. Thus, an updated value of soil-moisture concentration will be obtained. Updated values of actual evaporation rate and of yield rate will also be obtained.

5. If the surface temperature is to be calculated, Equations (4.14)-(4.16) can be solved conjunctively with the equations of the force-restore method. In order to do that, estimates of the surface roughness and the initial deep soil temperature are necessary. In addition, knowledge of several meteorological variables at each time step will be necessary in order to estimate the changing value of e_p , which influences the thermal and water balance equations at the surface.

8.2 Conclusions

The model was tested using simulated rainstorm events for two contrasting climates and in both cases it was found to agree reasonably well with the solution of the numerical model. It was also tested against real measurements of soil-moisture during an evaporation period, and again it was found that it made very accurate predictions.

Thus, from the results obtained in this research, it can be stated that a simple second-order Budyko-type parameterization of the landsurface, compares favorably with "exact" numerical solutions for exchanges of water through the surface. Also, the parameterization suggested here is an improvement over the first-order Budyko-type model of Manabe (1969).

A range of depths of the soil-moisture layer was found for both tested climates, within which the cumulative evaporation and yield fluxes were rather insensitive to the layer depth. This range appears to include the actual root-zone depth.

In order to estimate the surface temperature, it was found that the force-restore method is superior to the application of the thermodynamic equilibrium equation, but again difference with real measurements, although small, did exist. It must also be pointed out that in order to apply the force-restore method conjunctively with the analytical soil-moisture model developed here, parameters such as the surface roughness and the initial deep soil temperature must be either known or fitted a priori to available data.

It should also be said that the very good agreement between analytical and numerical solutions for Santa Paula and for Clinton was obtained using soil properties derived from ecological optimality hypotheses. This provides one more indication of the applicability of these hypotheses.

8.3 Suggestions for Further Research

Using as a basis the simple landsurface parameterization developed in this study, the following additional studies should be carried out:

1. Test the model at other catchments particularly under soil-controlled conditions and for longer simulation periods.
2. Compare the model with other simple parameterizations in addition to the one suggested by Manabe (1969).
3. Investigate cases where $k_v \neq 1$ and possibly test the analytical model with more accurate numerical models which include vegetation.
4. Investigate the relation between the soil-moisture layer thickness and the soil properties $k(1)$ and c for different climates.
5. Further investigate the sensitivity of the force-restore method with respect to the surface roughness coefficient and the deep soil temperature.
6. Use the short-term water balance model developed in this study conjunctively with measurements of soil moisture (obtained for example by

remote sensing). Thus, one equation representing system dynamics and one vector of observations will be available to apply optimal linear estimation techniques (linear filtering) and to make predictions of soil moisture.

REFERENCES

- Anderson, E. A. (1976). A Point Energy and Mass Balance Model of a Snow Cover, NOAA Technical Report NWS19.
- Anderson, M. D. and Linville, A. (1969). Temperature Fluctuations at a Wetting Front: I. Characteristic Temperature-Time Curves. Soil Science Society Proceedings.
- Anderson, M. et al. (1963). Temperature Fluctuations at a Wetting Front: II. The Effect of Initial Water Content of the Medium on the Magnitude of the Temperature Fluctuations, Soil Science Society Proceedings.
- Arakawa, A. (1972). Design of the UCLA General Circulation Model. Numerical Simulation of Weather and Climate, Technical Report No. 7, Department of Meteorology, UCLA, 116 pp.
- Bhumralkar, C. M. (1975). Numerical Experiments on the Computation of Ground Surface Temperature in an Atmospheric General Circulation Model, Journal of Applied Meteorology, Volume 14, pp. 1246-1258.
- Bhumralkar, C. M. (1976). Parameterization of the Planetary Boundary Layer in Atmospheric General Circulation Models. Reviews of Geophysics and Space Physics, Volume 14, No. 2.
- Barton, I. J. (1979). A Parameterization of the Evaporation from Nonsaturated Surface, Journal of Applied Meteorology, Volume 18.
- Blackadar, A. K. (1976). Modeling the Nocturnal Boundary Layer. In Proceedings of the Third Symposium on Atmospheric Turbulence, Diffusion and Air Quality, pp. 46-49, American Meteorological Society, Boston, Massachusetts.
- Blake, G. J. (1975). The Interception Process. In Prediction in Catchment Hydrology, T. G. Chapman and F. X. Dunin (Eds.), Australian Academy of Sciences, pp. 59-81.
- Brutsaert, W. and H. Stricker (1979). An Advection-Aridity Approach to Estimate Actual Regional Evapotranspiration. Water Resources Research, 15, 2, pp. 443-450.
- Budyko, M. I., "The Heat Balance of the Earth's Surface," (in Russian) Leningrad, 1956 (Translated by N. A. Stepanova, Office of Technical Services, U. S. Department of Commerce, Washington, D. C. 1958).
- Deardorff, J. W. (1978). Efficient Prediction of Ground Surface Temperature and Moisture with Inclusion of a Layer of Vegetation. Journal of Geophysical Research, 83, C4, pp. 1189-1903.
- Eagleson, P. S., Dynamic Hydrology, McGraw-Hill, New York, 1970.
- Eagleson, P. S., "Climate, Soil, and Vegetation. 1. Introduction to Water Balance Dynamics," Water Resources Research, 14(5), 1978a.

- Eagleson, P. S., "Climate, Soil, and Vegetation. 2. The Distribution of Annual Precipitation Derived from Observed Storm Sequences," Water Resources Research, 15(5), 1978b.
- Eagleson, P. S., "Climate, Soil, and Vegetation. 3. A Simplified Model of Soil Moisture Movement in the Liquid Phase," Water Resources Research, 14(5).
- Eagleson, P. S., "Climate, Soil, and Vegetation. 4. The Expected Value of Annual Evapotranspiration," Water Resources Research, 14(5), 1978d.
- Eagleson, P. S., "Climate, Soil, and Vegetation. 5. A Derived Distribution of Storm Surface Runoff," Water Resources Research, 14(5), 1978e.
- Eagleson, P. S., "Climate, Soil, and Vegetation. 6. Dynamics of the Annual Water Balance," Water Resources Research, 14(5), 1978f.
- Eagleson, P. S., "Climate, Soil, and Vegetation. 7. A Derived Distribution of the Annual Water Balance," Water Resources Research, 14(5), 1978g.
- Eagleson, P. S., "Dynamic Hydrothermal Balances at Macroscale", MIT, Cambridge Massachusetts, January 1981.
- Eagleson, P. S., "Ecological Optimality in Water-Limited Natural Soil-Vegetation Systems. 1. Theory and Hypothesis", Water Resources Research, Volume 18, No. 2, pp. 325-340, April 1982.
- Eagleson, P. S., "Ecological Optimality in Water-Limited Natural Soil-Vegetation Systems. 2. Tests and Applications", Water Resources Research, Volume 18, No. 2, pp. 341-354, April 1982.
- Edlefsen, N. E. and A. B. C. Anderson, Thermodynamics of Soil Moisture, Hilgardia, 15(2), 1943.
- Federer, C. A. (1977). Leaf Resistance and Xylem Potential Differ Among Broad-leaved Species. Forest Science, 23, pp. 411-419.
- Federer, C. A. (1979). A Soil-plant-atmosphere Model for Transpiration and Availability of Soil Water. Water Resources Research, 15, 3, pp. 555-562.
- Federer, C. A. and D. Lash (1978). Brook: A Hydrologic Simulation Model for Eastern Forests. Res. Rept. No. 19, Water Resource Research Center, University of New Hampshire, Durham, New Hampshire.
- GARP (1978), JOC Working Group on Land Surface Processes, Report of Dublin Meeting, May 8-12, 1978, Geneva, 32 pp.
- Gates, W. L. and M. E. Schlesinger, "Numerical Simulation of the January and July Global Climate with a Two-Level Atmospheric Model," Journal of the Atmospheric Sciences, Volume 34, 1977.

- Jackson, R. D., "Diurnal Changes in Soil Water Content During Drying", Field Soil Water Regime, SSSA Special Publication No. 5, March 1976.
- Lettau, H. (1969). Evaporation Climatology, a New Approach to Numerical Prediction of Monthly Evapotranspiration, Runoff, and Soil Moisture Storage. Monthly Weather Review, 97, 10, pp. 691-699.
- Lin, J. D., "On the Force-Restore Method for Prediction of Ground Surface Temperature", Journal of Geophysical Research, Volume 85, No. C6, pp. 3251-3254, June 1980.
- Lin, J. D., P. Bock, J. Alfano, "Formulation of Ground Hydrologic Model II for GISSO-GCM", Interim Report, University of Connecticut, Department of Civil Engineering, February 1976.
- Linacre, E. T. (1968). Estimating the Net-Radiation Flux. Agricultural Meteorology, 5, pp. 49-63.
- Linsley, R. K. and N. H. Crawford (1960). Computation of a Synthetic Streamflow Record on a Digital Computer Pub. No. 51, International Association of Scientific Hydrology, pp. 526-538.
- Lowry, W. P. (1959). The Falling Rate Phase of Evaporative Soil Moisture Loss: A Critical Evaluation. Bull. Amer. Meteor. Soc., 40, p. 605.
- Manabe, S. (1969). Climate and the Ocean Circulation. 1. The Atmospheric Circulation and the Hydrology of the Earth's Surface. Monthly Weather Review, 97, 11, pp. 739-774.
- Manabe, S., D. G. Hahn and J. L. Hollway, Jr. (1974). The Seasonal Variation of the Tropical Circulation as Simulated of a Global Model of the Atmosphere. Journal of the Atmospheric Sciences, 31, pp. 43-83.
- McNaughton, K. G. (1976-a). Evaporation and Advection I: Evaporation from Extensive Homogeneous Surfaces. Quarterly Journal of the Royal Meteorological Society, 102, pp. 181-191.
- Milly, P. C. P. and Eagleson, P. S. (1980). The Coupled Transport of Water and Heat in a Vertical Soil Column Under Atmospheric Excitation, MIT, Technical Report No. 258.
- Monteith, J. L. (1965). Evaporation and Environment. Symposium of the Society for Experimental Biology, No. 19, pp. 205-234.
- Monteith, J. L. (1979). Principles of Environmental Physics. American Elsevier Pub. Company, Incorporated, New York, 241 pp.
- Morton, F. I., "Potential Evaporation and River Basin Evaporation," Proc. ASCE, Journal of the Hydraulics Division, HY6, 4534, pp. 67-97.
- Morton, F. I., "Evaporation and Climate", Scientific Series No. 4, Inland Waters Branch, Canadian Department of Energy, Mines and Resources Ottawa, Canada 1968., 32 pp.

- Morton, F. I., "Catchment Evaporation and Potential Evaporation-Further Development of a Climatologic Relationship", Journal of Hydrology, Volume 12, pp. 81-99, 1971.
- Mualem, Y., "A New Model for Predicting the Hydraulic Conductivity of the Un-saturated Porous Media", Water Resources Research, Volume 12, No. 3, June 1976.
- Philip, J. R. (1957). Evaporation and Moisture and Heat Fields in the Soil. Journal of Meteorology, 14, pp. 354-366.
- Philip, J. R. (1969). Theory of Infiltration. In Advances in Hydrosience, 5, V. T. Chow (Ed.), Academic Press, New York, pp. 215-296.
- Philip, J. R. and D. A. deVries, "Moisture Movement in Porous Materials Under Temperature Gradients," Trans. A.G.U., Volume 38, 1957.
- Priestley, C. H. B. and R. J. Taylor (1972). On the Assessment of Surface Heat Flux and Evaporation Using Large-scale Parameters. Monthly Weather Review, 100, 2, pp. 81-92.
- Rasmussen, E. M. (1977). Hydrological Application of Atmospheric Vapor Flux Analyses. Operational Hydrology Report No. 11, WMO - No. 476, WMO, Geneva 50 pp.
- Restrepo, P. and Eagleson P. S., "Fortran Programs for the Interpretation and Analysis of NOAA Hourly Precipitation Data Tapes, MIT, Technical Note No. 22, September 1979.
- Rijtema, P. E. (1965). An Analysis of Actual Evapotranspiration. Agriculture Research Report 659, Wanenihgen, Netherlands.
- Sasamori, T., "A Numerical Study of Atmospheric and Soil Boundary Layers," Journal of Atmospheric Sciences, Volume 27, 1970.
- Slatyer, R. O. and I. C. McIlroy (1961). Practical Microclimatology, UNESCO, Paris, 310 pp.
- Solomon, S. (1967). Relationship Between Precipitation, Evaporation, and Run-off in Tropical-Equatorial Regions, Water Resources Research, 3, 1, 163-173.
- Somerville, R. C. J., et al. (1974). The GISS Model of the Global Atmosphere. Journal of the Atmospheric Sciences, 31, pp. 84-117.
- Tanner, C. B. and M. Fuchs (1968). Evaporation from Unsaturated Subsurfaces: A Generalized Combination Method. Journal of Geophysical Research, 75, 4, pp. 1299-1304.
- Tellers, T. E. and P. S. Eagleson (1980). Estimation of Effective Properties of Soils from Observations of Vegetation Density. R. M. Parsons Laboratory, Report No. 254, MIT, Department of Civil Engineering, 126 pp.

- Van Bavel, C. H. M. (1966). Potential Evaporation: The Combination Concept and its Experimental Verification. Water Resources Research, 2, 3, pp. 455-467.
- Van de Honert, T. H. (1948). Water Transport in Plants as a Catenary Process. Discuss. Faraday Soc., 3, pp. 146-153.
- de Vries, D. A. and J. H. Philip, "Temperature Distribution and Moisture Transfer in Porous Materials," Journal of Geophysical Research, Volume 64, March 1959.
- de Vries, D. A., "Simultaneous Transfer of Heat and Moisture in Porous Media," Trans. Amer. Geophys. Union, 39(5), 909-916, 1958.

APPENDIX 1

FORTRAN PROGRAMS FOR SIMULATING SOIL-MOISTURE
AT THE SURFACE LAYER

1. PROGRAM TAYLOR.FORTRAN

```

C *****
C THIS PROGRAM GENERATES RAINSTORM EVENTS, STORM DURATIONS
C AND INTERSTORM PERIODS WHICH PRESERVE THE HISTORICAL STATISTICS.
C IT CALCULATES THE SOIL MOISTURE OVER A DEPTH CLOSE TO THE SURFACE
C EVERY HALF HOUR .IT PLOTS THE EVAPOTRANSPIRATION
C FUNCTION,THE SURFACE RUNOFF AND PERCOLATION FUNCTIONS.IT ALSO
C PLOTS THE DAILY SOIL MOISTURE DURING THE RAINY SEASON LENGTH.
C IT CALCULATES THE TOTAL STORAGE CHANGE, THE CUMULATIVE
C EVAPORATION AND YIELD AT THE END OF EVERY RAINY OR
C INTERSTORM PERIOD
C IT HAS THE OPTION OF USING MANABE'S MODEL
C TO CALCULATE THE MOISTURE FLUXES
C THE VALUE OF THE POTENTIAL EVAPOTRANSPIRATION RATE
C IS SET EQUAL TO ITS ANNUAL AVERAGE VALUE

C *****
C CLIMATIC AND SOIL VARIABLES
c epr=average annual evapotranspiration rate(cm/day)
c mtb=mean time between storms(days)
c mtr=mean storm duration(days)
c mpa=mean annual precipitation(cm)
c mtau=mean rainy season length(days)
c ta=average annual air temperature(C)
c mnu=mean number of storms per year
c n=soil porosity
c k1=saturated intrinsic permeability(cm2)
c c=pore disconnectedness index
c Zr=surface layer thickness(cm)
c Mo=vegetation cover
c Kv=plant coefficient
c k=parameter of gamma distributed storm depths
c Lamda=parameter of gamma distributed storm depths
C *****

real min,mo,m,n,nu,k1,mtb,mtr,mh,in
real sjk(20),yi(20),soj(20),a77(20),b77(20),b78(20)
real da(365),SKP(365),st(365),b79(20),a79(20),ys(20),yg(20)
real a78(20),day(365)
fi(d,so)=1./(d*(1.-so)**(1.45-.0375*d)+5./3.)
external plot_$setup (descriptors)
external plot_$scale (descriptors)
external plot_ (descriptors)
character*10 xaxis,yaxis
fi(em)=10.**(.66+.55/em+.14/em**2.)
k11=1
ran=1.
print,'To use Manabes parameterization type 2 , otherwise 1'
input,mnb
if(mnb.eq.1) go to 3020
print,'Input the initial soil moisture so'
input,so
go to 3021
3020 print,'Input the average annual soil moisture so'
input,so
print,'Input Time step (in days) '
input,tis

C NR=Number of rainstorm events you want to generate

```

```

3021 print,'Input NR'
input,NR
print,'Input storm properties k and Lamda'
input,xk,am1
if(mnb.eq.2) go to 3040
print,'For daily fluxes type 1,for half hour fluxes type 2 '
input,f1
print,'To plot S(t) type 2,otherwise 1'
input,lot
print,'For cumulative fluxes after each storm and interstorm period type 2, otherwise 1'
input,ucu
print,'To plot S(t) for different values of Zr type 2 ,otherwise 1'
input,szr
print,'To print the cumulative fluxes only at the end of the rainy season type 2 , otherwise 1'
input,fcu
3040 print,'To print the rainstorm events type 2 , otherwise 1'
input,rae
i1=1
3003 print,'epr,mtb,mtr,mpa,mtau,ta,mnu,n'
input,epr,mtb,mtr,mpa,mtau,ta,mnu,n
if(mnb.eq.2) go to 3022
2020 print,'Mo,Kv,k1,c,Zr'
input,vg,vk,k1,cs,zr
if(vg.eq.1) stop
if(ran.eq.2) go to 3004
if(dif.eq.2) go to 3004
C J(s)=evapotranspiration efficiency function
C Ys(s)=surface runoff function
C Yg(s)=ground water percollation function

1000 print,'To plot J(s) and y(s) type 2 , otherwise 1'
input,p1
if(p1.eq.1) go to 3004
if(k11.eq.2) go to 3004
print,'To draw different curves for J(s) for different climates type 2, otherwise 1'
input,dif
double precision sum1,mean1,mean2,mean3,828
double precision sum2
double precision sum3
3004 if(ran.eq.2) go to 807
3022 if(rae.eq.1) go to 42
print,'STORM DEPTH STORM DURATION TIME BETWEEN '
print,' (cm) (days) (days) '

42 i1=1

C *****
C GENERATION OF RAISTORM EVENTS
C *****

C R1(I)=storm depth(cm)
C R2(I)=storm duration(days)
C R3(I)=interstorm duration(days)

real R(500),WK(1000),R1(500),R2(500),R3(500)
double precision DSEED
DSEED=123765.ODO
A=xk
B=1./am1
call ggamr(DSEED,A,NR,WK,R)

```



```

do 5 I=1,NR
R(I)=B*R(I)
5 continue
do 41 I=1,NR
R1(I)=R(I)
41 continue
DSEED=3478758.ODO
A=1.
B=mtr

call ggamr(DSEED,A,NR,WK,R)
do 7 I=1,NR
R(I)=B*R(I)
7 continue
do 21 I=1,NR
R2(I)=R(I)
21 continue
DSEED=649853.ODO
A=1.
B=mtb
call ggamr(DSEED,A,NR,WK,R)
do 9 I=1,NR
R(I)=B*R(I)
9 continue
do 30 I=1,NR
R3(I)=R(I)
30 continue
if(ran.eq.2) go to 807
if(rae.eq.1) go to 3023
go to 3024
3023 if(mnb.eq.2) go to 3025
go to 807
3024 do 11 I=1,NR
write(6,17) R1(I),R2(I),R3(I)
17 format(f10.6,4x,f10.6,4x,f10.6)
11 continue

807 m=2./(cs-3.)
d=cs-1./m-1
dE=2.+1./m
fied=fie(dE)
C *****
C COMPUTE WATER CONSTANTS
C *****

call WATCHN(ta,sut,nu,gamsw)
C *****
C COMPUTE CLIMATIC PARAMETERS
C *****
delta=1./mtr
mh=mpa/(mtau/(mtb+mtr))
amnu=mtau/(mtb+mtr)
mi=mh/mtr
eta=1./mh
alpha=1./mi
pi=3.14159
beta=1./mtb
C *****
C COMPUTE DERIVATIVE OF J WITH RESPECT TO so
C *****

```

```

den=(1.425-0.0375*d)
if(pl.eq.1) go to 802
k=0
so=0.
805 so=so+0.05
go to 802
802 ds=(1.-so)**den
dds=ds*d
deno=dds+(5./3.)
denom=deno**(4./3.)
soo=1.-so
so1=soo**(-4./3.)
denos=2*soo*deno
dt=(2.425-0.0375*d)
so2=soo**dt
deos1=so2*d*den
nom=-denos-deos1
nom1=nom*so1
der=nom1/(denom*3)
fic=fi(m)
si1=sqrt(n/(k1*fic))*sut/gamsw
si11=si1*so**(-1./m)
bk1=k1*gamsw/nu
sigc=n*eta**2.*bk1*si1/(pi*m*delta)*72000.
sigc1=sigc**0.3333333
dersig=sigc1*der
sia=5*n*bk1*86400*si1/(3*m*pi)
sigma=(sigc/deno*(1.-so)**2. )**0.3333333
g=alpha*bk1*86400*.5*(1.+so**cs)
g1=log10(sigma)
xp=(1.766*g1)+(0.980*(g1**2.))
xp1=-.806-xp
CSI=10.**xp1
xp2=(1.96*g1)+1.766
U=-dersig*xp2/sigma
co=alpha*86400*bk1/2.*cs*so**(cs-1.)
co1=U-co
C2=co1*CSI*exp(-g)
C38=mtau*86400*bk1*cs/mpa*so**(cs-1.)
C3=C38/2.
if(vg.eq.0) go to 80
go to 90

80 E=2.*beta*n*bk1*si1*fied/(pi*m*ep**2.)*86400*so**(d+2.)
if(E.ge.88.) E=88.
z1=(1.+E*sqrt(2.))*exp(-E)
z2=gamma(1.5)-gamt(1.5,E)
z2=z2*sqrt(2.*E)
sj=1.-z1+z2
if(pl.eq.1) go to 803
k=k+1
sjk(k)=sj
if(k.eq.20) go to 804
go to 805
803 ag=gamma(1.5)-gamt(1.5,E)
g1=exp(-E)*sqrt(2.)
g2=E*sqrt(2.)+1.
g2=g2*exp(-E)

```

```

g3=ag*sqrt(2.)/(2.*sqrt(E))
g4=exp(-E)*sqrt(E)*sqrt(2*E)
gg=-g1+g2+g3-g4
E11=2.*beta*n*bk1*si1*fied/(pi*m*epr**2.)*86400
E12=(d+2.)*so**(d+1.)
derij=gg*E11*E12
  C1=derij
  if(C1.le.0) C1=0.0
  go to 100
90 B=(1.-vg)/(1.+(vg*vk))
B=B+(vk*vg**2.)/(2.*(1.+(vg*vk))**2.)
  C=1./(2.*(vg*vk)**2.)
E1=2.*beta*n*bk1*si1*fied/(pi*m*epr**2.)*86400
E=2.*beta*n*bk1*si1*fied/(pi*m*epr**2.)*86400*so**(d+2.)
o1=B*((vg*vk)+1)
o1=-o1+sqrt(B*2.)
o11=B*E*sqrt(2.*B)
o1=o1-o11
o1=o1*exp(-B*E)
o1=o1*E1*(d+2.)
o1=o1*(so**(d+1.))
o2=-vg*vk*C
o2=o2+sqrt(2*C)
o2=o2-(C*sqrt(2*C)*E)
  C88=C*E
  if(C88.ge.88) C88=88.
o2=o2*exp(-C88)*E1*(d+2.)
o2=o2*(so**(d+1.))
  CE=C*E
  BE=B*E

a1=(vg*vk)+1.
a2=E*sqrt(2.*B)
a3=a1+a2
  if(BE.ge.88.) BE=88.
a3=a3*exp(-BE)
a4=vg*vk
a4=a4+(E*sqrt(2.*C))
  if(CE.ge.88.) CE=88.
a4=a4*exp(-CE)
a5=gamt(1.5,CE)-gamt(1.5,BE)
a5=a5*sqrt(2.*E)
a6=a3-a4-a5
a6=a6*(1.-vg)/(1.-vg+(vg*vk))
sj=1.-a6
  if(pl.eq.1) go to 806
k=k+1
sjk(k)=sj
  if(k.eq.20) go to 804
go to 805
806 o3=gamt(1.5,CE)-gamt(1.5,BE)
o3=o3*sqrt(2.*E1)
o3=(1.+d/2.)*o3*(so**(d/2.))
o31=-C*E1*(so**(d+2.))
o31=(C**1.5)*exp(o31)
o32=-B*E1*(so**(d+2.))
o32=(B**1.5)*exp(o32)
o33=o31-o32
o33=o33*(E1**1.5)
o33=o33*(2.+d)

```

```

o33=o33*(so**((1.5*d)+2.))
o33=o33*sqrt(2.*E)
o3=o3+o33
derj=o1-o2-o3
derj=derj*(1.-vg)
derj=-derj/((vg*vk)+1.-vg)
  C1=derj
if(C1.le.0) C1=0.0
B28=mtau*bk1*86400/mpa*so**cs
C *****

C C1=Derivative of J with respect to s
C C2=Derivative of Ys with respect to s
C C38=Derivative of Yg with respect to s
C sj=J(so)
C si11=psi evaluated at so
C bk1=saturated hydraulic conductivity (cm/sec)

C *****

100 print101,C1,C2,C38,sj,si11,bk1
101 format(3hC1=,f10.6,4x,3hC2=,f10.6,4x,3hC3=,f10.6,4x,2hJ=,f10.6,4x,3hMH=,f10.2,4x,f20.10)
SK=so
804 p=mpa/(mnu*mtr)
  C1=C1*epr
B1=sj*epr

if(p1.eq.1) go to 808
so=0.
k=0
811 so=so+0.05
ds=d*(1.-so)**den
deno=ds+(5./3.)
sigma=(sigc/deno*(1.-so)**2.)*.333333
808 B22=sigma**(-sigma)
sigm=sigma+1.
B22=B22*gamma(sigm)
B2=B22*exp(-g-(2*sigma))
B28=mtau*bk1*86400/mpa*so**cs
B4=B2*p
B5=B28*p*mnu*mtr/mtau
if(p1.eq.1) go to 809
k=k+1
ys(k)=B4
yg(k)=B5
soj(k)=so
if(k.eq.20) go to 810
go to 811
809 if(ucu.eq.2) go to 1816
  print,' S(t)      i(cm/day)      Et(cm/day)      yield(cm/day)      DAY '
go to 1815
C *****
C CALCULATE THE SOIL MOISTURE CONCENTRATION AND THE
C CUMULATIVE EVAPORATION AND YIELD AT THE END OF
C EVERY RAISTORM AND INTERSTORM PERIOD
C *****

1816 print,'SOIL.MOIST. CUM.EVAP. CUM.YIELD'
1815 if(p1.eq.1) go to 812
810 if(k11.eq.2) go to 3001

```

```

C *****
C PLOT J VERSUS s
C *****

call plot_$setup(' ','s','J',1,0,0,0)
call plot_$scale(0.,1.,0.,1.)
3001 i=0
k11=2
do 813 j=1,20
i=i+1
b77(i)=sjk(j)
a77(i)=soj(j)
813 continue
call plot_(a77,b77,20,1,' ')
if(dif.eq.1) go to 3002
go to 3003
3002 read(5,)
C *****
C PLOT Ys AND Yg VERSUS s
C *****

call plot_$setup(' ','SOIL MOISTURE','SURFACE RUNOFF',1,0,0,0)
call plot_$scale(0.,1.,0.,2.)
i=0
do 814 j=1,20
i=i+1
b78(i)=ys(j)
a78(i)=soj(j)
814 continue
call plot_(a78,b78,20,1,' ')
read(5,)
call plot_$setup(' ','SOIL MOISTURE','GROUNDWATER RUNOFF',1,0,0,0)

call plot_$scale(0.,1.,0.,2.)
i=0
do 834 j=1,20
i=i+1
b79(i)=yg(j)
a79(i)=soj(j)
834 continue
call plot_(a79,b79,20,1,' ')
go to 1000
812 if(szr.eq.1) go to 817
do 2001 i1=1,2
print,'Input Zr(cm)'
input,zr
817 a=n*zr
Dt=tis
K=0
KP=0
I=0
LM=0

SK3=0.0
SK2=0.0
LMM=0
yieldc=0.0
evapc=0.0
400 if(ucu.eq.1) go to 401
if(szr.eq.2) go to 401

```

```

if(fcu.eq.2) go to 401
write(6,1701)SK,evapc,yieldc
1701 format(f8.5,4x,f8.5,4x,f8.5)
C *****
C CALCULATE THE VALUE OF SOIL MOISTURE EVERY HALF HOUR
C DURING A PRECIPITATION EVENT
C *****

401 Dt1=0.
yt=0.0
sia1=sia*f11(d,SK)
sia2=2*(1.-SK)*sqrt(sia1)
Ao=bk1*86400/2.
if(SK.le.0) go to 215
ao1=Ao*(1.+(SK**cs))
go to 216
215 ao1=Ao
216 I=I+1
r2=R2(I)
in=R1(I)/r2
To1=2*in*(in-ao1)
to2=sia2**2./To1
to3=2.*(in-ao1)
to4=1.+(ao1/to3)
To=to2*to4
300 Dt1=Dt1+Dt
if(Dt1.ge.r2) go to 200
LM=LM+1
if(Dt1.ge.To) yt=1
if(SK2.lt.SK3) yt=0.0
SK1=SK+(in-p*((B2*yt)+(B28*mnu*mtr/mtau))-p*(SK-so)*((C2*yt)+(C3*mnu*mtr/mtau)))*Dt/a
SK2=SK1
SK3=SK
if(SK1.ge.0.999) go to 211
go to 212
211 SK1=0.999
yield=in
yieldc=yieldc+(in*tis)
go to 213
212 yield=p*((B2*yt)+(B28*mnu*mtr/mtau))+p*(SK-so)*((C2*yt)+(C3*mnu*mtr/mtau))
yieldc=yieldc+(yield*tis)
213 SK=SK1
if(f1.eq.1) go to 250
if(szr.eq.2) go to 300
write(6,210) SK,in,yield
210 format(f8.5,4x,f8.5,22x,f8.5)
go to 300
250 tiss=1./tis
if(LM.ge.tiss) go to 251
go to 300
251 LM=0
LMM=LMM+1
if(LMM.gt.mtau) go to 900
KP=KP+1
SKP(KP)=SK
da(KP)=LMM
if(ucu.eq.2) go to 300
if(szr.eq.2) go to 300
write(6,252) SK,in,yield,LMM

```

```

252 format(f8.5,4x,f8.5,22x,f8.5,9x,15)
go to 300
200 if(ucu.eq.1) go to 201
if(fcu.eq.2) go to 201
write(6,1700) SK,yieldc,yt
1700 format(f8.5,16x,f8.5,4x,f3.1)
C *****
C CALCULATE THE VALUE OF SOIL MOISTURE EVERY HALF HOUR
C DURING AN INTERSTORM PERIOD
C *****

201 Dt1=0.
500 Dt1=Dt1+Dt
r3=R3(I)
if(Dt1.ge.r3) go to 400
LM=LM+1
evap=B1+(C1*(SK-so))
if(evap.ge.epr) go to 600
evapp=evap/epr
if(evapp.le.vg) go to 701
SK1=SK-(evap+(B28*p*mnu*mtr/mtau)+(C3*p*mnu*mtr*(SK-so)/mtau))*Dt/a
evapc=evapc+(evap*tis)
go to 700
600 evap=epr
evapc=evapc+(evap*tis)
SK1=SK-(epr*Dt/a)-((B28*p*mnu*mtr/mtau)+(C3*p*mnu*mtr*(SK-so)/mtau))*Dt/a
go to 700
701 evap=epr*vg
evapc=evapc+(evap*tis)
SK1=SK-(evap*Dt/a)-((B28*p*mnu*mtr/mtau)+(C3*p*mnu*mtr*(SK-so)/mtau))*Dt/a
700 yield=(B28*p*mnu*mtr/mtau)+(C3*p*mnu*mtr*(SK-so)/mtau)
if(yield.le.0.0000001) yield=0.0000001
yieldc=yieldc+(yield*tis)
SK=SK1
if(f1.eq.1) go to 750
if(szr.eq.2) go to 757
write(6,220) SK,evap,yield
220 format(f8.5,16x,f8.5,10x,f8.5)
757 K=K+1
if(K.ge.1000) stop
go to 500
750 tiss=1./tis
if(LM.ge.tiss) go to 751
go to 500
751 LM=0
LMM=LMM+1
if(LMM.le.mtau) go to 901
write(6,905) SK,evapc,yieldc
905 format(f8.5,4x,f8.5,4x,f8.5)
go to 900
901 KP=KP+1
SKP(KP)=SK
da(KP)=LMM
if(ucu.eq.2) go to 500
if(szr.eq.2) go to 500
write(6,752) SK,evap,yield,LMM
752 format(f8.5,16x,f8.5,10x,f8.5,9x,15)
go to 500
900 if(szr.eq.2) go to 2008
if(ran.eq.2) go to 2031

```

```

C *****
C CALCULATE THE STATISTICAL PROPERTIES OF THE GENERATED
C RAINSTORM EVENTS
C *****

print,'Statistical properties of the simulated rainstorm characteristics'
sum1=0.000
sum2=0.000
sum3=0.000
do 1001 IL=1,I
sum1=sum1+R1(IL)
sum2=sum2+R2(IL)
sum3=sum3+R3(IL)
1001 continue
mean1=sum1/(float(I))
mean2=sum2/(float(I))
mean3=sum3/(float(I))
var1=0.0
var2=0.0
var3=0.0
do 1002 IL=1,I
var1=var1+((R1(IL)-mean1)**2.)
var2=var2+((R2(IL)-mean2)**2.)
var3=var3+((R3(IL)-mean3)**2.)
1002 continue
vari1=var1/float(I-1)
vari2=var2/float(I-1)
vari3=var3/float(I-1)
print,'AVER.h(cm)      AVER.tr(days)      AVER.tb(days) '
write(6,1003) mean1,mean2,mean3
1003 format(f10.6,6x,f10.6,6x,f10.6)
print,'      VAR.h      VAR.tr      VAR.tb'
print 1004,vari1,vari2,vari3
1004 format(f8.2,4x,f8.2,10x,f8.2)
ran=2.
2031 if(1ot.eq.2) go to 2030
go to 2020
2030 read(5.)
2008 if(i1.gt.1) go to 2003

C *****
C PLOT THE SOIL MOISTURE CONCENTRATION WITHIN THE
C LAYER OF THICKNESS Zr VERSUS TIME DURING THE
C RAINY SEASON LENGTH
C *****

call plot_$setup(' ','DAYS','SOIL MOISTURE',1,0,0,0)
call plot_$scale(1.,220.,0.,1.)
2003 i=0
do 910 j=1,LMM
i=i+1
st(i)=SKP(j)
day(i)=da(j)
910 continue
if(i1.eq.1) go to 2004
if(i1.eq.2) go to 2005
2005 call plot_(day,st,mtau,3,')
go to 2001
2004 call plot_(day,st,mtau,1,')
if(szr.eq.1) go to 2000

```



```

2001 continue
C *****
C CALCULATE THE MOISTURE FLUXES USING MANABE'S PARAMETERIZATION
C *****

3025 if(mnb.eq.1) go to 2000
print,'S(t)      CUM.EVAP.      CUM.YIELD'
SK=so
Dt=1./48.
I=0
yieldc=0.0
evapc=0.0
Dt11=0.0
3031 write(6,3033) SK,evapc,yieldc
3033 format(f8.5,4x,f8.5,4x,f8.5)
Dt1=0.0
I=I+1
r2=R2(I)
in=R1(I)/r2
3028 Dt1=Dt1+Dt
Dt11=Dt11+Dt
if(SK.ge.0.42) go to 3029
SK1=SK+in*Dt/(n*100)
SK=SK1
if(Dt1.ge.r2) go to 3027
go to 3028
3029 yield=(in-epr)*Dt
yieldc=yieldc+yield
if(Dt1.ge.r2) go to 3027
go to 3028
3027 write(6,3030) SK,evapc,yieldc
3030 format(f8.5,4x,f8.5,4x,f8.5)
Dt1=0.0
r3=R3(I)
3032 Dt1=Dt1+Dt
Dt11=Dt11+Dt
evap=epr
if(SK.lt.0.315) evap=epr*SK/0.315
SK1=SK-evap*Dt/(n*100)
evapc=evapc+(evap*Dt)
SK=SK1
if(Dt11.ge.mtau) stop

if(Dt1.ge.r3) go to 3031
go to 3032
2000 read(5,)
stop
end
C *****

subroutine WATCHN(ta,sut,nu,gamsw)

C *****

real nu,nut
dimension sutt(11),nut(11),gamst(11)
data sutt/75.6,74.9,74.2,73.5,72.80,72.1,71.4,70.7,70.0,69.3,68.6/
data nut/17.93e-3,15.18e-3,13.09e-3,11.44e-3,10.08e-3,8.94e-3,
& 8.e-3,7.2e-3,6.53e-3,5.97e-3,5.94e-3/
data gamst/0.99987,0.99999999,0.99973,0.99913,0.99823,0.99708,

```

```

& 0.99568,0.99406,0.99225,0.99025,0.98807/
if(ta.gt.50.)go to 10
ita=ifix(ta*.2)+1
frac=ta-float(5*(ita-1))
ita1=ita+1
sut=(sutt(ita1)-sutt(ita))*0.2*frac+sutt(ita)
nu=(nut(ita1)-nut(ita))*0.2*frac+nut(ita)
gamsw=((gamst(ita1)-gamst(ita))*0.2*frac+gamst(ita))*980.
return
10 sut=sutt(11)
nu=nut(11)
gamsw=gamst(11)
return
end
c *****
c this function computes the gamma incomplete function
c *****
function gamt(a,x)
if(x.eq.0)go to 40
if(x.gt.100)go to 50
sum=1./a
an=1.0
old=sum
33 old=old*x/(a+an)
if(old/sum-1.e-6)20,10,10
10 an=an+1.
sum=sum+old
if(an-300.)33,33,12
12 continue
20 xxx=(a*log(x)+log(sum)-x)
if(xxx.lt.-80.)go to 40
gamt=(exp(xxx))
go to 60
40 gamt=0.0
go to 60
50 gamt=gamma(a)
60 return
end
c *****
c This function computes the gamma function by a Stirling approx.
c *****
function gamma(y)
x=y+1.
pi=3.14159
stir1=1./(12.*x)
stir2=1./(288.*x**2.)
stir3=-139./(51840.*x**3.)
stir4=-571./(2488320.*x**4.)
stir=1+stir1+stir2+stir3+stir4
gamma=exp(-x)*x**(x-.5)*sqrt(2.*pi)*stir/y
end
function fie(d)
dimension y(6)
data y/0.18,0.11,0.077,0.056,0.044,0.034/
if(d.gt.7.)go to 10
x=d-1.
i=ifix(x)
frac=x-float(i)
y1=log(y(i))
y2=log(y(i+1))

```

```
fie=exp((y2-y1)*frac+y1)
return
10 fie=.034
return
end
```

2. PROGRAM ARIZ.FORTRAN

```

C *****
C THIS PROGRAM CALCULATES THE AVERAGE SOIL MOISTURE CONCENTRATION
C OVER 1m DEPTH EVERY HALF HOUR , DURING AN EVAPORATION PERIOD WITH
C A CHANGING VALUE OF THE POTENTIAL EVAPORATION RATE.
C IT ALSO CALCULATES THE SURFACE TEMPERATURE USING THE FORCE-
C RESTORE METHOD OR THE THERMODYNAMIC EQUILIBRIUM EQUATION.
C THE POTENTIAL EVAPORATION RATE IS CALCULATED EITHER USING
C PENMAN'S EQUATION OR THE AERODYNAMIC EQUATION.
C ATMOSPHERIC INSTABILITY CRITERIA ARE USED.
C THE SHORT-TERM WATER AND THERMAL BALANCES CAN BE SOLVED SIMULTANEOUSLY
C AND THE SOIL MOISTURE CONCENTRATION AND SURFACE TEMPERATURE
C CAN BE CALCULATED AND PLOTED
C THIS PROGRAM READS FROM FILE 31 THE METEOROLOGIC
C VARIABLES AND THE SOIL MOISTURE CONCENTRATION MEASUREMENTS,
C WHICH ARE GIVEN EVERY HALF HOUR.
C *****

```

```

C THE CLIMATIC VARIABLES AND SOIL PARAMETERS USED AS INPUTS
C TO THIS MODEL ARE DESCRIBED BELOW.

```

```

c epr=annual average potential evaporation rate(cm/day)
c mpa=mean annual precipitation(cm)
c mtr=mean storm duration(days)
c mtau=mean rainy season length(days)
c mnu=mean number of storms per year
c J=evapotranspiration efficiency
c C1=derivative of J with respect to s
c C3=derivative of percolation rate with respect to s
c so=average annual soil moisture
c SK=initial soil moisture at 1m depth
c n=porosity
c Zr=surface layer thichness
c K(1)=saturated hydraulic conductivity (cm/sec)
c c=pore disconectedness index
c a(1,1)=net radiation(ly/min)
c a(i,2)=air temperature(C)
c a(i,3)=water vapor pressure of air (mb)
c a(i,4)=wind speed(cm/sec)
c a(i,5)=average soil moisture content in 0-10cm
c a(i,6)=average soil moisture content in 10-50cm
c a(i,7)=average soil moisture content in 50-100cm
c a(i,8)=ground temperature at 1cm (C)

c Tg=calculated surface temperature(C)
c T2=deep soil temperature(C)
c (cH)n=drag coefficient under neutral conditions

```

```

C *****
real a(337,8),epi(337),hr(337),ASK(337)
real epp(337),hrr(337)
real Ask(337),SK2(337),hr1(337),SK3(337),hr2(337)
real Ask1(337),TgCC(337),TgC1(337),TgKK(337)
real TgCM(337)
external plot_$setup (descriptors)
external plot_$scale (descriptors)
external plot_(descriptors)
real mpa,mtau,mtr,mnu,k1,m
fi(em)=10.**( .66+.55/em+.14/em**2.)
double precision B,ga,gd,gd1,bet,deno,T,es,dif,H,nom,ep,B28

```

```

print,'epr,mpa,mtr,mtau,mnu,J,C1,C3,so,SK,n,Zr,K(1),c'
input,epr,mpa,mtr,mtau,mnu,sj,C1,C3,so,SK,un,zr,bk1,cs
read(31,)((a(i,j),i=1,337),j=1,8)
print,'To print file31 type2, otherwise type 1'
input,ty
print,'To plot ep type 1,otherwise type 2'
input,pr
print,'To print ep write 2 ,otherwise 1'
input,pr1
print,'To print soil moisture type 2 ,otherwise1'
input,pt
print,'To calculate the surface temperature type 2, otherwise 1'
input,tmr
if(tmr.eq.1) go to 200
print,'Input the initial surface temperature Tg, T2 (in degrees Celcius) and (cH)n'
input,TgC,T2,cHn
print,'To solve simultaneously the equations for soil moisture
& and temperature using the aerodynamic equation and
& the instability criteria type 2 , otherwise 1'
input,aer
print,'To use the thermodynamic equation type 2 , otherwise 1'
input,thm
if(thm.eq.1) go to 305
print,'Input k(1),Ta'
input,k1,ta

m=2./(cs-3.)
fic=fi(m)
C *****
C COMPUTE WATER CONSTANTS
C *****

call WATCN(ta,sut,nu,gamsw)
s11=sqrt(un/(k1*fic))*sut/gamsw
305 T2=T2+273.16
TgK=TgC+273.16
TgF=(9.*TgC/5.)+32.
TgKK(1)=TgK
200 if(ty.eq.1) go to 41
do 40 i=1,337
write(6,20) a(i,1),a(i,2),a(i,3),a(i,4),a(i,5),a(i,6),a(i,7),a(i,8)
20 format(f10.4,2x,f10.4,2x,f10.4,2x,f10.4,2x,f10.4,2x,f10.4,2x,f10.4,2x,f10.4)
40 continue
41 h=-0.5
sum=0.0
do 46 i=1,337
C *****
c CALCULATE ep USING PENMAN'S EQUATION
C *****

ga=(a(i,2)*0.013)+0.42
gd1=1./ga
gd=gd1-1.
deno=597.*gd1
bet=200./0.03
bet=log(bet)
bet=bet**2.
B=10.**(-7)
B=1.222*B
B=B*a(i,4)*60.

```

```

B=B/bet
T=273.16+a(i,2)
es=273.16/T
es=1.-es
es=es*(5.00650+19.83923)
es=exp(es)
es1=(273.16/T)**5.00650
es=es*es1*6.11
dif=es-a(i,3)
H=597.*B*dif*gd
nom=H+a(i,1)
64 ep=nom/deno
ep=ep*60.*24.
h=h+0.5
epi(i)=ep
hr(i)=h
sum=sum+epi(i)
if(pr1.eq.1) go to 46
write(6,45) ep
45 format(f10.4)
46 continue
avep=sum/337.
write(6,60) avep
60 format(2x,f10.4)
  if(pr.eq.2) go to 61
  call plot_$setup('Potential Evaporation','Hours','ep',.1,0,0,0)
  call plot_$scale(0.,168.,-0.15,2.)
61 i=0
do 51 j=1,337
i=i+1
epp(i)=epi(j)
hrr(i)=hr(j)
51 continue
if(pr.eq.2) go to 63
  call plot_(hrr,epp,337,1,' ')
C *****
C CALCULATE THE UPDATED SOIL MOISTURE
C *****

63 ai=un*zr
hr8=-0.5
p=mpa/(mnu*mtr)
B28=mtau*bk1*86400./mpa*so**cs
Dt=1./48.
  C33=C3/2.
do 100 i=1,337
ASK(i)=(0.10*a(i,5))+(0.40*a(i,6))+(0.50*a(i,7))
B1=sj*epr
  c1=C1*epr
yt=0.0
evap=B1+(c1*(SK-so))
if(i.le.196) go to 108
if(evap.lt.epi(i)) go to 107
108 evap=epi(i)
yt=1.0
107 Ask(i)=ASK(i)/0.35
ASKK=Ask(i)
SK2(i)=SK
hr1(i)=hr8+0.5
SK1=SK-(evap+(B28*p*mnu*mtr/mtau)+(C33*p*mnu*mtr*(SK-so)/mtau))*Dt/ai

```

```

if(pt.eq.1) go to 102
write(6,101) ASKK,SK,yt
101 format(f10.4,4x,f10.4,4x,f3.1)
102 SK=SK1
hr8=hr1(i)
100 continue
if(tmr.eq.2) go to 290

C *****
C PLOT THE CALCULATED AND MEASURED SOIL MOISTURE CONCENTRATION
C AT DEPTH OF 1m , USING PENMAN'S EQUATION TO CALCULATE ep
C *****

call plot_$setup(' ', 'HOURS', 'SOIL MOISTURE', 1, 0, 0, 0)
call plot_$scale(0., 170., 0.62, 0.70)
i=0
do 110 j=1, 337
i=i+1
ASK1(i)=ASK(j)
SK3(i)=SK2(j)
hr2(i)=hr1(j)
110 continue
call plot_ (hr2, SK3, 337, 3, '.', '.')
call plot_ (hr2, ASK1, 337, 1, ' ')
290 Dt=1800.
if(tmr.eq.1) go to 210

Ev1=-10.
SUM=0.0
L=1
print, 'Average Daily Evaporation Rate(cm/day)'
SK=SK2(1)

C *****
C CALCULATE ep USING THE AERODYNAMIC EQUATION AND THE
C ATMOSPHERIC INSTABILITY CRITERIA(surface roughness 0.05cm)
C *****

do 250 i=1, 337
TgA=a(i,2)+273.16
SK2(i)=SK
est=6.11+(0.339*(TgF-32.))
if(i.le.196) go to 260
Ev11=B1+(c1*(SK2(i)-so))
Ev1=Ev11/86400
260 Ri=2.*981*100.*(TgA-TgK)/((TgA+TgK)*(a(i,4)**2.))
if(Ri.ge.0.2) rat=0.0
if(Ri.lt.0.2.and.Ri.ge.0.1) rat=(-2.*Ri)+0.4
if(Ri.lt.0.1.and.Ri.ge.0.0) rat=(-8.*Ri)+1.
if(Ri.lt.0.0.and.Ri.ge.-0.1) rat=1.30
if(Ri.lt.-0.1.and.Ri.ge.-0.2) rat=1.8
if(Ri.lt.-0.2.and.Ri.ge.-0.3) rat=2.2
if(Ri.lt.-0.3.and.Ri.ge.-0.4) rat=2.45
if(Ri.lt.-0.4) rat=2.7
CH=cHn*rat
Ev=cH*(730.5e-9)*a(i,4)*(est-a(i,3))
if(i.le.196) go to 262
if(Ev.ge.Ev1) Ev=Ev1
if(thm.eq.1) go to 262
if(Ev.lt.Ev1) go to 262

```



```

C *****
C CALCULATE THE SURFACE TEMPERATURE USING THE
C THERMODYNAMIC EQUILIBRIUM EQUATION
C *****

est1=Ev1/(cH*(730.5e-9)*a(1,4))
est=est1+a(1,3)
s111=s11*SK**(-1./m)

ex=981.*s111/((2.876e+6)*TgK)
rh=exp(ex)
TgF1=est-(rh*6.11)+(0.339*32.*rh)
TgF=TgF1/(0.339*rh)
j=i+1
TgKK(j)=(5.*(TgF-32.)/9.)+273.16
TgK=TgKK(j)

262 if(aer.eq.1) go to 261
SK1=SK-((Ev*86400.)+(B28*p*mnu*mtr/mtau)+(C33*p*mnu*mtr*(SK-so)/mtau))/(48.*a1)
SK=SK1
if(Ev.1t.Ev1) go to 261
if(i.le.196) go to 261
if(thm.eq.2) go to 250
261 Hs=cH*(285.48e-6)*a(1,4)*(TgK-TgA)
Le=597.3-(0.57*TgC)
G=(a(1,1)/60.)-Hs-(Le*Ev)
j=i+1
C *****
C COMPUTE SURFACE TEMPERATURE
C *****

TgKK(j)=TgKK(i)+(2.*G*Dt/7.37)-((72.72e-6)*Dt*(TgKK(i)-T2))
TgC=TgKK(j)-273.16
TgF=(9.*TgC/5.)+32.
TgK=TgKK(j)
T2=T2+(G*Dt/249.68)
SUM=SUM+(Ev*86400.)
L=L+1
if(L.1t.48) go to 250
AEV=SUM/48.
write(6,400) AEv
400 format(2x,f8.4)
L=1
SUM=0.0
250 continue
C *****
c PLOT CALCULATED AND MEASURED SURFACE TEMPERATURE
C USING THE AERODYNAMIC EQUATION
C *****

call plot_$setup(' ','HOURS','SURFACE TEMPERATURE',1,0,0,0)
call plot_$scale(0.,170.,-2.,40.)
do 270 i=1,337
TgCC(i)=TgKK(i)-273.16
270 continue
i=0
do 280 j=1,337
i=i+1
TgCM(i)=a(j,8)
TgC1(i)=TgCC(j)

```

```

hr2(i)=hr1(j)
280 continue
  call plot_ (hr2,TgC1,337,3,'.')
  call plot_ (hr2,TgCM,337,1,' ')
  if(aer.eq.1) go to 210
  read(5,)
  call plot_$setup(' ','HOURS','SOIL MOISTURE',1,0,0,0)
  call plot_$scale(0.,170.,0.61,0.70)
  i=0
  do 300 j=1,337
  i=i+1
  SK3(i)=SK2(j)
  AsK1(i)=AsK(j)
  hr2(i)=hr1(j)
  300 continue
C *****
C PLOT CALCULATED AND MEASURED SOIL MOISTURE DERIVED BY
C USING THE AERODYNAMIC EQUATION FOR ESTIMATING ep
C *****

  call plot_ (hr2,SK3,337,3,'.')
  call plot_ (hr2,AsK1,337,1,' ')
210 stop
end

C *****
  subroutine WATCHN(ta,sut,nu,gamsw)
C *****
  real nu,nut
  dimension sutt(11),nut(11),gamst(11)
  data sutt/75.6,74.9,74.2,73.5,72.80,72.1,71.4,70.7,70.0,69.3,68.6/
  data nut/17.93e-3,15.18e-3,13.09e-3,11.44e-3,10.08e-3,8.94e-3,
  & 8.e-3,7.2e-3,6.53e-3,5.97e-3,5.94e-3/
  data gamst/0.99987,0.999999999,0.99973,0.99913,0.99823,0.99708,
  & 0.99568,0.99406,0.99225,0.99025,0.98807/
  if(ta.gt.50.) go to 10
  ita=ifix(ta*.2)+1
  frac=ta-float(5*(ita-1))
  ita1=ita+1
  sut=(sutt(ita1)-sutt(ita))*0.2*frac+sutt(ita)
  nu=(nut(ita1)-nut(ita))*0.2*frac+nut(ita)
  gamsw=((gamst(ita1)-gamst(ita))*0.2*frac+gamst(ita))*980.
  return
10 sut=sutt(11)
  nu=nut(11)
  gamsw=gamst(11)
  return
end

```

APPENDIX 2

DOCUMENTATION OF THE COMPUTER PROGRAM SPLASH

Documentation of the Computer Program SPLASH

A complete documentation of the computer program SPLASH.FORTRAN is given by Milly and Eagleson (1980). Here, only the procedure to achieve convergence of the results will be described and the way of attaching a file to it, including the boundary conditions of the area under investigation.

Two parameters were varied in order to achieve convergence. Those were:

1. XERR

The parameter XERR represents the maximum allowed change of soil-moisture at every node and at every time-step. That is,

$$XERR = \max_{\text{nodes } i} \left[\left| \theta_i(t+\Delta t) - \theta_i(t) \right| \right].$$

As this parameter decreases, the accuracy of calculations increases. In studying the catchments of Santa Paula and Clinton, it was found that convergence of the results occurs when $XERR = 0.0005$.

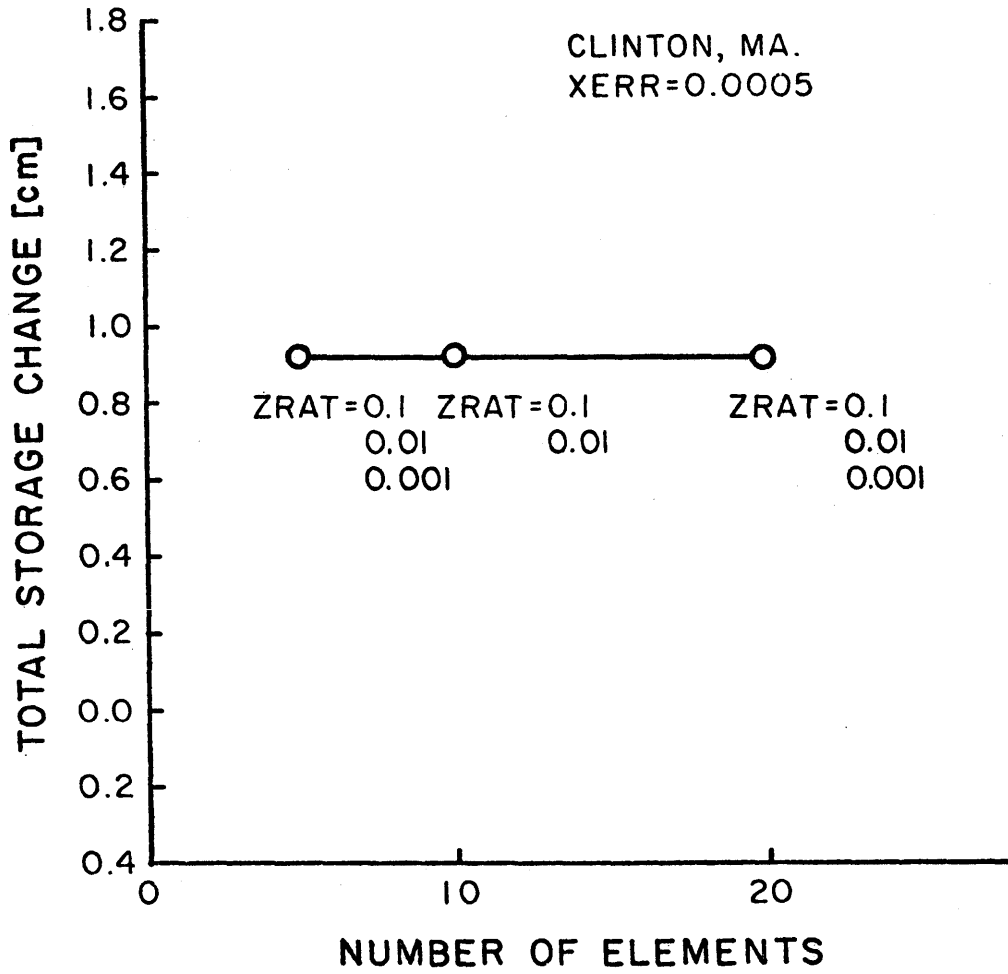
2. ZRAT

The parameter ZRAT is given by:

$$ZRAT = \frac{(\text{length of top element}) \times (\text{number of elements})}{(\text{total column length})}$$

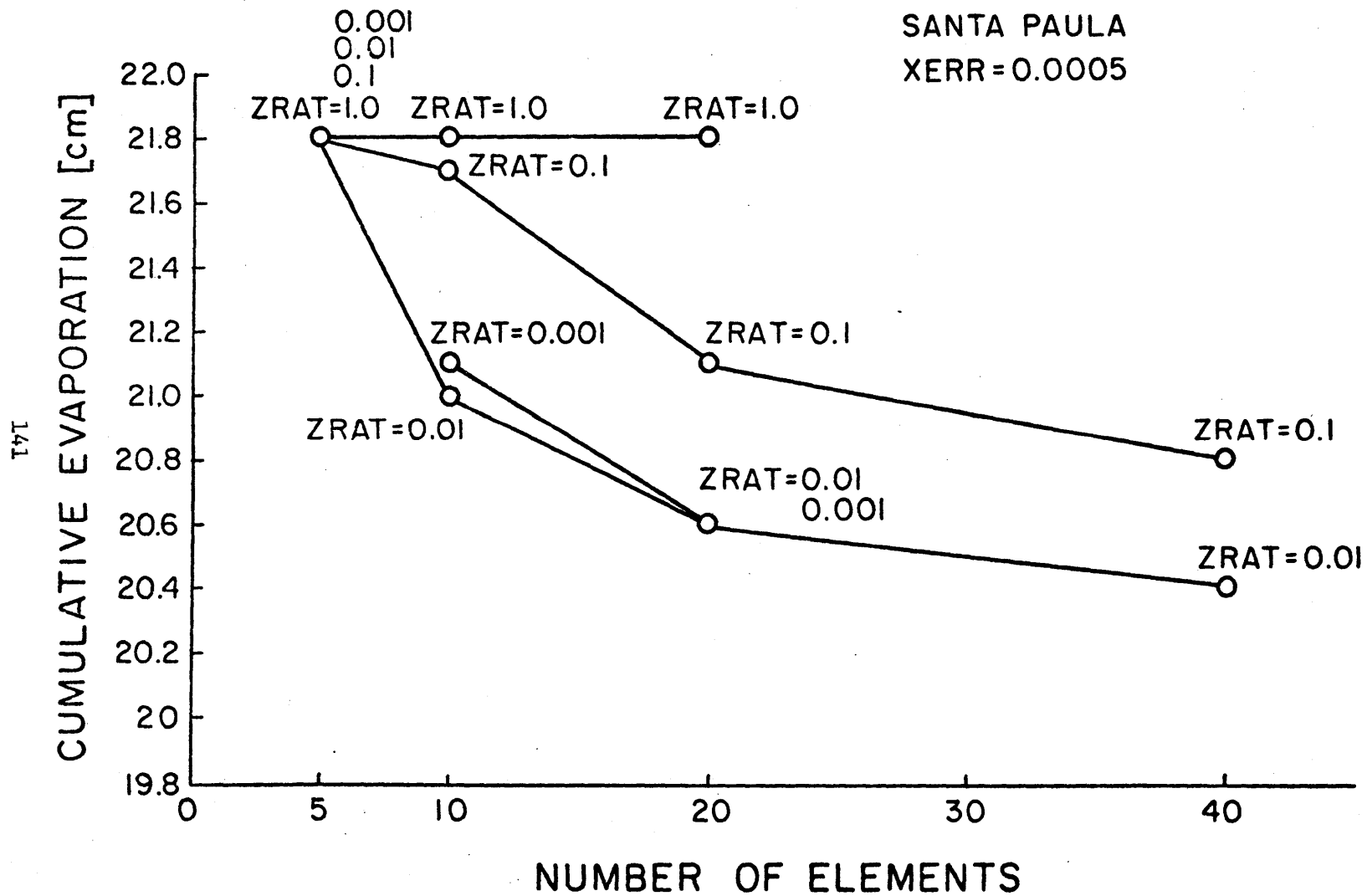
For a fixed number of nodes, the value of ZRAT was varied until satisfactory convergence was achieved. The results for Clinton, Massachusetts and Santa Paula, California are shown in Figures 31 and 32, respectively.

It was found that satisfactory convergence is achieved for Clinton, when $XERR = 0.0005$, $ZRAT = 0.01$ and $n = 21$. For Santa Paula it was found that convergence can be considered achieved when $XERR = 0.0005$, $ZRAT = 0.01$, and $n = 41$.



Convergence Experiments (Clinton, Massachusetts)

FIGURE 31



Convergence Experiments (Santa Paula, California)

FIGURE 32

Inputs for SPLASH

First the program "input" described by Milly and Eagleson (1980) must be run, in which the number of nodes and the manner of setting up the nodes is established, and also the parameters XERR and initial $\psi(s)$ are defined.

By running "input" File 98 is created. This file must then be combined with a file including the soil properties and the atmospheric boundary conditions of the area under investigation. This file is also described with details by Milly and Eagleson (1980). By combining those two files, File 15 is created.

Then, the program SPLASH.FORTRAN is ready to run, using as input File 15.